MERCURY CONCENTRATIONS AND FEEDING ECOLOGY OF FISHES IN ALASKA

By

Andrew Philip Cyr, B.S.

A Dissertation Submitted in Partial Fulfillment of the Requirements
for the Degree of Doctor of Philosophy

In

Fisheries

University of Alaska Fairbanks

May 2019

Andrew P. Cyr

APPROVED:

Dr. Juan Andrés López, Committee Chair

Dr. Todd O'Hara, Committee Member

Dr. Matthew Wooller, Committee Member

Dr. Andrew Seitz, Committee Member

Dr. Milo Adkison, Chair *Department of Fisheries*

Dr. Bradley Moran, Dean *College of Fisheries and Ocean Sciences*

Dr. Michael Castellini *Dean of the Graduate School*

Abstract

Mercury (Hg) is a ubiquitous contaminant found in nearly every fish species analyzed. Certain forms of Hg accumulate efficiently in fish tissues, sometimes reaching concentrations of concern for human and wildlife health when consumed. This has motivated considerable research and interventions surrounding fish consumption with Hg concentrations as the underlying cause of over 80% of fish consumption advisories in the United States and Canada. The ecological and physiological drivers that influence the concentrations of Hg in fishes are complex and vary among taxa spatially and temporally. Studying these drivers and their respective influences on Hg concentrations can help elucidate observed differences in Hg concentrations across space and time, which can then be used to improve management and consumption strategies. Here I present a series of studies focused on the chemical feeding ecology of Hg by measuring total Hg (THg) concentrations and ratios of nitrogen and carbon stable isotopes in multiple fish species from three regions in Alaska. In Chapter 2 I described foundational field collection efforts to characterize the fish communities from West Creek and the Taiya River in Klondike Gold Rush National Historical Park, and the Indian River in Sitka Historical National Park, Alaska. This chapter and agency report presents a survey of the fish species assemblage of the rivers and laid the framework for the regional analyses I conducted in the study presented in Chapter 3. In Chapter 3 I report inter- and intra-river comparisons of THg concentrations and associated feeding ecology of riparian Dolly Varden, separated by anadromous barriers in each system. I concluded that resident Dolly Varden that co-habit riverine locations with spawning salmon consume more salmon eggs than resident Dolly Varden from other locations of the same river that do not co-habit with spawning salmon. This is reflected in the isotopic composition of their tissues, and subsequently the THg concentrations of these fish are lower relative to Dolly Varden from parts of the same river above anadromous barriers. In Chapter 4, I describe regional patterns of THg concentrations and stable isotope values of carbon and nitrogen in nine species of fish and invertebrates from the Bering Sea and North Pacific Ocean along the Aleutian Islands, using Steller sea lion management zones as a spatial framework. I determine that most species from the Western Aleutian Islands have greater THg concentrations, and more negative $\delta^{13}C$ values than those from the

Central Aleutian Islands, indicating ecosystem-wide differences in THg concentrations and fish feeding ecology. I also determined that Amchitka Pass, a well-documented oceanographic and ecological divide along the Aleutian Island chain, aligns better with differences in THg concentrations than the boundary between Steller sea lion management zones. In Chapter 5, I report THg and methylmercury concentrations in fishes of Kotzebue Sound, including seven species that are important for subsistence users. I determined that fork length influences Hg concentrations within individual species, and that trophic relationships within a food web, a factor associated with biomagnification, influences Hg concentrations across the entire food web. I also observed that muscle tissues from virtually every individual fish had Hg loads below the State of Alaska's criteria for unlimited consumption. Taken together, the work conducted in this dissertation helps us better understand the ecological dynamics of Hg in aquatic food webs and has contributed to Hg monitoring of fish resources across parts of Alaska.

Acknowledgements

This dissertation would not have been possible without the tireless efforts and patience of my friends and colleagues. I would like to thank my committee for all their assistance, patience and guidance at every step of the process. Similarly, I would like to thank my coauthors for their valuable insight and guidance on each step of each manuscript. Todd O'Hara and J. Andrés López were enormously helpful through all aspects of my research, and continually provided me with new and exciting opportunities to expand my skill sets and professional development. Collectively, the support of all those behind the scenes helped keep me focused and to take charge of my research to make the difficult decisions at the right moments.

I would like to thank the Wildlife Toxicology Lab community for their assistance. To my fellow graduate students John Harley, Stephanie Kennedy, Marianne Lian, and Stephanie Crawford for all their help corralling me and keeping me moving forward despite my frustrations, limitations, and self-imposed restrictions. Similarly, I would like to thank the many undergraduate students that assisted me throughout the laboratory portion of my research. The many hours of work they contributed are the only reason the immense amount of lab work required for this project was ever completed. A well-deserved thank you to Maggie Castellini for keeping the lab running despite the chaos I brought to it, and my ability to break things and make her blood boil. It goes without saying that none of this would have been possible without her hard work, guidance, knowledge, and of course her patience. I would also like to thank Cathy Griseto for being the ever-present smart ass to keep things in perspective and helping me with all manner of paperwork, logistics, and staying on track in general.

None of the research presented here would have been even remotely possible without the generous support of numerous funding groups and agencies. I would like to thank the National Park Service, the Alaska Department of Environmental Conservation, the North Pacific Research Board (NPRB), Biomedical Learning and Student Training (BLaST), and the Graduate School for a Thesis Completion Fellowship, all of which contributed funding for various portions of my research and degree.

In particular, I would like to thank the BLaST program. Not only did they fund a significant portion of my research, they also provided me with more opportunities for mentoring, outreach, conferences and trainings than most graduate students ever receive. The support of the BLaST program and staff has been instrumental in assisting me throughout my research and guiding my interests both throughout graduate school, as well as into the future.

A collective thank you to the many friends, family, coworkers, and random other people that encouraged me in some capacity to pursue a graduate degree in this research field. This includes Anna Bryan, Bobbie Sandwich, Erin Gleason, Aaron Wells, Brian Jackson, J.J. Frost, Adrian Gall, and countless others that I have forgotten to mention here.

Finally, I would like to thank my friends and family. My parents and sister might not have a clue what I do (don't worry, neither do I!), but they have supported me and encouraged me every step of the way. And I promise you Mom and Dad, I will get a real job sometime, maybe even after I finish this degree. Maybe… Finally, I would like to thank my girlfriend Stephanie Kennedy who has miraculously maintained composure and patience with me while I struggled and couldn't find the traction and confidence to move forward. Thank you.

Table of Contents

Page

List of Figures

Page

List of Tables

Page

Chapter 1 - **Introduction**[1]

[1]Cyr, A.

1.1 Introduction

Mercury (Hg) is considered a "global contaminant" and consequently Hg contamination attracts worldwide attention, with particular interest on Hg contamination of aquatic organisms. The ecological and chemical processes underlying the Hg cycle enable efficient accumulation in aquatic food webs, particularly in the tissues of fish and top predators in fish-based ecosystems. As evidence of this, Hg has been detected in almost every fish species that has been measured from North America in the last several decades (AMAP 2011; Eagles-Smith et al. 2016). Due to the concentrations measured in some fish species, Hg is now responsible for over 80% of fish consumption advisories in the United States and Canada (Environment Canada, 2013; USEPA, 2011).

1.2 Mercury Exposure

Human and wildlife exposure to Hg is influenced by environmental chemistry, biochemistry and inter- and intra-species variation in feeding ecology. Hg is efficiently absorbed through the gastrointestinal wall as the bioavailable form of monomethyl Hg ($MeHg^+$), with an assimilation efficiency greater than 85% (Wang, 2012). The methylation of divalent Hg (Hg^{2+}) to $MeHg^+$ in the environment is highly variable and is influenced by environmental factors, notably the bacterial species present, water pH (Kelly et al., 2003), temperature (Johnson et al., 2016), ultraviolet light (Lehnherr and St. Louis, 2009), and the presence of dissolved cations or organic matter (Boening, 2000; Douglas et al., 2012). Fish also have limited capacity for redistributing, demethylating or eliminating total Hg (THg) or $MeHg^+$, which leads to the variable accumulation and retention of THg or $MeHg^+$ in muscle and other tissues (Amlund et al., 2007; Trudel and Rasmussen, 1997).

$MeHg^+$ is a potent neurotoxin, involving oxidative stress and inhibiting selenium dependent enzymes (Farina et al., 2011; Ralston and Raymond, 2010). The ecotoxicological and biochemical properties of $MeHg^+$ have led to considerable concern surrounding Hg exposure from dietary resources, and in particular the consumption of fish. A thorough understanding of the drivers of Hg accumulation in

the food web, and the importance of effective monitoring, is therefore vital for providing meaningful and targeted consumption advice.

1.3 Linking Humans and Fish Together

Fish are an especially important resource for many Alaskans. They represent a significant cultural connection for many Alaskans through family, history, and education (Barnhardt and Kawagley, 2005). Fish are also an important commercial resource for many communities in Alaska. Importantly, fish contribute significantly to the diet of many subsistence users in Alaska year-round. It is estimated that rural subsistence fishers in Alaska consume over 100 kg of fish annually (Fall, 2018; Robert J Wolfe, 2000). This level of consumption indicates a potential for significant dietary exposure to Hg. These details highlight the importance of understanding Hg concentrations ([Hg]) in Alaskan fish resources, and effective monitoring of the drivers that influence those [Hg] over time and space.

Because the Hg cycle is linked to the aquatic environment, dietary exposure to Hg is most prevalent through the consumption of contaminated fishes and aquatic invertebrates. However, dietary exposure to Hg is highly variable and dependent on numerous factors, such as species of fish, tissue type, fish age and size, feeding ecology, and area where they were caught. This variability in [THg] has generated considerable interest and research into how these factors influence [THg] in different settings.

1.4 A Notable Human Dietary Exposure Example

One of the most notable examples of Hg toxicosis from consuming fish is the Minamata Bay, Japan disaster. The Chisso Corporation discharged $MeHg^+$, a by-product of acetaldehyde synthesis, into the bay from the 1930s until the 1960s. Once in the water, the $MeHg^+$ settled into the sediments, entered the food chain and then biomagnified through the food web. In the 1950s, many of the infants and young children from families that consumed large quantities of fish were exhibiting signs and symptoms of neurotoxicosis. In 1953, the first documented case of $MeHg^+$ poisoning from the town of Minamata was recognized, and in 1956, the phrase Minamata Disease was coined to describe neurotoxicological impacts

of $MeHg^+$ (Ekino et al., 2007). $MeHg^+$ had accumulated in the Minamata Bay fish and reached concentrations that could be dangerous, and even lethal, to humans and other animals. It is estimated that 1,043 people died from $MeHg^+$ toxicosis, and over 2,200 were left with severe, lifelong neurological damage (Harada, 1995). The Minamata Bay disaster represents one of the worst events of poisoning by dietary exposure to a Hg compound, notably from fishes, and is a salient example of the importance of ongoing monitoring of fish resources. Adequate monitoring ensures the resources people consume are safe for consumption to prevent such disasters. Muscle [$MeHg^+$] of fish from Minamata Bay were reported to be as high as 23 mg/kg wet weight (ww), concentrations that are approximately 100–200 times higher than those commonly observed in most fish tissues today (Fujiki and Tajima, 1992). Changing climate and ecological conditions coupled with ongoing anthropogenic release of Hg remind us that ongoing monitoring of Hg concentrations in fishes should remain a priority to prevent adverse impacts to human health.

1.5 Ecological Research Tools for Examining Food Webs

Analysis of stable isotope ratios of carbon and nitrogen can provide valuable information about feeding ecology and location. Carbon and nitrogen occur naturally as heavy and light isotopes, (e.g., N^{15} and N^{14}, and C^{13} and C^{12}). Following ingestion of prey items, physiological processes result in differential accumulation of these stable isotopes, whereby, for example, the lighter isotope is preferentially excreted, and the heavier isotope is preferentially retained. This causes slight changes in the ratio of heavy to light isotopes, resulting in small changes in $\delta^{13}C$ or $\delta^{15}N$ values. The degree of fractionation varies across ecosystems, species and populations; however, a general approximation for the change of these values with each trophic level is estimated to be ~1 ‰ for $\delta^{13}C$, and ~3.4 ‰ for $\delta^{15}N$ (Post, 2002). The ratio of the heavy to light isotopes are typically expressed relative to the isotopic ratio of a known standard (such as Vienna Pee-Dee Belemnite, or atmospheric Air), resulting in $\delta^{13}C$ (‰) and $\delta^{15}N$ (‰) values (delta notation).

[Hg] can increase in fishes through a food web in a process called biomagnification, which is driven by the feeding ecology of fishes at different trophic levels (McIntyre and Beauchamp, 2007; Power et al., 2002). Stable isotopes of nitrogen reflect feeding ecology. They provide information about trophic interactions in the food web and provide an indication of the relative trophic level of individuals, species, or different trophic guilds, and consequently can be indicators of biomagnification.

The $\delta^{13}C$ values of organisms are a reflection of the source of carbon used to generate the primary production at the base of the food chain (Budge et al., 2008; Wang et al., 2014). As a result, carbon isotopes can provide an indication of feeding location, and can differentiate between sources of primary production, such as marine versus terrestrial sources (Fry, 2006; McGrew et al., 2014), or benthic versus pelagic sources (Boyle et al., 2012; Doi et al., 2010). This is important because the area where fishes feed can provide access to prey resources with varying [Hg], which can then result in heterogeneous [Hg] in the food web (Burger et al., 2011; Burger and Gochfeld, 2006; Cyr et al., 2017).

Together, stable isotope ratios of carbon and nitrogen can be used to elucidate key aspects of the ecology of individuals and species groups, such as describing niche space, breadth, or overlap (Fry, 2006). In turn, understanding the trophic relationships of organisms can provide information about Hg exposure, either through proximity to sites of Hg methylation, or through prey resources with varying [$MeHg^{+}$].

Finally, [Hg] in fishes can increase over time with age, in a process called bioaccumulation (Burger and Gochfeld, 2007; Coelho et al., 2013; Scott and Armstrong, 1972). Fish age is commonly determined by examining markers of growth increments in otoliths. In cases where direct estimation of age is not feasible, fish length can be serve as an indicator of age (Scott and Armstrong, 1972). Fish fork length was measured and recorded for all the fishes from this project and then used to draw inferences about the influence of age on [Hg].

1.6 Organization of Dissertation

My dissertation research aims to improve understanding of the ecological and biological drivers that influence [Hg] in three regions of Alaska: two rivers of southeast Alaska, the western and central areas of the Aleutian Islands, and Kotzebue Sound. Fish are effective sentinels for environmental monitoring of Hg and many species are also directly relevant to human consumption advisories. As part of my research, I measured [THg] and [$MeHg^{+}$] in muscle from dozens of fish species thus contributing to efforts aimed at establishing effective monitoring protocols and consumption guidelines.

Chapter 2 characterized fish communities of two freshwater streams in Southeast Alaska. This work was published as Cyr et al., 2014, a National Park Service report. The information generated in this work laid the framework for Chapter 3, which examined the influence of feeding ecology on [THg] in Dolly Varden populations separated by barriers to upstream movement of migrating salmon. The goal of the project was to determine if [THg] and feeding ecology of Dolly Varden were significantly influenced by stream type with and without glacial influence or by overlap with spawning salmon. This work has been published as Cyr et al., 2017, in Science of the Total Environment. Chapter 4 investigated the Hg feeding ecology of nine groundfish species from the Bering Sea and North Pacific Ocean in close proximity to the Aleutian Islands. The goal of this project was to examine regional patterns in the magnitude and variability of [THg] (as seen in Steller sea lions and other vertebrates) and feeding ecology in part of the fish food web from the Aleutian Islands, discretely separated by Steller sea lion management regions as well as regions with known oceanographic differences. This work has been published as Cyr et al., 2019, in Science of the Total Environment. Chapter 5 further explored feeding ecology concepts and investigated the [THg], [$MeHg^{+}$], and stable isotopes of carbon and nitrogen in fishes from Kotzebue Sound, Alaska, focusing on species of particular interest to the subsistence user community. This work has been prepared for submission to Science of the Total Environment and will be submitted in the near future. In sum, my research has helped shape our understanding of the role species, region, time, and

feeding ecology play in driving [Hg]. Additionally, my research has helped contribute to monitoring Hg in fish resources across Alaska and will be an integral part of future consumption advice guidelines.

1.7 Works Cited

Amlund, H., Lundebye, A.K., Berntssen, M.H.G., 2007. Accumulation and elimination of methylmercury in Atlantic cod (Gadus morhua L.) following dietary exposure. Aquat. Toxicol. 83, 323–330. doi:10.1016/j.aquatox.2007.05.008

Arctic Monitoring Assessment Program (AMAP), 2011. AMAP Assessment 2011: Mercury in the Arctic. Oslo, Norway.

Barnhardt, R., Kawagley, A.O., 2005. Indigenous knowledge systems and the Alaskan Native ways of knowing. Anthropol. Educ. Q.

Boening, D.W., 2000. Ecological effects, transport, and fate of mercury: a general review. Chemosphere 40, 1335–1351. doi:10.1016/S0045-6535(99)00283-0

Boyle, M.D., Ebert, D.A., Cailliet, G.M., 2012. Stable-isotope analysis of a deep-sea benthic-fish assemblage: evidence of an enriched benthic food web. J. Fish Biol. 80, 1485–1507. doi:10.1111/j.1095-8649.2012.03243.x

Budge, A.M., Wooller, M.J., Springer, A.M., Iverson, S.J., McRoy, C.P., Divoky, G.J., 2008. Tracing carbon flow in an arctic marine food web using fatty acid-stable isotope analysis. Oecologia 157, 117–129. doi:10.1007/s00442-008-1053-7

Burger, J., Gochfeld, M., 2007. Risk to consumers from mercury in Pacific cod (Gadus macrocephalus) from the Aleutians: fish age and size effects. Environ. Res. 105, 276–284. doi:10.1016/j.envres.2007.05.004

Burger, J., Gochfeld, M., 2006. Locational differences in heavy metals and metalloids in Pacific Blue Mussels Mytilus [edulis] trossulus from Adak Island in the Aleutian Chain, Alaska. Sci. Total Environ. 368, 937–950. doi:10.1016/j.scitotenv.2006.04.022

Burger, J., Jeitner, C., Gochfeld, M., 2011. Locational differences in mercury and selenium levels in 19 species of saltwater fish from New Jersey. J. Toxicol. Environ. Heal. - Part A Curr. Issues 74, 863–874. doi:10.1080/15287394.2011.570231

Coelho, J.P., Mieiro, C.L., Pereira, E., Duarte, A.C., Pardal, M.A., 2013. Mercury biomagnification in a contaminated estuary food web: effects of age and trophic position using stable isotope analyses. Mar. Pollut. Bull. 69, 110–115. doi:10.1016/j.marpolbul.2013.01.021

Cyr, A., López, J.A., Rea, L., Wooller, M.J., Loomis, T., Mcdermott, S., O'Hara, T.M., 2019. Mercury concentrations in marine species from the Aleutian Islands: spatial and biological determinants. Sci. Total Environ. 664, 761–770. doi:10.1016/j.scitotenv.2019.01.387

Cyr, A., Sergeant, C., Lopez, J.A., O'Hara, T., 2014. Developing a Freshwater Contaminants Monitoring Protocol for the Southeast Alaska Network Summary of 2013 Fish and Habitat Sampling in Klondike Gold.

Cyr, A., Sergeant, C.J., Lopez, J.A., O'Hara, T., 2017. Assessing the influence of migration barriers and feeding ecology on total mercury concentrations in Dolly Varden (Salvelinus malma) from a glaciated and non-glaciated stream. Sci. Total Environ. 580, 710–718. doi:10.1016/j.scitotenv.2016.12.017

Doi, H., Kikuchi, E., Shikano, S., Takagi, S., 2010. Differences in nitrogen and carbon stable isotopes between planktonic and benthic microalgae. Limnology 11, 185–192. doi:10.1007/s10201-009-0297-1

Douglas, T.A., Loseto, L.L., MacDonald, R.W., Outridge, P., Dommergue, A., Poulain, A., Amyot, M., Barkay, T., Berg, T., Chetelat, J., Constant, P., Evans, M., Ferrari, C., Gantner, N., Johnson, M.S., Kirk, J., Kroer, N., Larose, C., Lean, D., Nielsen, T.G., Poissant, L., Rognerud, S., Skov, H., Sørensen, S., Wang, F., Wilson, S., Zdanowicz, C.M., 2012. The fate of mercury in Arctic terrestrial and aquatic ecosystems, a review. Environ. Chem. 9, 321–355. doi:10.1071/EN11140

Eagles-Smith, C.A., Ackerman, J.T., Willacker, J.J., Tate, M.T., Lutz, M.A., Fleck, J.A., Stewart, A.R., Wiener, J.G., Evers, D.C., Lepak, J.M., Davis, J.A., Flanagan Pritz, C., 2016. Spatial and temporal patterns of mercury concentrations in freshwater fish across the Western United States and Canada. Sci. Total Environ. doi:10.1016/j.scitotenv.2016.03.229

Ekino, S., Susa, M., Ninomiya, T., Imamura, K., Kitamura, T., 2007. Minamata disease revisited: An update on the acute and chronic manifestations of methyl mercury poisoning. J. Neurol. Sci. 262, 131–144. doi:10.1016/j.jns.2007.06.036

Environment Canada, 2013. Mercury: fish consumption advisories [WWW Document]. URL https://www.canada.ca/en/environment-climate-change/services/pollutants/mercury-environment/health-concerns/fish-consumption-advisories.html (accessed 7.10.18).

Fall, J.A., 2018. Regional Patterns of Fish and Wildlife Harvests in Contemporary Alaska Author (s): James A . Fall Published by : Arctic Institute of North America Stable URL : https://www.jstor.org/stable/43871398 Regional Patterns of Fish and Wildlife Harvests in Cont 69, 47–64.

Farina, M., Aschner, M., Rocha, J.B.T., 2011. Oxidative stress in MeHg-induced neurotoxicity. Toxicol. Appl. Pharmacol. 256, 405–417. doi:10.1016/j.taap.2011.05.001

Fry, B., 2006. Stable Isotope Ecology. Springer Science + Business Media, LLC, New York.

Fujiki, M., Tajima, S., 1992. The pollution of Minamata Bay by mercury. Water Sci. Technol. 25, 133–140. doi:doi.org/10.2166/wst.1992.0284

Harada, M., 1995. Minamata Disease: Methylmercury Poisoning in Japan Caused by Environmental Pollution. Crit. Rev. Toxicol. 25, 1–24. doi:10.3109/10408449509089885

Johnson, N.W., Mitchell, C.P.J., Engstrom, D.R., Bailey, L.T., Coleman Wasik, J.K., Berndt, M.E., 2016. Methylmercury production in a chronically sulfate-impacted sub-boreal wetland. Environ. Sci. Process. Impacts 18, 725–734. doi:10.1039/C6EM00138F

Kelly, C.A., Rudd, J.W.M., Holoka, M.H., 2003. Effect of pH on mercury uptake by an aquatic bacterium: implications for Hg cycling. Environ. Sci. Technol. 37, 2941–2946. doi:10.1021/es026366o

Lehnherr, I., St. Louis, V.L., 2009. Importance of ultraviolet radiation in the photodemethylation of methylmercury in freshwater ecosystems. Environ. Sci. Technol. 43, 5692–5698. doi:10.1021/es9002923

McGrew, A.K., Ballweber, L.R., Moses, S.K., Stricker, C.A., Beckmen, K.B., Salman, M.D., O'Hara, T.M., 2014. Mercury in gray wolves (Canis lupus) in Alaska: increased exposure through consumption of marine prey. Sci. Total Environ. 468–469, 609–613. doi:10.1016/j.scitotenv.2013.08.045

McIntyre, J.K., Beauchamp, D.A., 2007. Age and trophic position dominate bioaccumulation of mercury and organochlorines in the food web of Lake Washington. Sci. Total Environ. 372, 571–584. doi:10.1016/j.scitotenv.2006.10.035

Post, D.M., 2002. Using stable isotopes to estimate trophic position: models, methos, and assumptions. Ecology 83, 703–718. doi:10.2307/3071875

Power, M., Klein, G.M., Guiguer, K.R.R.A., Kwan, M.K.H., 2002. Mercury accumulation in the fish community of a sub-Arctic lake in relation to trophic position and carbon sources. J. Appl. Ecol. 39, 819–830. doi:10.1046/j.1365-2664.2002.00758.x

Ralston, N.V.C., Raymond, L.J., 2010. Dietary selenium's protective effects against methylmercury toxicity. Toxicology 278, 112–123. doi:10.1016/j.tox.2010.06.004

Scott, D.P., Armstrong, F.A.J., 1972. Mercury concentration in relation to size in several species of freshwater fishes from Manitoba and Northwestern Ontario. J. Fish. Res. Board Canada 29, 1685–1690. doi:10.1139/f72-268

Trudel, M., Rasmussen, J.B., 1997. Modeling the elimination of mercury by fish. Environ. Sci. Technol. 31, 1716–1722. doi:10.1021/es960609t

USEPA, 2011. National Listing of Fish Advisories.

Wang, S.W., Budge, S.M., Gradinger, R.R., Iken, K., Wooller, M.J., 2014. Fatty acid and stable isotope characteristics of sea ice and pelagic particulate organic matter in the Bering Sea: tools for estimating sea ice algal contribution to Arctic food web production. Oecologia 174, 699–712. doi:10.1007/s00442-013-2832-3

Wang, W.-X., 2012. Biodynamic understanding of mercury accumulation in marine and freshwater fish. Adv. Environ. Res. 1, 15–35. doi:10.12989/aer.2012.1.1.015

Wolfe, R.J., 2000. Subsistence in Alaska: A Year 2000 Update. Div. Subsist. Alaska Dep. Fish Game 1–4.

Chapter 2 - **Developing a freshwater contaminants monitoring protocol for the Southeast Alaska Network**[2]

Summary of 2013 fish and habitat sampling in Klondike Gold Rush and Sitka National Historical Parks

[2] Cyr, A., C.J. Sergeant, J.A. Lopez, and T.M. O'Hara. 2014. Developing a freshwater contaminants monitoring protocol for the Southeast Alaska Network: Summary of 2013 fish and habitat sampling in Klondike Gold Rush and Sitka National Historical Parks. Natural Resource Data Series NPS/SEAN/NRDS—2014/679. National Park Service, Fort Collins, Colorado

2.1 Abstract

The National Park Service (NPS) Southeast Alaska Network (SEAN) is developing a long-term freshwater contaminants monitoring protocol for Glacier Bay National Park and Preserve (GLBA), Klondike Gold Rush National Historical Park (KLGO), and Sitka National Historical Park (SITK) in cooperation with partners at the University of Alaska Fairbanks (UAF) and University of Alaska Southeast (UAS). This report summarizes the results of fish and habitat sampling completed in summer 2013. The goal of this field effort was to collect fish in KLGO and SITK to compare the relative levels of a suite of contaminants among fish species and among freshwater locations with four different characteristics: 1) glacial influence with anadromous fish present; 2) glacial influence without anadromous fish present; 3) non-glacial influence with anadromous fish present; and 4) non-glacial influence without anadromous fish present.

Minnow traps, beach seines, and hook and line capture techniques were employed in suitable habitats in four different rivers (Taiya River, Nourse River, West Creek, and the Indian River) over the span of 13 fishing days for a total of 3,747 trapping hours. Throughout this capture effort, Dolly Varden (*Salvelinus malma*), Coastrange sculpin (*Cottus aleuticus*), juvenile coho salmon (*Oncorhynchus kisutch*), rainbow trout (*Oncorhynchus mykiss*), an unknown juvenile salmonid, and spawning pink salmon (*Oncorhynchus gorbuscha*) were captured. A subset of individuals from those captured were euthanized and retained for contaminant analysis. We determined the location of apparent anadromous barriers on the Taiya River, West Creek, and the Indian River by observing the presence or absence of spawning salmon. Dolly Varden was the only species caught in each location (freshwater locations with the four different river characteristics), except above the apparent anadromous barrier on the Taiya River, thereby enabling a consistent comparison of fish biology and contaminant concentrations across sites and rivers. Coho and coastrange sculpin were caught in the Taiya and Indian rivers below the apparent anadromous barriers. Pink salmon were observed and caught from the Taiya and Indian rivers.

Length-at-age data was recorded in the lab, along with removal of the otoliths from each fish for age determination. Fish contaminant concentrations will be analyzed by fall 2014. The contaminant data, together with the ecological and length-at-age data generated from this field effort will be compiled and summarized into manuscripts for peer-reviewed publication in a fisheries journal and an ecotoxicology journal. In addition, this work will be used to enable a graduate student to complete their thesis for the completion of their Master of Science degree at the UAF.

2.2 Introduction

The National Park Service (NPS) Southeast Alaska Network (SEAN) is developing a long-term freshwater contaminant monitoring protocol for Glacier Bay National Park (GLBA), Klondike Gold Rush National Park (KLGO), and Sitka National Historical Park (SITK) in cooperation with partners at the University of Alaska Fairbanks (UAF) and University of Alaska Southeast (UAS). This report summarizes the results of fish and habitat sampling completed in 2013. The goal of this effort was to collect fish in KLGO and SITK to compare the relative levels of a suite of contaminants among fish species and among freshwater sites with four different characteristics 1) glacial influence with anadromous fish; 2) glacial influence without anadromous fish; 3) non-glacial influence with anadromous fish; and 4) non-glacial influence without anadromous fish.

With respect to many criteria, fish are an ideal biological medium (sentinel) to detect and monitor contaminant presence in the freshwater environment. Species with high lipid contents can incorporate lipophilic contaminants on a time scale ranging from months to years, and thus act as spatial and temporal integrators of bioavailable contaminants in a system (Ewald et al., 1998; Letcher et al., 2010; Zhang et al., 2001). Bioaccumulation and biomagnification processes increase the concentrations of many contaminants, making many easily detectable in tissues of fish and enabling consistent detection across the various analytical chemistry methods and classes of chemicals (Jewett & Duffy, 2007; Zhang et al., 2001). Collection and laboratory analysis of widely distributed and abundant fish species can be cost effective and efficient. Additionally, when comparing contaminant concentrations to fish consumption

advisory levels for humans and wildlife (Eagles-Smith et al., 2014), many of the studied fish species offer a relevant and direct comparison as important food items.

Contaminants analyses are underway and will be completed by the fall 2014. The results of this work will be used to support the development of standardized methodology and analysis techniques for comprehensive and efficient long-term freshwater contaminants monitoring within SEAN.

2.3 Methods

2.3.1 River description and selection

River selection for each park unit was based on locality specific criteria, which will be described in detail below. For more extensive descriptions of each river and watershed, see Sergeant and Johnson (2014).

2.3.1.1 Klondike Gold Rush National Historical Park

Three rivers or streams were sampled in or adjacent to KLGO: the Taiya River; the Nourse River; and West Creek. All three are glacially influenced, with documented annual salmon migrations. No sampling activities took place in the Skagway River, the only other major river present within KLGO, because it drains a different watershed from the Taiya River, does not currently host any long-term monitoring activities, and only the uppermost headwaters of the river are contained within the park (Figure 2.2).

2.3.1.1.1 Taiya River

The Taiya River (Figures 2.2 and 2.3) is approximately 25.7 km long, with a watershed of approximately 170 km^2 (Hood et al, 2006). It is currently the only river in the park with long-term monitoring activities (streamflow and water quality). The river flows south and it is almost entirely contained within park boundaries. The historic Chilkoot trail runs parallel to the Taiya River, providing ample opportunity for fish and habitat sampling. All Taiya River sites in our field sampling were accessed via the Chilkoot Trail. The proximity of the trail to the river ranges from mere centimeters to almost a

kilometer. The Chilkoot trail, road access, and a few structures along the last mile of the river are the full extent of human development along the Taiya River.

2.3.1.1.2 Nourse River

The Nourse River (Figure 2.2) originates from a large proglacial lake west of the park and flows south. It drains into the Taiya River approximately 14.5 km upstream from the mouth. The Nourse River is approximately 11 km long and drains a watershed of approximately 205 km^2 (Hood et al., 2006). Although the river traverses large portions of KLGO, it is not easily accessed. Fish and habitat sampling opportunities were limited. We accessed the Nourse River via the historic Chilkoot Trail, where we crossed the Taiya River on the suspension bridge at Canyon City, then hiked off-trail to reach the river.

2.3.1.1.3 West Creek

West Creek, which flows east and drains into the Taiya River approximately 5 km upstream from the mouth, is adjacent to the park. West Creek is approximately 13 km long, and drains a watershed of 115 km^2 (Hood et al., 2006). West Creek was accessed by walking from the West Creek road. This road turns west off the main Dyea Road and proceeds uphill, paralleling the creek. We were able to drive to within 300 m of each sampling site on the creek. Except for the road that parallels the creek, there is no other human development along the creek.

2.3.1.2 Sitka National Historical Park

2.3.1.2.1 Indian River

The Indian River is a 10-km-long mature river with a watershed encompassing approximately 32 km^2 (Moynahan et al 2008). It is the only river flowing through SITK. Long-term streamflow and water quality monitoring occur just upstream of park boundaries (Sergeant and Johnson 2014). The Indian River is not glacially influenced. It includes spawning and rearing habitat for anadromous salmon populations. The Indian River watershed has no lakes contained within its drainage boundaries (Moynahan et al., 2008). We accessed the river via the Indian River Trail. There are varying degrees of urban development

on all sides of the park, including city streets, residential development, water treatment facilities, an abandoned asphalt plant, a fish hatchery, and both personal and commercial boat use in nearby marine waters.

2.3.2 Fish species selected

Target species were selected by reviewing the existing literature on the fish fauna of the region and target drainages. The literature search included NPS surveys and reports, observations reported in peer-reviewed articles, and the NPS Certified Species List. Local residents, anglers, and NPS staff were also consulted. Based on the literature review and consultation, eight species were identified as potential study targets: Dolly Varden (*Salvelinus malma*), coho salmon (*Oncorhynchus kisutch*), pink salmon (*Oncorhynchus gorbuscha*), sockeye salmon (*Oncorhynchus nerka*), threespine stickleback (*Gasterosteus aculeatus*), ninespine stickleback (*Pungitius pungitius*), coastrange sculpin (*Cottus aleuticus*), and slimy sculpin (*Cottus cognatus*).

2.3.3 Permits, animal care and use authorizations

The project was permitted to collect eight different species of freshwater fish, varying in life stage, and quantity (e.g. 10 adult pink salmon from each river, 50 juvenile or adult Dolly Varden from each river, etc.; Alaska Department of Fish and Game permit SF2013-227, and NPS permits KLGO-2013-SCI-003 and SITK-2013-SCI-003). Collection, handling and euthanasia practices were approved by UAF IACUC permit 449319-3.

2.3.4 Sample site selection

Prior to the start of field work, a set of potential sampling sites were selected using the following criteria: 1) whether a site was above or below a known or hypothesized barrier to anadromous migration, and 2) the proximity of the site to the access road or trail. Long-term monitoring sites must have reasonable access for field crews to conduct work in an efficient and safe manner. The suitability of these

potential sites for long-term monitoring was further assessed on-site by considering habitat conditions such as terrestrial or aquatic vegetation, substrate, water depth, and streamflow.

Sample sites on the Taiya River and West Creek were upstream of some human development such as a campground and a short trail system, but the watershed is largely free of development. The lower portion of the Indian River is influenced by some human development, such as roads and bridges, residential areas, and a water diversion structure. Sampling sites on the lower, anadromous section of the Indian River spanned a range of urban development. Four sites were in the park and downstream of development, while two sites were approximately 300 meters upstream from any of the residential homes, streets, or other direct anthropogenic influences. Sites in the upper watershed were above an apparent anadromous barrier and absent of adult pink salmon during peak migration and spawning time periods.

2.3.5 Trapping and fish handling

Fish were trapped using Gees G-40 minnow traps (22.8 cm x 44.5 cm with 2.5 cm opening) baited with salmon eggs from sockeye salmon or pink salmon. Bait was placed in securely tied small cloth bags. Baited traps were deployed in water depths ranging from 0.3-2.0 m, and tied off to bank vegetation or rocks. Traps were labeled with a plastic tag listing the project, personnel involved, contact information, trap number, and all the applicable permit numbers. Stream characteristics (eddy, backwater, main channel, side channel, slough, lake, pond), habitat (vegetation, woody debris, etc.) and water information (color, odor, substrate type and color) were recorded. Pictures of each trap and the site were taken, along with site coordinates as determined by a handheld GPS device. Traps were left in the water for variable lengths of time based on access logistics. The contents of each trap were emptied into a 2-ga plastic bucket partially filled with river water. All of the fish in a trap were counted, identified to species (species identification was conducted on-site by qualified NPS personnel or a UAF fisheries biologist), then either euthanized and retained for analysis, or released unharmed. Fish lengths and mass were recorded post-thaw in a laboratory setting at the University of Alaska Fairbanks.

Fish that were retained for contaminant analysis were handled using Nitrile gloves, euthanized by blunt force trauma to the head (following reviewed and approved animal care protocol, UAF IACUC protocol #449319-3), immediately triple-wrapped in Ultra-Clean Supremium Aluminum Foil (VWR International; see Figure 2.1) and then placed inside Ziplock Freezer bags and placed in a -20°C freezer within 8 hours.

2.4 Results

Dolly Varden, coho salmon, coastrange sculpin, pink salmon, rainbow trout (*Oncorhynchus mykiss*), Pacific staghorn sculpin (*Leptocottus armatus*), and starry flounder (*Platichthys stellatus*) were caught during sampling efforts. Dolly Varden were caught in each river within each park unit.

2.4.1 Klondike Gold Rush National Historical Park

2.4.1.1 Taiya River

From July 25 to August 2, 2013, we placed 85 traps at 19 different sites, for a total sampling effort of 1,500 trap-hours across all sites (Table 2.1). Trapping effort at the thirteen sampling sites located downstream of an apparent anadromous barrier was 805 trap-hours. Trapping effort at the remaining six sites upstream of this apparent barrier was 691 trap-hours (Figures 2.2 and 2.3). We caught fish at 11 (85%) of the lower sites (Figure 2.3, downstream of the apparent barrier) and 0% of the higher sites (Figure 2.2, upstream of the apparent barrier). Dolly Varden were the most numerous (n=256), followed by coastrange sculpin (n=19), then by juvenile coho salmon (n=7). Some of these fish were retained for contaminant analysis: 14 Dolly Varden (mean weight [range] = 7.9 g [1.0-24.4 g], mean length = 87.5 mm [49.0-132.0 mm]); 19 coastrange sculpin (mean weight = 7.7 g [3.8-14.3 g], mean length = 84.8 mm [69.0-105.0 mm]); 7 juvenile coho (mean weight = 5.2 g [3.5-7.6 g], mean length = 76.9 mm [65.0-88.0 mm]).

During the sampling period, thousands of adult pink salmon were observed in the lower reaches of the river. We observed adult pink salmon as far upstream as Pleasant camp, at approximately mile 7 of

the Chilkoot Trail. Ten adult pink salmon were caught by hook and line in the lower reaches of the river on August 5 (mean weight = 1244 g [804-1700 g], mean length = 507 mm [465-560 mm]) and retained for contaminant analysis. Beach seines were also employed for 12 different sets at four sites on the lower Taiya River and the intertidal flats on August 2. Catch was minimal, consisting of six Dolly Varden, four coastrange sculpin, two Pacific staghorn sculpin, and one starry flounder, none of which were retained for contaminant analysis. No catch efforts are reported for the beach seine sampling effort. Habitat and general site information for each of the sites is located in Table 2.4.

2.4.1.2 Nourse River

From July 31 to August 1, we placed 13 traps at two different sites, for a total sampling effort of 246 trap-hours, (Table 2.2). We caught one Dolly Varden, which was not retained for analysis (no mass or length data recorded in the field) and no other fish. One site was located directly on the main channel of the river, which contained very few eddies in which to place traps, had very high velocity water, and did not appear likely to sustain juvenile salmonids. The second site was located in a shallow side channel that appeared to be suitable habitat for juvenile salmonids. However, due to strong diurnal changes in flows, the water dropped 20-30 cm overnight, and we did not catch any fish at that site. During the period of sampling, no adult salmon of any species were observed in the river. Habitat and general site information for each of the sites is located in Table 2.5.

2.4.1.3 West Creek

From July 25 to July 28, we placed 24 traps at five different sites, for a total sampling effort of 532 trap-hours, (Table 2.3). We caught fish at every site. Trapping effort at the three sites upstream of the apparent barrier was 420 trap-hours. Trapping effort at the two sites downstream of the apparent barrier was 112 trap-hours. Dolly Varden were present at every site and were the only species caught in West Creek (n=64). 36 Dolly Varden were retained for contaminant analysis (12 from downstream of the apparent barrier: mean weight = 5.8 g [1.9-11.7g], mean length = 80.2 mm [60-104 mm]. 24 from

upstream of the apparent barrier: 23.7 g [9.5-44.8g], mean length = 131.8 mm [97-162 mm]). During the period of sampling several adult pink salmon were observed in the lower reaches of the river, above and below the road crossing. Habitat and general site information for each of the sites is located in Table 2.6.

2.4.1.4 KLGO sampling summary

Sampling period

July 25 to August 2, 2013

Field participants

Andrew Cyr (field project lead, UAF graduate student), Chris Sergeant (SEAN ecologist), Andres Lopez (UAF assistant professor), Jessica Wilbarger (NPS physical science technician)

Sampling gear

Minnow traps, beach seine, hook and line

Access methods

Vehicle and foot

Sampling sites

20 sites sampled in Taiya River: 19 with minnow traps, 1 with beach seines and hook and line

4 sites sampled along the tidal flats of the Taiya River with beach seines

2 sites sampled with minnow traps in Nourse River

5 sites sampled with minnow traps in West Creek

2.4.2 Sitka Historical National Park

During the mid-August sampling period, pink salmon were observed migrating and spawning in the river. They were observed in great numbers in each pool and riffle for the length of the first 3-4 miles of the river. The water levels were low during the sampling period, which further concentrated the salmon. The river was accessible along the Indian River Trail, leading up to a waterfall near the headwaters, which marked the three most upstream sampling sites (7-9) of the project. We were able to follow the distribution of the adult pink salmon along the length of the river, and did not observe any at the most upstream sampling sites (7-9). Above Site 8, we found an apparent barrier (a 2-3 m high natural log jam with water trickling through the debris but not over the top). Site 9 was above a large waterfall approximately 20 m high. Except for one vandalized trap (removed from the water with dead fish inside), only permitted species were euthanized and retained for contaminants analysis, with one exception. One trap was vandalized during its deployment period. It was pulled from the water, causing mortality of several fish that had previously been captured. These mortalities were retained for contaminants analysis.

From August 14 to August 17, we placed 76 traps in 9 different sites, for a total sampling effort of 1,469 trap-hours (Table 2.7). One trap was vandalized during its deployment period. It was pulled from the water, causing mortality of several fish that had previously been captured. These mortalities were retained for contaminants analysis. We caught fish at all sites except Site 9, the most upstream sampling site and the only one upstream of a large waterfall. Dolly Varden were abundant at all sites that yielded fish (n=714). Coho salmon were present at the six lower sites (n=202), rainbow trout/cutthroat trout were present in four of the lowest six sites (n=83), and coastrange sculpin were present in low numbers in the lowest four sites (n=15). Some of the fish caught were retained for contaminant analysis: 54 Dolly Varden (mean weight = 17.9 g [0.8-52.8 g], mean length = 112.1 mm [46-174 mm]); 40 coho salmon (mean weight = 3.6 g [0.7-10.9 g], mean length = 65 mm [43-93 mm]); 4 rainbow trout (mean weight = 14.9 g [7.3-35.0 g], mean length = 104.3 mm [87-150 mm]); 15 coastrange sculpin (mean weight = 5.3 g [1.1-12.0 g], mean length = 76.9 mm [48-114 mm]); and 1 unknown salmonid (13.9 g; 110 mm). Ten adult

pink salmon were caught with hook and line at Site 5 on August 14 (mean weight = 1260 g [849-1542 g]; mean length = 490 mm [420-530 mm]). Habitat and general site information for each of the sites is presented in Table 2.8

2.4.2.1 SITK sampling summary

SITK sampling summary

Sampling period

August 14 to August 17, 2013

Field participants

Andrew Cyr (field project lead, UAF graduate student), Chris Sergeant (SEAN ecologist), Emily Noyd (University of Washington intern at SITK), Steve Bryan (NPS volunteer)

Sampling gear

Minnow traps, hook and line

Access methods

Vehicle and foot

Sampling sites

Nine sites sampled with minnow traps on Indian River, one of the nine sites also sampled with hook and line

2.5 Discussion

The field work conducted during the summer of 2013 contributed to knowledge of the presence and distribution of fish species across the rivers studied and was an important step to advance the freshwater contaminants monitoring program. The primary objective of identifying suitable sampling sites

and determining the presence and abundance of appropriate species was accomplished during this field session. Across both parks, one fish species, Dolly Varden, was collected from all rivers, including at locations above and below apparent anadromous barriers in two of the rivers. Several additional species were also caught and retained for contaminants analysis to provide additional qualitative information regarding detectable contaminants in these systems. In summary, we collected specimens from each of the four locations within the research question framework: glacial river, above anadromous barrier; glacial river, below anadromous barrier; non-glacial river, above anadromous barrier; non-glacial river, below anadromous barrier.

Additional objectives including exploring site access, study site selection, and validation of field collection methods as proof of principle were also met. Species presence and distribution data will be paired with future contaminant analyses to examine whether salmon and glacial melt influence contaminant concentrations within these freshwater biota.

2.6 Next steps

Lab work has been ongoing since completion of field work. At the time of preparation of this report, all fish have been processed through the preliminary stages of laboratory analysis. Each specimen has been photographed to validate species identification, and basic morphometric measurements have been taken and recorded (length and mass). Individual fish with uncertain species identification had fin clip samples removed for further genetic-based species identification. Due to anticipated inconsistencies in the content of and quality of sample preservation between individuals, all organs of the viscera were removed. Otoliths were extracted from all pink salmon, coho salmon, Dolly Varden and rainbow trout specimens, but not from the sculpins.

Dolly Varden lengths and masses varied greatly, suggesting the presence of more than one age cohort. This could directly affect the contaminants concentrations among individuals, with larger, older fish feeding at higher trophic levels and potentially having higher contaminants concentrations than

smaller, younger fish. Age estimation and classification could provide a method of standardization for contaminant concentrations assessment for a species. The possibility of completing carbon and nitrogen stable isotope analysis on muscle for a subsample of the fish will also be considered. This analysis could provide valuable insight into potential differences in trophic levels and feeding dynamics within species, between the different fish species, sample sites, and rivers.

Specimens will either be homogenized individually for larger fish or in pools of individuals for smaller fish. The homogenates will then be prepared for detection and quantification of a suite of inorganic (mercury, lead, arsenic, nickel, cadmium, copper, zinc) and organic contaminants (several PCBs, PBDEs, current-use and legacy pesticides, etc.) using Atomic Absorption spectroscopy (AA), a Direct Mercury Analyzer (DMA80), and Gas Chromatography - Mass Spectrometry (GC/MS).

Approximately 45 Dolly Varden samples were collected from three watersheds in GLBA in 2012 and will also be analyzed in the near future. These analyses may provide sufficient information to move forward with protocol development for Glacier Bay without additional sample collection.

2.7 Figures

Figure 2.1 - Photos demonstrating sample collection techniques using ultra-clean foil and nitrile gloves.

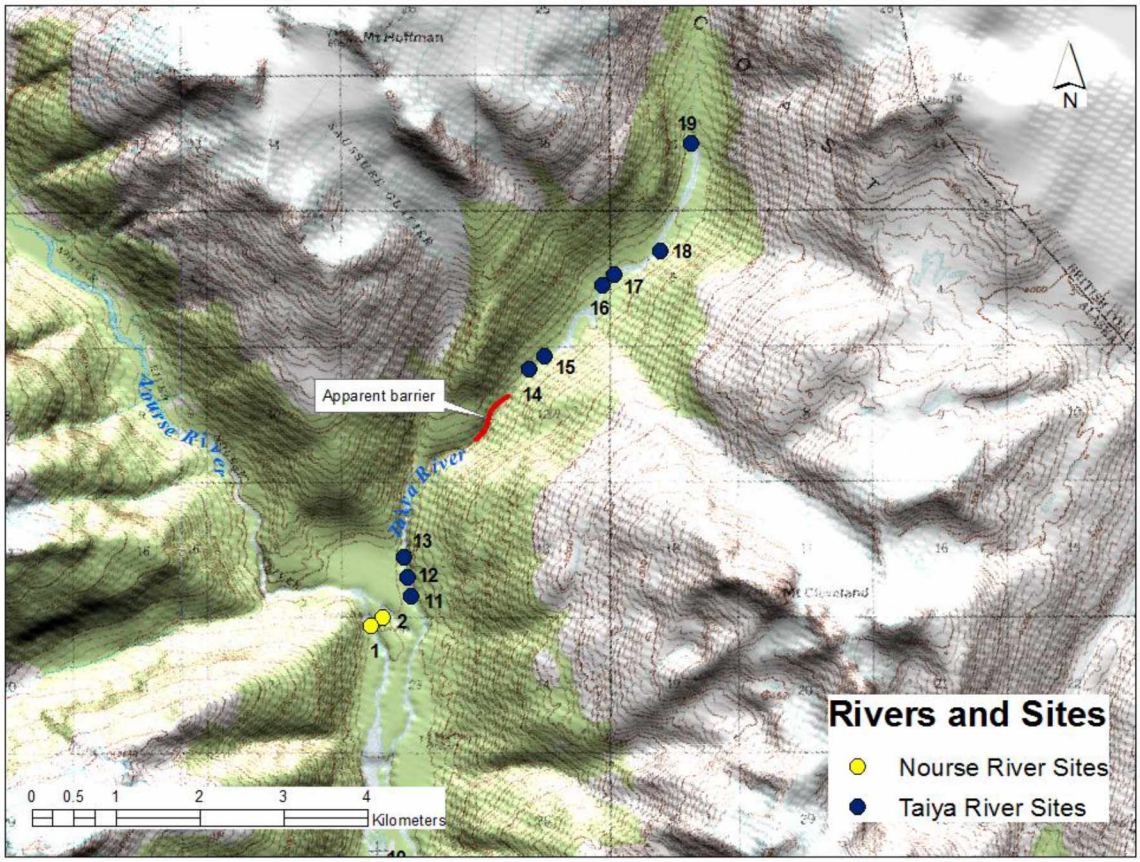

Figure 2.2 - Upper watershed sampling sites in KLGO, including Taiya (blue dots) and Nourse (yellow dots) Rivers.

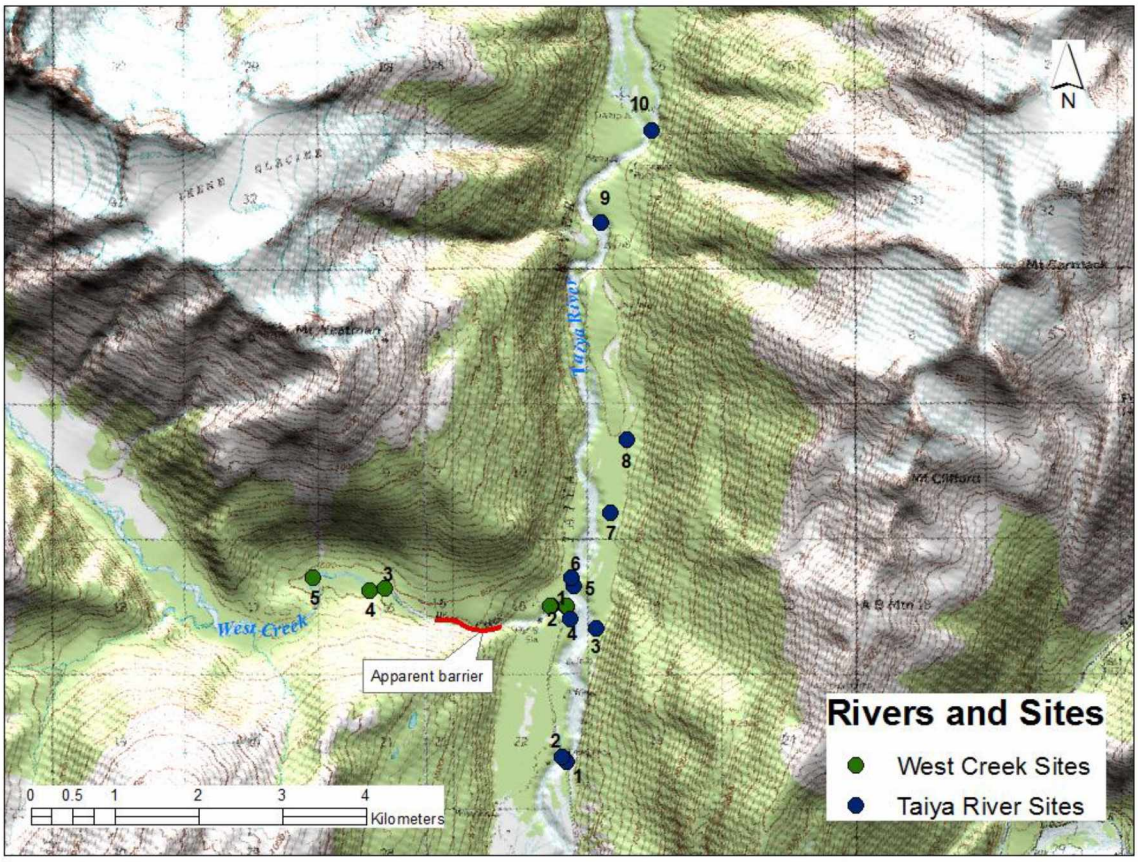

Figure 2.3 - Lower watershed sampling sites in KLGO, including Taiya River (blue dots) and West Creek (green dots).

Figure 2.4 - Representative photos of riverine habitat in KLGO (West Creek: *left picture*-above apparent barrier; *right picture*-below apparent barrier). Note the proximity of the glaciers to the study site, the density of the riparian vegetation, and the glacial silt color of the water.

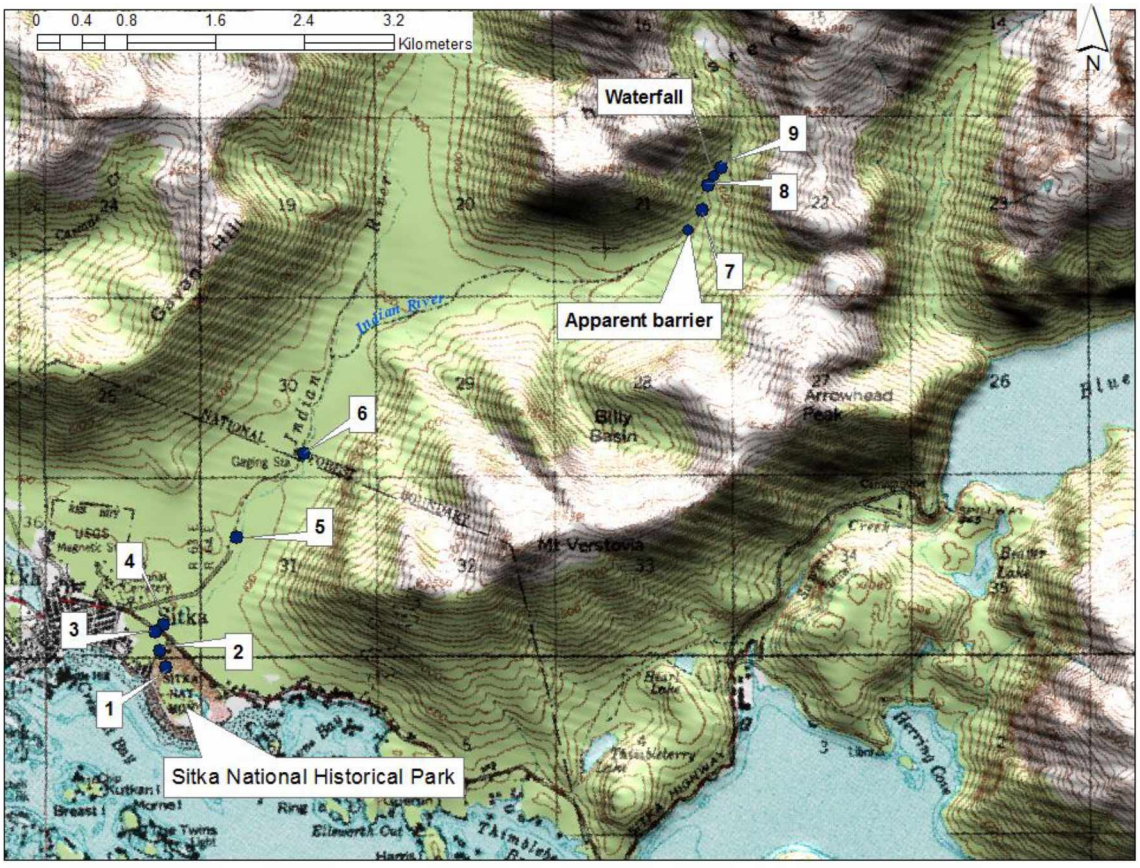

Figure 2.5 - Sampling site locations in Indian River (SITK).

2.8 Tables

Table 2.1 - Trapping effort, fish counts, and catch per unit effort (CPUE) at sample sites on the Taiya River in KLGO (July 25 to August 2, 2013).

				Dolly Varden		Coho		Coastrange Sculpin			
Site	Trap hr	# traps	Total trap hr	Count	CPUE[1]	Count	CPUE[1]	Count	CPUE[1]	Total count	Total CPUE
1	18.9	4	75.7	28	0.4	0	0.0	14	0.2	**42**	**0.6**
2	18.9	2	37.8	73	1.9	2	0.1	0	0.0	**75**	**2.0**
3	21.8	2	43.7	16	0.4	3	0.1	0	0.0	**19**	**0.4**
4	18.4	3	55.1	18	0.3	0	0.0	1	0.0	**19**	**0.3**
5	18.2	3	54.5	19	0.3	1	0.0	1	0.0	**21**	**0.4**
6	18.1	3	54.3	33	0.6	0	0.0	0	0.0	**33**	**0.6**
7	23.3	3	70.0	22	0.3	1	0.0	0	0.0	**23**	**0.3**
8	21.4	4	86.3	0	0.0	0	0.0	0	0.0	**0**	**0.0**
9	21.6	3	64.7	19	0.3	0	0.0	3	0.0	**22**	**0.3**
10	0.6	4	2.3	0	0.0	0	0.0	0	0.0	**0**	**0.0**
11	19.9	5	99.4	10	0.1	0	0.0	0	0.0	**10**	**0.1**
12	20.1	5	100.5	5	0.0	0	0.0	0	0.0	**5**	**0.0**
13	20.2	3	60.6	8	0.1	0	0.0	0	0.0	**8**	**0.1**
14	19.2	7	134.2	0	0.0	0	0.0	0	0.0	**0**	**0.0**
14 (2)	18.0	5	90.0	0	0.0	0	0.0	0	0.0	**0**	**0.0**
15	17.2	5	85.8	0	0.0	0	0.0	0	0.0	**0**	**0.0**
15 (2)	18.9	5	94.6	0	0.0	0	0.0	0	0.0	**0**	**0.0**
16	15.4	5	77.1	0	0.0	0	0.0	0	0.0	**0**	**0.0**
17	16.1	5	80.5	0	0.0	0	0.0	0	0.0	**0**	**0.0**
18	14.9	5	74.4	0	0.0	0	0.0	0	0.0	**0**	**0.0**
19	13.6	4	54.4	0	0.0	0	0.0	0	0.0	**0**	**0.0**

trapping effort: mean=71.2 hr/site; SD=27.4 hr; range=2.3 hr-134.2 hr

[1] CPUE = # fish per trap-hour fished

Table 2.2 - Trapping effort, fish counts, and catch per unit effort (CPUE) at sample sites on the Nourse River in KLGO (July 31 to August 1, 2013).

				Dolly Varden		Coho		Coastrange Sculpin			
Site	**Trap hr**	**# traps**	**Total trap hr**	**Count**	**CPUE[1]**	**Count**	**CPUE[1]**	**Count**	**CPUE[1]**	**Total count**	**Total CPUE**
1	19.60	3	58.8	1	0.0	0	0.0	0	0.0	**1**	**0.0**
2	18.70	10	187.3	0	0.0	0	0.0	0	0.0	**0**	**0.0**

[1] CPUE = # fish per trap-hour fished

Table 2.3 - Trapping effort, fish counts, and catch per unit effort (CPUE) at sample sites on West Creek in KLGO (July 25 to July 28, 2013).

				Dolly Varden		Coho		Coastrange Sculpin			
Site	**Trap hr**	**# traps**	**Total trap hr**	**Count**	**CPUE[1]**	**Count**	**CPUE[1]**	**Count**	**CPUE[1]**	**Total count**	**Total CPUE**
1	18.5	3	55.6	8	0.1	0	0.0	0	0.0	**8**	**0.1**
2	18.8	3	56.3	24	0.4	0	0.0	0	0.0	**24**	**0.4**
3	19.3	6	115.5	16	0.1	0	0.0	0	0.0	**16**	**0.1**
4	19.8	6	118.6	10	0.1	0	0.0	0	0.0	**10**	**0.1**
5	31.0	6	186.0	6	0.0	0	0.0	0	0.0	**6**	**0.0**

trapping effort: mean=106.4 hr/site; SD=54.0 hr; range=55.6 hr-186.0 hr

[1] CPUE = # fish per trap-hour fished

Table 2.4 - Site coordinates (WGS84) and descriptions for the Taiya River in KLGO.

Site	Latitude	Longitude	Barrier	Description
1	59° 30'42.7"	135° 20'48.5"	Below	Main channel of the Taiya River, at the road bridge, river left. Muddy and silty water with sand and boulder substrate (rip rap side banks).
2	59° 30'44.5"	135° 20'50.8"	Below	Main channel of the Taiya River, at the road bridge, river right. Muddy and silty water with sand and mucky substrate.
3	59° 31'30.0"	135° 20'27.3"	Below	Small back water channel of the Taiya River, with muddy and silty water, and some overhanging vegetation.
4	59° 31'37.3"	135° 20'45.6"	Below	Eddy in the main channel of the Taiya River, ~300 m downstream from confluence with West Creek. Muddy and silty water, with sand and gravel substrate. Both small and large woody debris, with overhanging bank vegetation.
5	59° 31'51.1"	135° 20'42.4"	Below	Main channel of the Taiya River, ~300 m upstream from confluence with West Creek. Muddy and silty water, with muck and sand substrate.
6	59° 31'51.7"	135° 20'42.8"	Below	Eddy in a side channel of the Taiya River, ~350 m upstream from the confluence with West Creek. Muddy and silty water, with muck and sand substrate. Large woody debris and overhanging vegetation.
7	59 32'18.7"	135 20'15.3"	Below	Small side channel of the Taiya River, muddy and silty water with overhanging vegetation.
8	59° 32'52.9	135° 19'59.9"	Below	Beaver pond complex, brown/red water, mucky substrate, large and small woody debris.
9	59° 34'08.9"	135° 20'14.6"	Below	Small, swift moving tributary to the Taiya River, silty water, sand and cobble substrate with overhanging vegetation.
10	59° 34'49.2"	135° 19'38.5"	Below	Small, slow side channel of Taiya River, at trail bridge crossing, mucky and leaf litter substrate, large woody debris and overhanging vegetation.
11	59° 36'38.4"	135° 19'40.0"	Below	Small eddies on the main channel of the Taiya River at the Canyon City bridge, muddy and silty water with cobble and boulder substrate, overhanging vegetation.
12	59° 36'46.1"	135° 19'44.8"	Below	Shallow water and small eddies on the main channel of the Taiya River ~0.5 km above Canyon City at base of the steps, sand and cobble substrate with overhanging vegetation.
13	59° 36'56.7"	135° 19'43.0"	Below	Small eddies on the main channel of the Taiya River ~1 km above Canyon City, ~50 m downhill, muddy and silty water with sand and cobble substrate, large woody debris and overhanging vegetation.
14	59° 38'08.8"	135° 17'56.6"	Above	Eddy in the main channel of the Taiya, 3.2 km above Canyon City. Silty water with cobble and boulder substrate, and overhanging vegetation.
15	59° 38'12.8"	135° 17'48.8"	Above	Log jam on a side channel of the Taiya River at Pleasant Camp. Silty water with mud and mucky substrate. Large and small woody debris.
16	59° 38'39.4"	135° 16'59.9"	Above	~Mile 12 of the trail (km 19.3), on a side channel of the Taiya River, at a log jam, muddy and silty water with sand and mucky substrate, large woody debris and overhanging vegetation.
17	59° 38'34.2"	135° 17'14.8"	Above	Main channel of the Taiya River, between mile 11 and 12 of the trail (km 17.7-19.3), muddy and silty water, large woody debris and overhanging vegetation.
18	59° 38'48.0"	135° 16'33.3"	Above	Small backwater eddy of the Taiya River, muddy and silty water, with overhanging vegetation.
19	59° 39'24.3"	135° 16'03.9"	Above	Small eddies on the main channel of the Taiya River directly in front of Sheep Camp ranger's station, muddy and silty water, cobble and boulder substrate.

Table 2.5 - Site coordinates (WGS84) and descriptions for the Nourse River in KLGO.

Site	Latitude	Longitude	Barrier	Description
1	59° 36'25.6"	135° 20'11.7"	Below	Small eddies on the main channel of the Nourse River, high velocity muddy and silty water with minimal overhanging vegetation.
2	59° 36'28.7"	135° 19'56.4"	Below	Small side channel of the Nourse River, muddy and silty water, sand and mucky substrate, overhanging vegetation. Strong diurnal flow rates. Channel was conveying 75% less water the following morning.

Table 2.6 - Site coordinates (WGS84) and descriptions for West Creek in KLGO.

Site	Latitude	Longitude	Barrier	Description
1	59° 31'42.7"	135° 20'52.6"	Below	Large eddy in the main channel of West Creek, ~100 m from the confluence with the Taiya River, muddy and silty water, sand and cobble substrate.
2	59° 31'43.7"	135° 20'56.7"	Below	Small eddies on main channel of West Creek, river left, ~50 m upstream of road bridge, muddy and silty water, sand and boulder substrate with overhanging vegetation.
3	59° 31'52.2"	135° 23'26.2"	Above	Small backwater eddy of the main channel of West Creek, muddy and silty water, sand and mucky substrate with overhanging vegetation.
4	59° 31'49.7"	135° 23'05.9"	Above	At West Creek foot bridge, main channel, muddy and silty water, cobble and boulder substrate with overhanging vegetation.
5	59° 31'53.1"	135° 24'01.2"	Above	Near the end of the road along West Creek, muddy and silty water, sand, cobble and mucky substrate with small woody debris and minimal overhanging vegetation.

Table 2.7 - Trapping effort, species counts, and catch per unit effort (CPUE) at sample sites on the Indian River in SITK (August 14 to August 17, 2013).

				Dolly Varden		Coho		Rainbow trout		Coastrange Sculpin			
Site	Trap hr	# traps	Total trap hr	Count	CPUE[1]	Count	CPUE[1]	Count	CPUE[1]	Count	CPUE[1]	Total count	Total CPUE
1	24.3	5	121.3	27	0.2	52	0.4	22	0.2	1	0.0	**102**	**0.8**
2	22.8	4	91.2	5	0.1	3	0.0	0	0.0	4	0.0	**12**	**0.1**
3	22.2	4	88.7	74	0.8	2	0.0	30	0.3	1	0.0	**107**	**1.2**
4	10.0	10	100.0	121	1.2	12	0.1	12	0.1	9	0.1	**153** [2]	**1.6**
5	22.2	15	333.5	147	0.4	129	0.4	10	0.0	0	0.0	**286**	**0.9**
6	18.0	10	180.0	85	0.5	4	0.0	9	0.1	0	0.0	**97**	**0.5**
7	19.8	8	158.3	56	0.4	0	0.0	0	0.0	0	0.0	**56**	**0.4**
8	20.1	15	300.8	199	0.7	0	0.0	0	0.0	0	0.0	**199**	**0.7**
9	19.1	5	95.3	0	0.0	0	0.0	0	0.0	0	0.0	**0**	**0.0**

trapping effort: mean=163.2 hr/site; SD=93.1 hr; range=88.7 hr- 333.5 hr

1 CPUE = # fish per trap-hour fished

2 1 unknown fish caught at Site 5, possibly a cutthroat trout

Table 2.8 - Site coordinates (WGS84) and descriptions for the Indian River in SITK.

Site	Latitude	Longitude	Barrier	Description
1	57° 02'59.7"	135° 19'03.6"	Below	~300 meters downstream of road bridge, within SITK park boundaries. Site was dominated by cobble and gravel with some small boulders, and large woody debris.
2	57° 03'02.6"	135° 19'04.2"	Below	~100 meters downstream of road bridge, within SITK park boundaries. Site was dominated by cobble and gravel with some small boulders.
3	57° 03'07.7"	135° 19'07.7"	Below	Just below road bridge, within SITK park boundaries. Site was dominated by cobble and gravel with some small boulders.
4	57° 03'10.0"	135° 19'03.0"	Below	Site of downstream water quality meter and stream gauge, 50 meters above road bridge. Site was dominated by cobble and gravel with some small boulders, large woody debris, and overhanging vegetation.
5	57° 03'34.9"	135° 18'24.1"	Below	200 meters above "urban influence", above location of the stream diversion and the end of city streets. Site was dominated by cobble and gravel with some small boulders, and large woody debris.
6	57° 04'03.0"	135° 17'44.1"	Below	At location of upstream stream gauge, ~2.4 km upstream from bridge. Site was dominated by cobble and gravel with some small and large boulders, numerous pieces of large woody debris, and overhanging vegetation.
7	57° 05'15.0"	135° 14'11.5"	Above	~300 meter below waterfall, no pink salmon observed here. The river was small here, with many small pools, and overhanging vegetation. The site was dominated by cobble and gravel with abundant small boulders and both large and small woody debris.
8	57° 05'17.1"	135° 14'12.8"	Above	At, and below waterfall, above a clear anadromous barrier, no pink salmon observed here. The river was very small here, with little water conveyance, many small pools, and overhanging vegetation. The site was dominated by cobble and gravel with abundant small boulders and both large and small woody debris.
9	57° 05'21.5"	135° 14'09.4"	Above	10-15 meters above the waterfall, no pink salmon observed here. The river was very small, dominated by tangled woody debris with a bare rock and gravel substrate.

2.9 Works Cited

Eagles-Smith, C.A., Willacker, J.J., Flanagan Pritz, C.M., 2014, Mercury in fishes from 21 national parks in the Western United States- Inter and intra-park variation in concentrations and ecological risk: U.S. Geological Survey Open- File Report 2014-1051.

Ewald, G., Larsson, P. E. R., Linge, H., Okla, L., & Szarzi, N. 1998. Biotransport of Organic Pollutants to an Inland Alaska Lake by Migrating Sockeye Salmon (Oncorhynchus nerka). Arctic 51(1):40–47.

Hood, E., Eckert, G., Nagorski, S., & Talus, C. 2006. Assessment of Coastal Water Resources and Estuarine Conditions in Klondike Gold Rush National Historical Park, Alaska. Technical Report NPS/NRWRD/NRTR-2006/349.

Jewett, S. C., & Duffy, L. K. 2007. Mercury in fishes of Alaska, with emphasis on subsistence species. The Science of the Total Environment 387(1-3):3–27.

Letcher, R. J., Bustnes, J. O., Dietz, R., Jenssen, B. M., Jørgensen, E. H., Sonne, C., … Gabrielsen, G. W. 2010. Exposure and effects assessment of persistent organohalogen contaminants in arctic wildlife and fish. The Science of the Total Environment 408(15):2995–3043.

Moynahan, B. J., Johnson, W. F., Schirokauer, D. W., Sharman, L. C., Smith, G., & Gende, S. 2008. Vital Signs Monitoring Plan: Southeast Alaska Network. Natural Resource Report NPS/SEAN/NRR-2008/059. National Park Service, Fort Collins, Colorado.

Sergeant, C. J. and W. F. Johnson. 2014. Southeast Alaska Network freshwater water quality monitoring program: 2013 annual report. Natural Resource Technical Report NPS/SEAN/NRTR—2014/840. National Park Service, Fort Collins, Colorado.

Zhang, X., Naidu, A. S., Kelley, J. J., Jewett, S. C., Dasher, D., & Duffy, L. K. 2001. Baseline concentrations of total mercury and methylmercury in salmon returning via the Bering Sea (1999-2000). Marine Pollution Bulletin 42(10):993–997.

Chapter 3 - **Assessing the influence of migration barriers and feeding ecology on total mercury concentrations in Dolly Varden (*Salvelinus malma*) from a glaciated and non-glaciated stream** [3]

[3]Cyr, A., Sergeant, C., López, J.A., O'Hara, T. 2017. Assessing the influence of migration barriers and feeding ecology on total mercury concentrations in Dolly Varden (*Salvelinus malma*) from a glaciated and non-glaciated stream. Science of the Total Environment. 580: 710-718. DOI: 10.1016/j.scitotenv.2016.12.017

3.1 Abstract

Assimilation of mercury (Hg) into food webs is directly influenced by ecological factors such as local habitat characteristics, species feeding behavior, and movement patterns. Total Hg concentrations ([THg]) in biota from Subarctic latitudes are driven both by broad spatial processes such as long-range atmospheric transport and more local influences such as biovectors and geology. Thus, even relatively pristine protected lands such as national parks are experiencing Hg accumulation. We analyzed [THg] and stable isotopes of carbon ($\delta^{13}C$) and nitrogen ($\delta^{15}N$) in 104 Dolly Varden (*Salvelinus malma*) collected from two rivers in southeastern Alaska, upstream and downstream of apparent anadromous migration barriers in watersheds with and without glacial coverage. To assess the potential magnitude of marine-derived THg returning to freshwater, we analyzed [THg] in ten adult pink salmon from each study system. There were no differences in Dolly Varden mean [THg] between sites after the data were standardized for fork length, but unadjusted [THg] varied relative to fish size and $\delta^{15}N$ values. While previous studies generally show that [THg] increases with higher $\delta^{15}N$ values, we found that Dolly Varden below migration barriers and foraging on salmon eggs had the highest $\delta^{15}N$ values among all sampled individuals, but the lowest [THg]. Dolly Varden residing below anadromous barriers had $\delta^{13}C$ values consistent with marine influence. Since salmon eggs typically have low [Hg], our results suggest that abundant salmon populations and the dietary subsidy they provide may reduce the annual exposure to [Hg] in egg-eating stream fishes such as Dolly Varden. In addition to identifying a suitable species for freshwater Hg monitoring in southeastern Alaska, our study more broadly implies that river characteristics, location within a river, fish size, and feeding ecology are important factors influencing Hg accumulation.

3.2 Introduction

The assimilation of mercury (Hg) into food webs is directly influenced by ecological factors such as local habitat characteristics, community composition, species' movement patterns, and feeding behavior (Downs et al., 1998; Jarman et al., 1996; Riget et al., 2000; Tran et al., 2015; and Zhang et al., 2001). In aquatic food webs, geologic and atmospherically transported Hg commonly enters food webs after it has been methylated (Wiener et al., 2013). It is estimated that more than 90% of Hg accumulates in upper trophic level fishes as monomethyl Hg ($MeHg^{+}$), a bioavailable and toxic form of Hg (Boening, 2000; Wang, 2012). Diadromous fish species, which migrate between freshwater and marine waterbodies, cross habitats and dynamic prey guilds with total Hg concentrations ([THg]) that vary over time and space (Evans et al., 2005; Riget et al., 2000; Tran et al., 2016). Generally, Hg bioaccumulates in individuals as they age and biomagnifies with increasing trophic level (Macdonald et al., 2002; Watras et al., 1998).

Total Hg concentrations in biota from Arctic and Subarctic latitudes are often driven by broad spatial processes (AMAP, 2011; Engstrom and Swain, 1997; Jaeglé, 2010). Mercury and other contaminants are subject to long-range atmospheric transport (LRAT), moving from warm environments to colder environments, and can ultimately accumulate via wet or dry deposition where they were neither produced nor used (Galloway et al., 1982; Macdonald et al., 2002). For example, despite recent declines in atmospheric Hg concentrations in North America (AMAP, 2011; Zhang et al., 2016), Hg accumulation is increasing in some high latitude sediments and biota (Engstrom and Swain, 1997; Drevnick et al., 2016). This phenomenon is thought in part to be the result of mercury transported from emissions from Asia (AMAP, 2011; Jaeglé, 2010). The northwestern coast of North America lies directly in the path of eastward air and ocean currents originating from Asia (Jaeglé, 2010). Local influences such as mining activities, geothermal activity, and the amount of wetland coverage can also introduce and transport Hg to freshwater environments on a smaller, regional scale (AMAP, 2011; Drevnick et al., 2016; Nagorski et al., 2014).

Due to the large spatial and temporal scales associated with LRAT, even organisms in remote and relatively pristine protected lands such as national parks accumulate Hg (Eagles-Smith et al., 2016). However, trends within some regions are increasing, while others are decreasing; thus, monitoring must be scaled appropriately to determine local landscape and ecological mechanisms that likely drive Hg bioaccumulation (AMAP, 2011). In southeastern Alaska, where our study was conducted, protected lands include some of the largest remaining icefields and most abundant salmon populations in the world. Previous research has demonstrated that glaciers have potentially important effects on local [THg] in freshwater ecosystems (Nagorski et al., 2014). Atmospherically transported Hg can become trapped in glacial ice after precipitation (Faïn et al., 2008; Faïn et al., 2009; Zheng et al., 2008) and later released during ablation, entering directly into the downstream ecosystem and potentially impacting a number of aquatic species, including Pacific salmon (*Onchorhynchus spp.*) (Bizzotto et al., 2009; Blais et al., 2001; Bogdal et al., 2009).

Migrating adult Pacific salmon are significant biovectors of marine-derived Hg to rivers and lakes in which they spawn (Baker et al., 2009; Blais et al., 2007; Krümmel et al., 2005, 2009). This transport of Hg from the marine environment to freshwater environments is in addition to Hg that is already present at background levels from geologic or atmospheric inputs. Depending on the species, approximately 95% or more of an anadromous salmon's growth occurs in the marine environment (Quinn et al., 2005; Zhang et al,. 2001), representing years of marine-derived Hg exposure and tissue accumulation. Salmon often densely congregate on spawning grounds by the thousands, releasing marine-derived contaminants during excretion, egg deposition, and decomposition. In smaller rivers, where species such as pink (*O. gorbuscha*) and chum salmon (*O. keta*) typically inhabit the lowest reaches of a river, and populations can include hundreds of thousands of fish, anadromous salmon can represent a disproportionately high input of marine-derived $MeHg^{+}$ relative to geologic or atmospheric input over these small spatial scales (Baker et al., 2009; Blais et al., 2007; Zhang et al., 2001). Sockeye salmon (*O. nerka*) returning to rivers and

lakes in Bristol Bay, Alaska transported approximately 21 kg of $MeHg^+$ over a 20-year period (Zhang et al., 2001).

When assessing Hg status of an ecosystem, it is important to choose appropriate monitoring targets. Many fish species offer several advantages over other taxonomic groups for assessing Hg status in the aquatic environment in part because of their ability to integrate Hg into their tissues over space and time. Dolly Varden (*Salvelinus malma*, hereafter "DV") in southeastern Alaska exhibit suitable traits that offer the potential to learn about contaminants and ecological links across regions and habitat types. DV forage opportunistically, integrating diverse components of freshwater and marine food webs including insects, salmon eggs, and small fish (Armstrong 1965, 1974; Tran et al., 2016). Isolated, resident, and anadromous populations occur below and above anadromous migration barriers and in streams with and without glacial influence (Armstrong, 1991; Cyr et al., 2014). The species' broad spatial distribution and diverse life history strategies provide an opportunity to explore the importance of glaciers, barriers to anadromous migration, and spawning salmon on Hg accumulation. Additionally, because DV are abundant, easily captured, long-lived, and feed at a relatively high trophic level, they are ideal candidates for assessing Hg trends and differences between rivers and locations, and can provide important survey design insights for long-term contaminants monitoring and research. Stable isotopes of nitrogen ($\delta^{15}N$) and carbon ($\delta^{13}C$) in DV tissue can further illuminate their feeding ecology and other potential mechanisms influencing Hg accumulation. The ratio of heavy to light isotopes of carbon and nitrogen changes in a predictable manner as prey items are consumed and assimilated into tissues (Fry, 2006).

Here, we present [THg] in DV collected above and below anadromous migration barriers in streams with and without glacial watershed coverage in southeastern Alaska. We analyzed $\delta^{15}N$ and $\delta^{13}C$ to estimate trophic position and degree of marine influence on diet. We explored four hypotheses: (1) [THg] increases with DV length; (2) glacial discharge from West Creek increases [THg] in DV; (3) spawning salmon transport of marine-derived Hg to freshwater systems increases [THg] in DV; and (4) [THg] increases with increasing $\delta^{15}N$ isotope values.

3.3 Methods

3.3.1 Study sites and fish sampling.

In July and August 2013, we collected DV from West Creek and the Indian River, both located in coastal southeastern Alaska, a region characterized by a wet maritime climate, steep, glacially formed topography, and temperate rainforest lowlands (Gallant et al., 1995). West Creek is a tributary to the Taiya River, which flows through Klondike Gold Rush National Historical Park near Skagway, Alaska and drains into Taiya Inlet, an extension of northern Lynn Canal (Figure 3.1). West Creek is approximately 13 km long and drains an area of 115 km^2 with 29% glacial watershed coverage (National Hydrography Dataset at http://nhd.usgs.gov; Randolph Glacier Inventory 5.0 at http://www.glims.org/RGI/). The watershed is located in the mountains west of the national park border, and remains largely undeveloped (no paved roads, infrastructure, effluent release, etc.). A waterfall at river km 1.2 with a vertical rise of approximately 70 m over a 900 m horizontal distance is an apparent barrier to anadromous migration (USGS National Map Viewer at http://viewer.nationalmap.gov/viewer/; Figure 3.1).

The non-glacial Indian River is 19.8 km long and drains an area of 31 km^2 (Sergeant and Nagorski, 2015). The watershed is located near Sitka, Alaska (Figure 3.1) and has moderate development from the mouth upstream to approximately river km 2.4. While the lower 0.8 km flows through Sitka National Historical Park, the majority of the upper Indian River watershed remains undeveloped and within the Tongass National Forest. Pink salmon comprise >95% of annual salmon spawning activity in the river (Stark et al., 2012), with the remainder consisting mostly of chum and coho (*O. kisutch*) salmon. In 2013, the peak daily count of spawning pink salmon was approximately 295,000 on August 9 (Stopha, 2015). A series of logjams of approximately 2 m in height beginning at river km 7.5 in the eastern fork of the river was an apparent barrier to anadromous migration (Figure 3.1).

In both systems, actively migrating and spawning pink salmon were observed below the apparent migration barriers, but not above them. Above the barriers, we observed no previous evidence of

spawning activity such as disturbed gravel or salmon carcasses. DV collection sites were selected above and below anadromous migration barriers (Figure 3.1). All sites were located upstream of any significant anthropogenic development. DV were collected using Gees G-40 minnow traps (23 cm width x 44.5 cm length x 2.5 cm opening on each end). Traps were baited with sockeye (*O. nerka*) or pink salmon eggs washed in a 1/100 Betadine solution to minimize microbial contamination, deployed in a cloth sack. Traps were deployed in water depths of 0.3-2.0 m for 45 minutes to 24 hours depending on access logistics. Adult pink salmon from the Indian River were caught by hook and line angling to assess the potential magnitude of marine-derived Hg delivered to the river. DV and adult pink salmon retained for contaminant analysis were handled at all times using Nitrile gloves, euthanized by blunt force trauma to the head, wrapped in Ultra-Clean Supremium Aluminum Foil (VWR International), and frozen at -20°C within eight hours of field collection and remained frozen until fish tissue preparation in the laboratory.

Research activities were permitted by Alaska Department of Fish and Game Fish Resource Permit SF2013-227, University of Alaska Fairbanks Institutional Animal Care and Use Committee permit 449319-3, and National Park Service Research Permits KLGO-2013-SCI-003 and SITK-2013-SCI-003.

3.3.2 Fish tissue preparation

DV were removed from the foil wrapping and rinsed with ultrapure water. Fork length (mm) and wet mass (g) were recorded and viscera removed. When possible, both sagittal otoliths were removed, rinsed with ultrapure water, air dried and used for age estimation. Small DV (<13 g) of similar length were pooled to obtain a minimum sample mass of approximately 13 g. DV >13 g were analyzed individually. For pink salmon, approximately 5 g of muscle was removed from the left side between the dorsal and anal fins. Fish and tissue samples were homogenized using liquid nitrogen and a stainless steel mortar and pestle. Approximately 4 g of sample material were reserved for THg and C and N stable isotope analyses. Samples were freeze dried (Labcono, FreeZone 4.5 Liter) for a minimum of 48 h to remove all moisture.

3.3.3 Total mercury (THg) analysis

Samples were analyzed using a Milestone DMA-80 instrument, U.S. EPA method #7473-EPA30B, 2007 SW 846, and reported as ng/g wet weight (ww), using the percent water calculated from samples during the drying process (Harley et al., 2015; Knott et al., 2011; McHuron et al., 2014). The method detection limit for THg determination in whole fish homogenate and fish muscle was 12.5 ng/g. Quality assurance and quality control measures were based on method blanks, Standard Reference Materials (SRMs) of similar matrices, and check standards. All samples were run in triplicate, averaged, then any sample with a coefficient of variation >10% was re-analyzed until <10% was reached. The SRMs used were DORM-4 (National Resource Council Canada; 0.410 ± 0.055 mg/kg), DOLT-4 (Dogfish liver, National Resource Council Canada; 2.58 ± 0.22 mg/kg), and Lake Superior Fish (LSF, National Institute of Standards and Technology, Standard Reference Material® 1946; 0.433 ± 0.009 mg/kg ww). Mean percent recoveries (± SD) for each SRM were: 100 µg/kg (liquid standard), 99.3 ± 3.3%; DOLT-4, 105.3 ± 7.4%; DORM-4, 97.8 ± 3.6%; LSF, 103.8 ± 7.05%.

3.3.4 Carbon and nitrogen stable isotope analysis

Analysis of C and N stable isotopes were performed by the Alaska Stable Isotope Facility at the University of Alaska Fairbanks on 0.2-0.5 mg of freeze-dried samples prepared as described above (Knott et al., 2011; McGrew et al., 2014). Stable isotope data were obtained using continuous-flow isotope ratio mass spectrometry (CFIRMS) performed on a Thermo DeltaVPlus interfaced with a Costech ESC 4010 elemental analyzer using a ConfloIV system. Reference checks (Peptone: No. P-7750 meat based protein. Sigma Chemical Company, Lot #76f-0300) were run every 10th sample, and blanks were run every 20th sample. Stable isotope ratios were reported in δ notation as parts per thousand (‰) deviation from the international standards Vienna PeeDee Belemnite (VPDB, carbon) and AIR (nitrogen). Instrument precision is typically <0.2 ‰ for both carbon and nitrogen. The formula for calculating the isotope ratios is as follows:

$$\delta^{H}X = \frac{R_{Sample} - R_{Standard}}{R_{Standard}} * 1000 \text{ (Equation 3.1).}$$

Where *X* is the element of interest, *H* is the heavy isotope mass of that element, and *R* is the ratio of the heavy to light isotope measured for that element, *Sample* is the sample of interest, and *Standard* is the standard used, VPDB or AIR.

The presence of lipids, which are depleted in $\delta^{13}C$ relative to protein and carbohydrates, can affect stable isotope analysis by lowering the $\delta^{13}C$ enrichment signature (DeNiro and Epstein, 1977). Our C:N ratios were above the acceptable threshold of >3.7, and different between sites, indicating the need for lipid content correction based on Hoffman and Sutton (2010):

$$\delta^{13}C_{Extracted} = 0.42 * (\delta^{13}C_{Bulk}) - 9.92 \text{ (Equation 3.2).}$$

3.3.5 DV otolith estimation

When extracted and preserved successfully from an individual DV, the right sagittal otolith was mounted on a glass slide using Crystalbond thermoplastic glue perpendicular to the long axis. Each otolith was ground to the nucleus using a thin-section machine (Hillquist, Inc. Denver, Colorado), then remounted to the slide with the ground portion lying flat on the slide, and ground down to a final thickness of approximately 0.30 mm and hand polished with 1-µm diamond grit sandpaper. Each otolith was viewed under a compound microscope at 10X power with polarized light transmitted through the slide. Digital photographs were taken of each otolith and ages estimated by two independent readers provided with date of capture and fork length of each DV. Annuli were identified by alternating zones of opaque and hyaline zones (DeVries and Frie, 1996). To increase certainty of age estimates, we additionally aged left sagittal otoliths while viewed on a backlit dissecting microscope and immersed in a 10% solution of Liquinox (Heiser, 1966). Annuli were identified by the same methods described above. If a discrepancy between our independently estimated ages existed for an individual fish, we selected the age calculated for the majority of the estimated ages.

3.3.6 Statistical analysis

All analyses were performed using R statistical computing software, version 3.2.1 (R Core Team, 2015). To evaluate the ability of five predictor variables (individual river system, fish location relative to anadromous migration barrier, fish length, $\delta^{15}N$, and lipid-corrected $\delta^{13}C$) to estimate unadjusted [THg] in individual DV, multiple linear regression and an information-theoretic model selection process were employed (Burnham and Anderson, 2002). Thirty-two linear regression models were compared that included every combination of the five predictor variables and the intercept-only null model. Model support was determined by Akaike's information criteria bias-corrected for small samples (AICc).

We calculated ΔAICc, Akaike weights (w_i) and evidence ratios to improve our ability to distinguish the best approximating models for [THg] (Burnham and Anderson, 2002). ΔAICc is calculated by subtracting the lowest AICc across all models from each model's AICc. Models with ΔAICc <2 are considered to perform similarly to the best model (Burnham and Anderson, 2002). Values for w_i range from zero to one and can be interpreted as the probability that model i is the best model for approximating [THg] across all candidates (Johnson and Omland, 2004). Higher w_i values indicate better support for a given model. Evidence ratios were calculated for all models using w_1/w_i, where w_1 is the Akaike weight for the top model. Although no specific threshold indicates a statistically significant difference between models, evidence ratios ≥3 represent relatively low support for a model (Burnham and Anderson, 2002). Considered in combination, ΔAICc, w_i, and evidence ratios provide an indication of how well or how poorly each model fits the given set of observations, allowing selection of the best model.

To estimate the relative importance of each predictor variable j, w_i were summed across all models in the set that included variable j. Each variable was ranked by this sum of Akaike weights ($w_+(j)$) to determine the order of importance for each variable in estimating [THg] in individual DV across all possible models (Burnham and Anderson, 2002).

We assessed relationships between [THg] and individual variables using a combination of linear regression, ANOVA, and graphical analysis. Results were considered significant at $\alpha \leq 0.05$. Before performing linear regression and ANOVA, all data were checked for normality and heteroscedasticity using QQ-normal plots and the Breusch-Pagan test. We calculated 95% elliptical confidence bound using R package 'ggplot2' to illustrate differences between each sampling site categories for carbon and nitrogen stable isotope relationships (Fox and Weisberg, 2011).

To account for any size-selection bias during field collections (allometric effects), and to compare [THg] within and among sites while controlling for length, we calculated length-standardized [THg] (Fleming and Gross, 1990; Tran et al., 2016):

$$M_i = MO_i * (\frac{L}{LO_i})^b \text{ (Equation 3.3).}$$

Where M_i is the adjusted $\log_{10}$ [THg] for the ith fish, MO_i is observed $\log_{10}$ [THg] for the ith fish, L is the mean fork length for all fish caught (110 mm), LO_i is the observed length of the ith fish, and b (0.645) is the slope of the $\log_{10}$ [THg] on $\log_{10}$ fork length across all fish.

3.4 Results

3.4.1 Descriptive overview

A total of 104 DV were sampled for THg and C and N stable isotopes analyses. Of the total samples, 66 (63.5% of samples) were large enough (>13 g) for individual tissue analyses (Supplementary Figure 3.1). The remaining 38 DV (35%) were combined into 11 separate groups for pooled tissue analyses (Table 3.1; Supplementary Table 3.1). Individuals within each pooled sample were similar in size and age; fork length standard deviations (SDs) for pooled samples ranged from 0-10 mm, while age SDs range from 0-0.7 years (Supplementary Table 3.1), so we considered these pooled samples to be appropriate surrogates for individuals and included them in all analyses. Among the DV sampled, fork length, mass, age, and [THg] varied across rivers and above and below anadromous migration barrier

sampling sites (Table 3.1). For all DV, mass and fork length ranged from 0.8 to 52.8 g (mean = 16.5 g ± 12), and 46 to 174 mm (mean = 110 mm ± 31), respectively. In general, larger and older DV with higher [THg] were captured above anadromous migration barriers (Table 3.1). Unadjusted [THg] for individuals and pooled samples ranged from 6 to 53 ng/g wet weight (ww) (geometric mean ± SD = 22 ng/g ww ± 1.5), and length-standardized $\log_{10}$[THg] ranged from 0.64 to 2.15 ng/g ww (mean ± SD = 1.28 ± 0.22). Values for $\delta^{15}N$ ranged from 3.24 to 11.80‰ (mean ± SD = 6.76 ± 2.74), while values for lipid-corrected $\delta^{13}C$ ranged from -22.67 to -19.69‰ (mean ± SD = -21.15 ± 0.89).

3.4.2 Modeling [THg] using Dolly Varden length, watershed characteristics, $\delta^{15}N$, and $\delta^{13}C$

Based on ΔAICc values, Akaike weights (w_i) and evidence ratios, four models were considered the best candidates for predicting [THg] in DV (Adj. r^2 = 0.486-0.491; Table 3.2; Supplementary Table 3.2). The top two models (Length + $\delta^{15}N$; and River + Length + $\delta^{15}N$) were two to three times more likely to be the best approximating model compared to the next two (Table 3.2). Out of the five predictor variables, only lipid-corrected $\delta^{13}C$ was not included in any of the best explanatory models. Fish length and $\delta^{15}N$ were clearly the most important predictors of [THg] in DV ($w_{+(j)}$ = 0.999 and 0.937, respectively), while fish location relative to anadromous barrier and individual river system had a moderate weight of support (Table 3.3).

3.4.3 Mean [THg] by fish and watershed characteristics

Across all sampled sites, unadjusted [THg] for all DV increased significantly with fork length, but fork length explained a relatively low proportion of overall variability (linear regression, r^2 = 0.27, P << 0.001; Figure 3.2). Neither river nor location relative to barrier had an independent influence on mean length-standardized $\log_{10}$[THg] (two-way ANOVA, barrier: $F_{(1,73)}$ = 0.38, P = 0.54; river: $F_{(1,73)}$ = 0.50, P = 0.48). However, the interaction of river and barrier was significant ($F_{(1,73)}$ = 4.71, P = 0.03). Within each sampling site category, linear relationships of unadjusted [THg] to fork length were significant, but had mixed slope directions. [THg] in DV collected below anadromous barriers decreased with length (Indian

River, $r^2 = 0.45$, slope = -0.13, P = 0.002; West Creek, $r^2 = 0.36$, slope = -0.09, P = 0.04), while [THg] in DV collected from above anadromous barriers increased with fork length (Indian River, $r^2 = 0.59$, slope = 0.29, $P << 0.001$; West Creek, $r^2 = 0.45$, slope = 0.14, $P << 0.001$).

3.4.4 [THg] in relation to C and N stable isotope values

Across all sites, DV collected below anadromous migration barriers had the lowest mean unadjusted [THg] and highest $\delta^{15}N$ values (Table 3.1 and Figure 3.3). Three data points were removed from stable isotope statistical analysis because they were beyond ± two standard deviations, and fell outside the 95% elliptical confidence bounds for C and N values (Figure 3.4). DV from Indian River below anadromous migration barriers showed some of the lowest [THg] while having much higher $\delta^{15}N$ values than the other three sampling sites (Table 3.1, Figure 3.3; $r^2 = 0.26$, slope = -8.09, P = 0.04). DV collected from Indian River above anadromous migration barriers showed the highest magnitude and variation in [THg], and the steepest [THg] increase in relation to increasing $\delta^{15}N$ values (Figure 3.3; $r^2 = 0.35$, slope = 13.26, P = 0.003). The [THg] at both West Creek sites generally increased with increasing $\delta^{15}N$ values, but the linear relationship was significant only for DV sampled below the anadromous migration barrier (Figure 3.3; $r^2 = 0.51$, slope = 1.33, P = 0.02).

3.4.5 Carbon and nitrogen isotope relationships

Lipid-corrected $\delta^{13}C$ values increased with higher $\delta^{15}N$ values (Figure 3.4) for DV from above and below anadromous barriers in West Creek (West/below: $r^2 = 0.48$, slope = 0.17, P= 0.03; West/above: $r^2 = 0.33$, slope = 0.30, P = 0.003). Linear relationships of $\delta^{15}N$ and lipid-corrected $\delta^{13}C$ for Indian River sites were not significant (Figure 3.4, Indian/below: P = 0.33; Indian/above: P = 0.42).

Between rivers, DV from the Indian River had higher lipid-corrected $\delta^{13}C$ values than DV from West Creek (Table 3.4). Within each river, DV collected from below anadromous barriers had higher lipid-corrected $\delta^{13}C$ values than DV from above anadromous barriers. DV from Indian River below anadromous barrier sites had higher $\delta^{15}N$ values than DV from West Creek below anadromous barrier

sites, whereas DV from West Creek above anadromous barrier sites had higher $\delta^{15}N$ than DV from Indian River above anadromous barrier sites. DV collected from the Indian River had higher $\delta^{15}N$ below anadromous barriers, while DV from West Creek were not different above and below anadromous barriers.

3.4.6 Spawning pink salmon contribution of THg to each river

Ten spawning pink salmon were caught from each river to assess the potential magnitude of marine-derived THg returning to the freshwater study systems. Indian River pink salmon mass ranged from 849 to 1542 g (mean ± SD = 1260 ± 212g), and from the Taiya River ranged from 804 to 1700 g (mean ± SD = 1244 ± 293 g). Indian River pink salmon fork length ranged from 420 to 530 mm (mean ± SD = 490 ± 32 mm), and from the Taiya River ranged from 465 to 570 mm (mean ± SD = 507 ± 31 mm). Unadjusted [THg] for Indian River pink salmon muscle ranged from 12.4 to 22.8 ng/g ww (geometric mean ± SD = 17 ± 1.2 ng/g), and Taiya River ranged from 15.3 to 26.5 ng/g ww (geometric mean ± SD = 20 ± 1.2 ng/g). Pink salmon were not aged because pink salmon uniformly return to spawn at two years of age with almost no exceptions (Quinn 2005).

There are no known spawning salmon counts for the Taiya River or West Creek, but the one-day peak spawning pink salmon count for the Indian River was approximately 295,000 on 9 August 2013 (Stopha, 2015). Using a minimum estimate of 50% of salmon mass as muscle (Rorå et al., 1998), average [THg] in pink salmon muscle (17 ng/g), and average pink salmon mass from the Indian River (1260 g), the peak one-day contribution of pink salmon THg to the Indian River was:

$$\frac{1260\ g * 0.5 * 17\ \frac{ng}{g}}{10^8} * 295{,}000 = 3.16\ g \text{ (Equation 3.4).}$$

3.5 Discussion

Our finding that fish length and $\delta^{15}N$ values were important factors in determining THg in DV is consistent with previous studies of Hg accumulation in fish (Evans et al., 2005; Jewett et al., 2003;

McIntyre and Beauchamp, 2007; van der Velden et al., 2012). Studying only two rivers (one with, and one without glacial influence) prevents us from drawing generalized conclusions about glacial influence on [THg] or accumulation trends in fish. However, we found evidence that river system and fish location relative to anadromous migration barriers had interacting effects on [THg]. After standardizing for fish length, mean [THg] in DV populations were not different between the Indian River (no glacial influence) and West Creek (glacial influence), or above and below barriers to anadromous movements, contrary to our hypotheses. The fork length and mass relationship of each sampled group of DV were similar (Supplemental information, Figure 3.1), indicating that the unadjusted differences in [Hg] were likely driven by differences in feeding ecology, which is controlled by the habitat occupied by an individual fish and locally available forage.

One mechanism potentially explaining the interaction between river and location is that DV below anadromous migration barriers are exposed to varying densities of spawning salmon. As salmon return from the sea, the marine-derived nutrients accumulated during their multi-year maturation process can subsidize natal freshwater ecosystems during their spawning and subsequent death (Gende et al., 2002). But, this prolonged exposure to the marine environment may also be responsible for transporting unique amounts and combinations of contaminants that differ from freshwater inputs. An important question to consider is whether the subsidies provided by salmon (for example, egg foraging opportunities to other stream fish) are intrinsically linked to contributions of marine-derived contaminants to watersheds. The answer is likely to be system-specific and dependent on unique habitat characteristics within each salmon-influenced watershed. However, while traveling upstream, anadromous migration barriers block migrating salmon from upstream reaches of a watershed, thereby preventing the extended transport and input of marine-derived nutrients and contaminants. Barriers to anadromous movements therefore provide both a physical and chemical separation within a river. In contrast to the larger glacial watershed of West Creek, the annual transport of marine-derived Hg to the lower reaches of the Indian River by spawning pink salmon has the potential to represent a larger proportion of the overall

contribution of Hg. Southeast Alaska encompasses thousands of medium-sized watersheds (30-200 km^2) similar to the Indian River in morphology and stream flow (Edwards et al., 2013; O'Neel et al., 2015; Shanley and Albert, 2014). In streams that receive large annual salmon runs, migrating salmon likely represent the largest external input of marine-derived Hg and other contaminants (Blais et al., 2007; Krümmel et al., 2009).

DV from the Indian River exhibited high $\delta^{15}N$ values below anadromous migration barriers, but [THg] decreased as $\delta^{15}N$ values increased (Figure 3.3). From 2010-2015, peak single-day estimates for pink salmon in the Indian River ranged from 80,000 in 2015 to 295,000 in 2013, the year of our study (Stopha, 2015). DV are known to feed on salmon eggs during the salmon spawning season (Armstrong, 1970; Sergeant et al., 2015), and have been shown to obtain most of their growth during the summer months when they have access to eggs and insect larvae feeding on decaying salmon carcasses (Jaecks and Quinn, 2014). DV have also been shown to exhibit seasonal shifts in their C and N stable isotope signatures depending on their access to salmon eggs (Ellings, 2003). One study determined that DV with access to sockeye salmon eggs can obtain the majority of their annual energy budget requirements exclusively from eating salmon eggs during an approximately five week spawning period (Armstrong and Bond, 2013). Salmon eggs have low [Hg], ranging from 3.4-14.7 ng/g ww (Zhang et al., 2001), but have higher $\delta^{15}N$ values than associated fish tissues, such as muscle or liver (Bilby et al., 1996; Jaecks and Quinn, 2014). Of the DV we sampled from Indian River, 73% from below anadromous barriers had eggs in their stomachs. These DV are likely feeding primarily on pink salmon eggs, which are abundant in the lower reaches of the river during the spawning season, resulting in relatively low [THg] but high $\delta^{15}N$ values in fish tissues. The $\delta^{15}N$ values of DV in the Indian River with access to salmon eggs are comparable to the $\delta^{15}N$ values of juvenile coho salmon that inhabit streams where sockeye salmon spawn (Smits et al., 2016). Soft tissue turnover in fish has been estimated to range from days to weeks, depending on species, metabolic requirements, growth rate, and diet shifts (Herzka and Holt, 2000; Vander Zanden et al., 1998), thus $\delta^{15}N$ values of pink salmon eggs could have been efficiently assimilated

by DV tissues. The relationship of Hg to $\delta^{15}N$ values observed in lower Indian River is contrary to the general understanding that Hg accumulates with increasing $\delta^{15}N$ values, particularly in systems where salmon spawn, representing increasing biomagnification as an individual feeds higher on the trophic scale (McIntyre and Beauchamp, 2007; Power et al., 2002).

In contrast to the Indian River, DV from West Creek were lower in $\delta^{15}N$. Observed differences in $\delta^{15}N$ values between the Indian River and West Creek could be attributed to the higher turbidity and greater hydrologic energy of glacially influenced West Creek. Prey detection rates of visual foraging fish can be reduced in swift and turbid environments (Henderson and Northcote, 1985; Miner and Stein, 1996). Forty-two percent of DV from West Creek had salmon eggs in their stomachs, which may be due to reduced ability to detect and consume fish eggs drifting through the water column. The $\delta^{15}N$ values of the Indian River DV from below anadromous barriers are similar to the $\delta^{15}N$ values from DV of other studies, whereas the $\delta^{15}N$ of the Indian River DV from above anadromous barriers and all West Creek DV were lower than DV from other studies (Jaecks and Quinn, 2014; Rinella et al., 2013). Taken together, these findings help explain that [THg] in DV can be driven by factors not immediately discernable based on $\delta^{15}N$ values, fish size, age, river type, and location.

Within a river, DV from below barrier sites were higher in $\delta^{13}C$ than above barrier sites, signifying the greater influence of marine carbon inputs, particularly from spawning salmon returning from the ocean. Marine-derived $\delta^{13}C$ values are higher than terrestrial $\delta^{13}C$ values because the process of fractionation of atmospheric carbon and bicarbonate in ocean water differs from the fractionation of atmospheric carbon by terrestrial plants (Fry, 2006). Thus, salmon migrating to the lower reaches of our study rivers appear to be contributing to the contaminant and C isotopic signatures found in spatially overlapping DV. The $\delta^{13}C$ values of the DV from this study were consistent with $\delta^{13}C$ values for fish analyzed in related studies (Fellman et al., 2015; Jaecks and Quinn, 2014).

Finally, we demonstrated that all four sampling groups of DV were distinctly different in their stable isotopic niche space, as defined by the relationship of $\delta^{15}N$ values to $\delta^{13}C$ values (Figure 3.4). These differences appear to be driven by variations in feeding ecology, and the source of the primary production for both carbon and nitrogen isotopic fractionation, which can be further explained by marine influences (e.g. spawning salmon), and watershed geology (i.e. glacial carbon inputs). Anadromous DV typically migrate to the marine environment from their natal systems at age three or four (fork length >150 mm), and upon returning to freshwater in the summer or fall they are larger than any fish we sampled (Armstrong, 1974; Underwood et al., 1996). We presume individual DV from this study had not fed or resided in any marine environment, suggesting that their [THg] and C and N stable isotopic signatures were reflective of the freshwater environment where they hatched and reared.

Mercury concentrations of DV analyzed in this study (range: 6.2-53.3 ng/g ww) were generally greater than Hg concentrations in freshwater-rearing age-0 coho salmon (range: 1.7-6.0 g/g ww), from the same watersheds (Nagorski et al., 2011). All of these Hg concentrations are well below the US Food and Drug Administration action level for human consumption of edible fish (1,000 ng/g ww, USFDA, 2016), or even the more conservative action level of 300 ng/g ww (USEPA 2001). The results of this study mainly describe ecological patterns of Hg accumulation and potential monitoring program considerations, and do not trigger any immediately obvious concerns for human consumption. DV are a popular sport fishing species; however, we did not sample typical sport-fishing sized individuals. Despite the large influx of marine-derived Hg to freshwater streams in southeastern AK and the potential for increased Hg deposition in the sediments (Nagorski et al., 2014), the THg trends observed in our study suggest that abundant salmon populations and the egg subsidies they provide to resident stream fish such as DV may serve to reduce [THg] in larger individuals. Thus, depressed salmon populations may indirectly increase [THg] in individual fish by decreasing the abundance of forage with lower [THg].

3.6 Conclusions

DV are an informative and readily available species for monitoring Hg in southeastern Alaska streams using simple field collection protocols. Other fish species have proven effective in other areas, such as three-spine stickleback (*Gasterosteus aculeatus*) (Kenney et al., 2012), northern pike (*Esox lucius*), Arctic grayling (*Thymallus arcticus*) (Jewett et al., 2003), and Arctic char (*S. alpinus*) (Evans et al., 2015). However, in many of the streams and river systems of southeastern Alaska, DV are ubiquitous, whereas other species like three-spine stickleback are typically absent or discontinuous in distribution in high gradient streams common in the region. In addition to identifying a suitable species for freshwater Hg monitoring in southeastern Alaska, our study more broadly implies that river characteristics, location within a river, as well as fish size and feeding ecology are important factors to consider that influence [THg]. High $\delta^{15}N$ values may not always equate to increasing [THg] and should be interpreted in the context of system-specific feeding ecology. With the knowledge gained through this research, future studies should expand on the spatial scope of sampling, inter- and intra-annual [THg] comparisons, extreme events monitoring (e.g. floods, significantly large or small salmon runs, etc.), and more inclusive food web analysis, including invertebrates and additional fish species.

3.7 Acknowledgments

The staff at Klondike Gold Rush and Sitka National Historical Parks provided field and logistical support, particularly T. Thibault, C. Farley, T. Jones, J. Wilbarger, and E. Noyd. S. Bryan graciously volunteered his time in the field. J. M. Castellini assisted with mercury analysis, including equipment maintenance, calibration, troubleshooting, and data interpretation. J. Harley provided statistical assistance and data interpretation throughout the project. E. Decker, A. Grimes, and H. Gerrish helped with sample processing, mercury analysis, and stable isotope analysis. M. Bower and S. Nagorski provided helpful preliminary manuscript reviews. This work was supported by the National Park Service Inventory and Monitoring Program and the Alaska Department of Environmental Conservation. The views expressed in this article do not necessarily represent the views of the United States National Park Service. Any use of

trade, firm, or product names is for descriptive purposes only and does not imply endorsement by the United States Government.

3.8 Figures

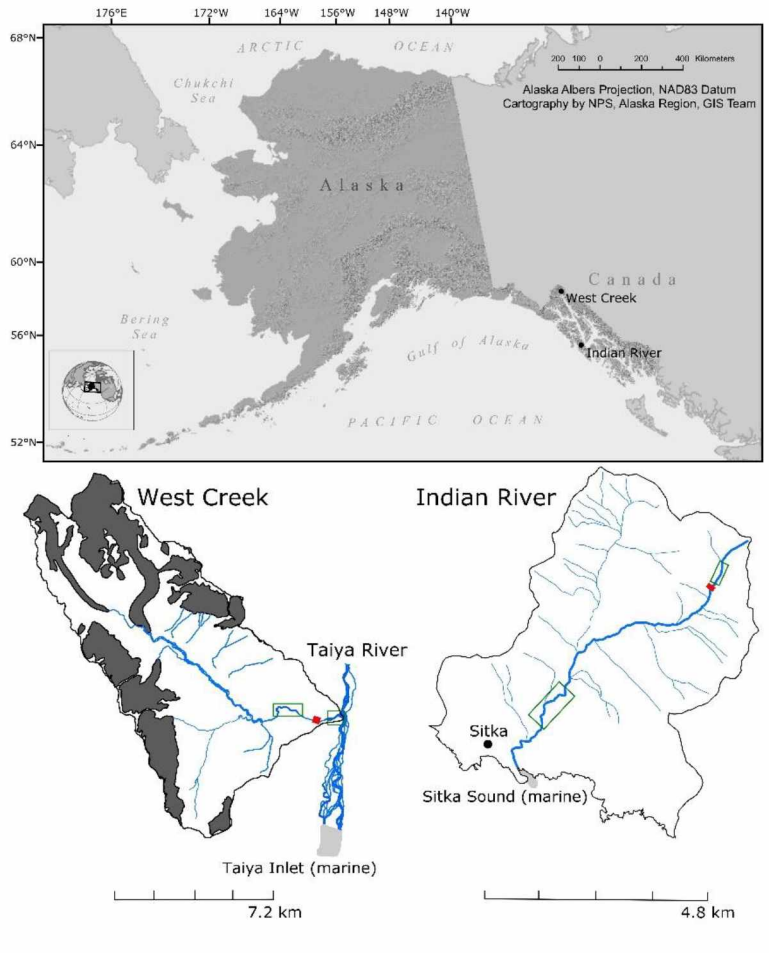

Figure 3.1 - Dolly Varden sampling reaches for West Creek and the Indian River. To maximize clarity, watersheds are not scaled relative to one another. Red rectangles represent apparent barriers to anadromous migration. Green boxes represent sampling reaches above and below barriers. Dark grey polygons represent glacier extent within the West Creek watershed.

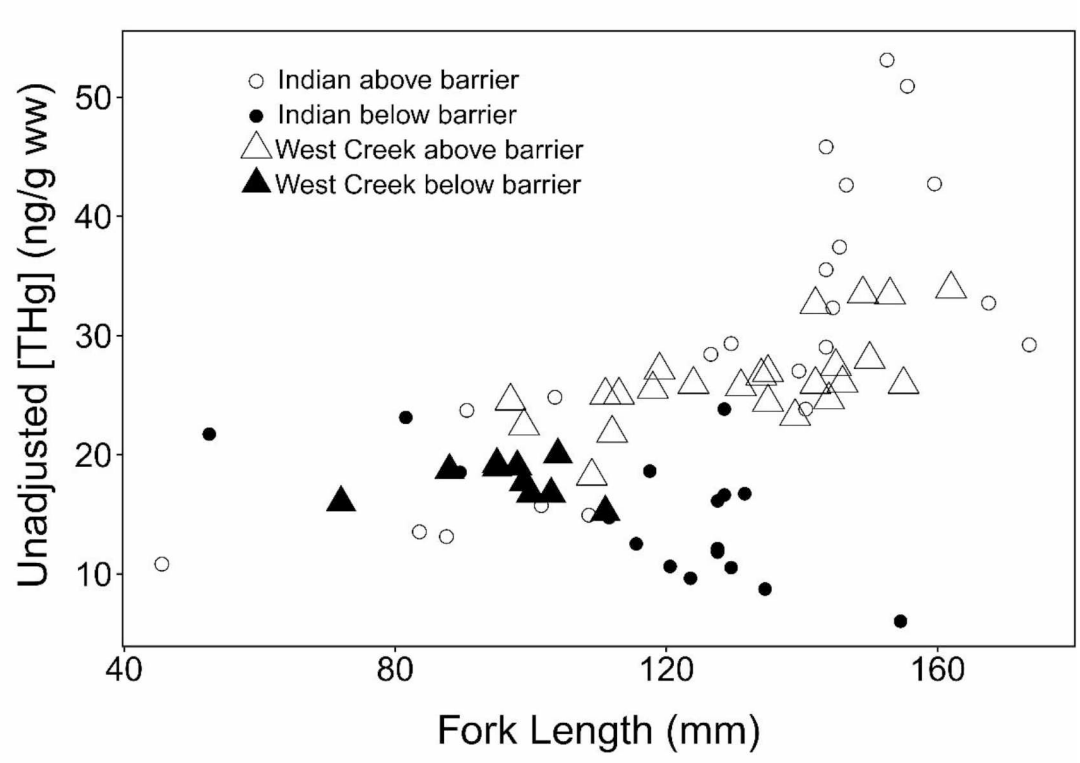

Figure 3.2 - Unadjusted THg concentrations across all sampling sites generally increase with Dolly Varden fork length (linear regression; $r^2 = 0.27$, $P << 0.001$). [THg] = Total mercury concentration.

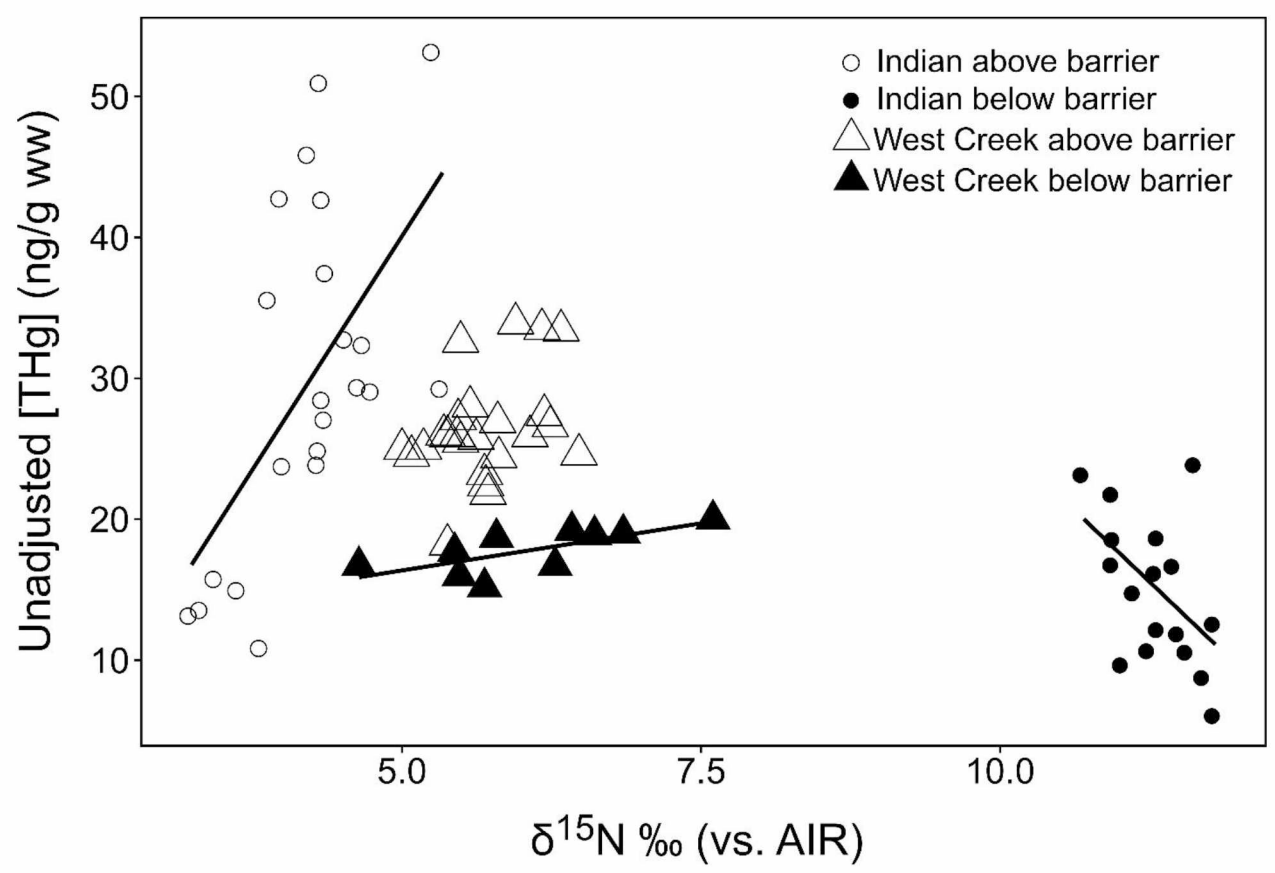

Figure 3.3 - Unadjusted THg concentrations (ng/g ww) and $\delta^{15}N$ (‰) for individual fish from Indian River and West Creek, categorized by above and below anadromous barriers. THg = Total mercury.

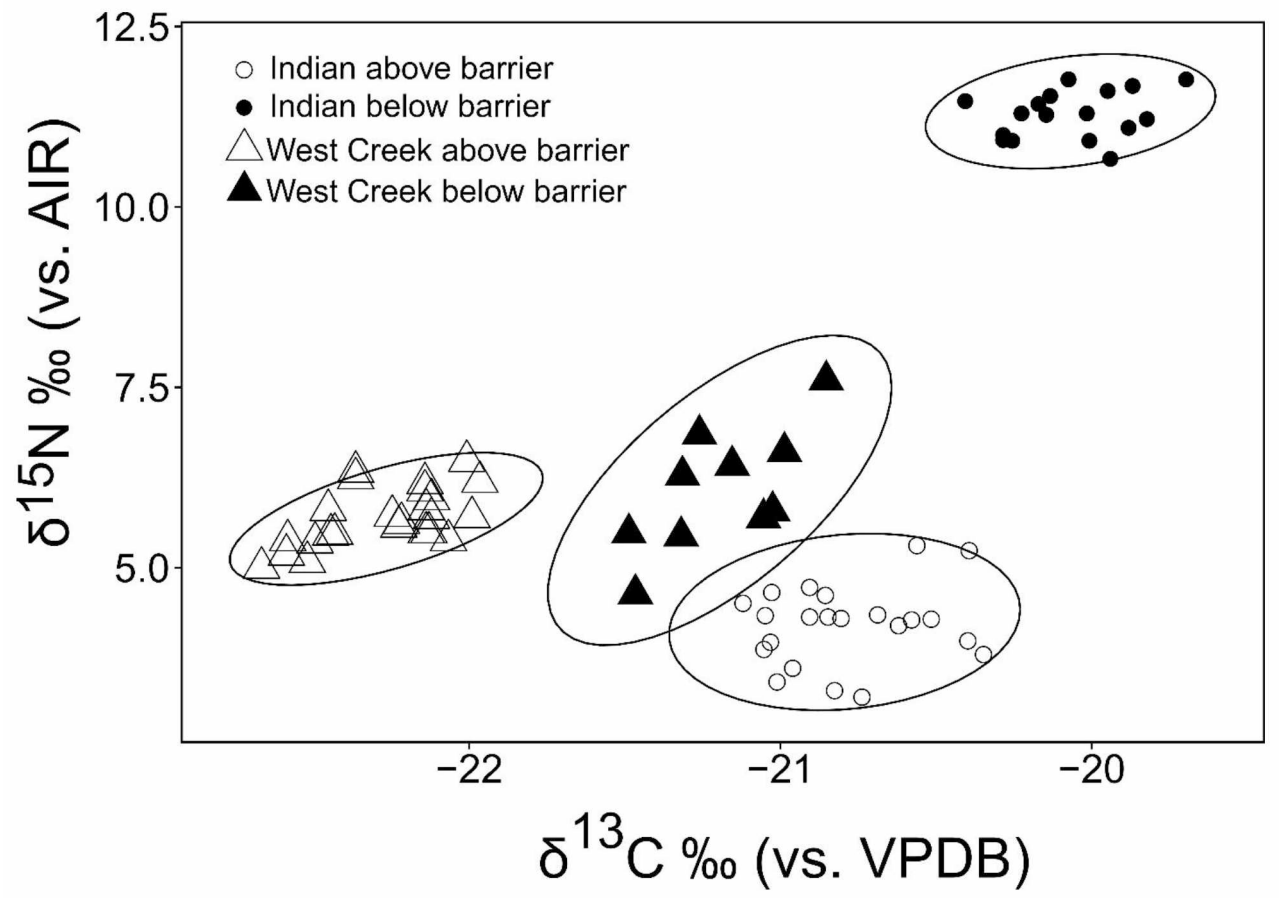

Figure 3.4 - $\delta^{15}N$ (‰) and $\delta^{13}C$ (‰) stable isotopic space for individual fish from the Indian River and West Creek, categorized by above and below anadromous barriers.

3.9 Tables

Table 3.1 - Morphometrics, age, mercury, and stable isotope values for Dolly Varden collected across sampling sites in West Creek and Indian River. Values are mean ± SD (note that both THg columns are reported as the geometric mean). N represents the total samples run for THg and stable isotope analysis. The numbers in parentheses represent how many samples out of N were smaller individuals pooled together to meet minimum tissue mass requirements (see Methods). [THg] = Total mercury concentration based on a ratio of girth to length as utilized by Rea et al. (2016).

Watershed *Barrier location*	N (pooled)	Fork Length (mm)	Mass (g)	Age (y)	[THg] (ng/g ww)	Length-standardized $\log_{10}$[THg] (ng/g ww)	δ^{15}N (‰)	Lipid- corrected δ^{13}C (‰)
West Creek (glacial)								
Below barrier	12 (5)	84 ± 19	6.9 ± 4.9	1.9 ± 0.3	17 ± 1	1.35 ± 1.16	6.7 ± 1.7	-21.2 ± 0.2
Above barrier	24 (0)	132 ± 18	23.7 ± 9.2	2.9 ± 0.5	26 ± 1	1.27 ± 1.08	5.7 ± 0.4	-22.7 ± 0.2
Indian River (non-glacial)								
Below barrier	19 (4)	104 ± 28	15.1 ± 10.3	1.9 ± 0.8	15 ± 1	1.15 ± 1.3	11.1 ± 0.8	-20.1 ± 0.2
Above barrier	22 (2)	120 ± 35	20.7 ± 15.0	3.2 ± 1.1	27 ± 2	1.32 ± 1.1	4.2 ± 0.6	-20.7 ± 0.2

Table 3.2 - The best set of candidate models describing the relationship between total mercury concentrations in individual Dolly Varden and fish length, watershed characteristics, and δ^{15}N composition. Length = individual fish length (mm); River = individual river system (West Creek or Indian River); Barrier = fish location relative to anadromous migration barrier (above or below).

Model parameters	Adj. r^2	AICc	ΔAICc	w_i	Evidence
Length + δ^{15}N	0.486	518.6	0.0	0.248	1
River + Length + δ^{15}N	0.490	519.3	0.7	0.176	1
Barrier + Length + δ^{15}N	0.489	519.5	0.9	0.160	2
River + Barrier + Length + δ^{15}N	0.491	520.5	1.9	0.098	3

Table 3.3 - Parameter Akaike weighs ($w_+(j)$) calculated from all candidate models describing the relationship between total mercury in individual Dolly Varden and fish length, watershed characteristics, and δ^{15}N composition. Length = individual fish length (mm); River = individual river system (West Creek or Indian River); Barrier = fish location relative to anadromous migration barrier (above or below).

Parameter	$w_+(j)$
Length	0.999
δ^{15}N	0.937
Barrier	0.415
River	0.401
Lipid-corrected δ^{13}C	0.271

Table 3.4 - ANOVA test results of mean stable isotope values (N, $\delta^{15}N$ (‰); and C, $\delta^{13}C$ (‰)). * denotes a significance of P = 0.001, ** denotes a significance of P = 0.0001, no asterisk denotes no significance.

	Lipid-extracted $\delta^{13}C$		$\delta^{15}N$	
Comparison	**F-values**	**More enriched**	**F-values**	**More enriched**
Between rivers:				
Above barrier sites	$F_{(1, 44)} = 519.2$**	Indian River	$F_{(1, 44)} = 106.9$*	West Creek
Below barrier sites	$F_{(1, 25)} = 202.4$*	Indian River	$F_{(1,25)} = 529.3$*	Indian River
Within a river:				
Indian River sites	$F_{(1, 37)} = 101.3$*	Below	$F_{(1, 37)} = 2214$*	Below
West Creek sites	$F_{(1, 32)} = 189$*	Below	$F_{(1, 32)} = 3.37$	NA

3.10 Appendices

Supplementary Table 3.1 - Morphometrics and age for pooled samples of Dolly Varden collected across sampling sites in West Creek and Indian River. Values are mean ± SD. N represents the number of individual fish comprising the pooled sample.

Watershed	N	Fork length	Mass (g)	Age (year)
West Creek				
Below barrier	9	64 ± 7	2.5 ± 0.8	1.0 ± 0.0
	4	79 ± 5	5.1 ± 1.2	1.5 ± 0.6
	2	88 ± 0	6.9 ± 0.1	2.0 ± 0.0
	2	94 ± 2	8.3 ± 0.3	2.0 ± 0.0
	2	97 ± 5	9.4 ± 0.2	2.0 ± 0.0
Indian River (non-				
Below barrier	5	71 ± 5	3.6 ± 0.7	1.2 ± 0.5
	3	77 ± 2	5.0 ± 0.4	1.0 ± 0.0
	2	97 ± 9	10.7 ± 3.2	2.5 ± 0.7
	2	117 ± 1	18.3 ± 0.5	2.5 ± 0.7
Above barrier	4	77 ± 10	4.6 ± 1.6	1.3 ± 0.5
	3	89 ± 6	7.2 ± 1.0	2.0 ± 0.0

Supplementary Table 3.2 - The full candidate set of 32 multiple linear regression models evaluating the ability of five predictor variables (individual river system, fish location relative to anadromous migration barrier, fish length, $\delta 1^5N$, and lipid-corrected $\delta^{13}C$) to estimate unadjusted total mercury concentration in individual DV. Length = individual fish length (mm); River = individual river system (West Creek or Indian River); Barrier = fish location relative to anadromous migration barrier (above or below).

Model	AICc	ΔAICc
Length + $\delta^{15}N$	518.6	0.0
River + Length + $\delta^{15}N$	519.3	0.7
Barrier + Length + $\delta^{15}N$	519.5	0.9
River + Barrier + Length + $\delta^{15}N$	520.5	1.9
Length + $\delta^{15}N$ + $\delta^{13}C$	520.8	2.2
River + Length + $\delta^{15}N$ + $\delta^{13}C$	520.9	2.3
Barrier + Length + $\delta^{15}N$ + $\delta^{13}C$	521.4	2.8
Barrier + Length	522.6	4.0
River + Barrier + Length + $\delta^{15}N$ + $\delta^{13}C$	522.8	4.1
River + Barrier + Length	524.5	5.9
Barrier + Length + $\delta^{13}C$	524.8	6.2
River + Barrier + Length + $\delta^{13}C$	526.8	8.2
Barrier	532.0	13.3
River + Barrier	533.4	14.8
Barrier + $\delta^{13}C$	533.8	15.1
Barrier + $\delta^{15}N$	533.8	15.2
River + Barrier + $\delta^{15}N$	535.0	16.4
Barrier + $\delta^{15}N$ + $\delta^{13}C$	535.5	16.9
River + Barrier + $\delta^{13}C$	535.7	17.1
River + Barrier + $\delta^{15}N$ + $\delta^{13}C$	537.3	18.7
River + Length + $\delta^{13}C$	537.9	19.3
Length + $\delta^{13}C$	541.1	22.5
River + $\delta^{15}N$ + $\delta^{13}C$	544.2	25.5
Length	544.9	26.3
$\delta^{15}N$	544.9	26.3
River + $\delta^{15}N$	545.3	26.7
$\delta^{15}N$ + $\delta^{13}C$	547.1	28.4
River + Length	547.1	28.4
River + $\delta^{13}C$	555.3	36.7
$\delta^{13}C$	561.8	43.2
Intercept-only null model	567.6	48.9
River	569.7	51.1

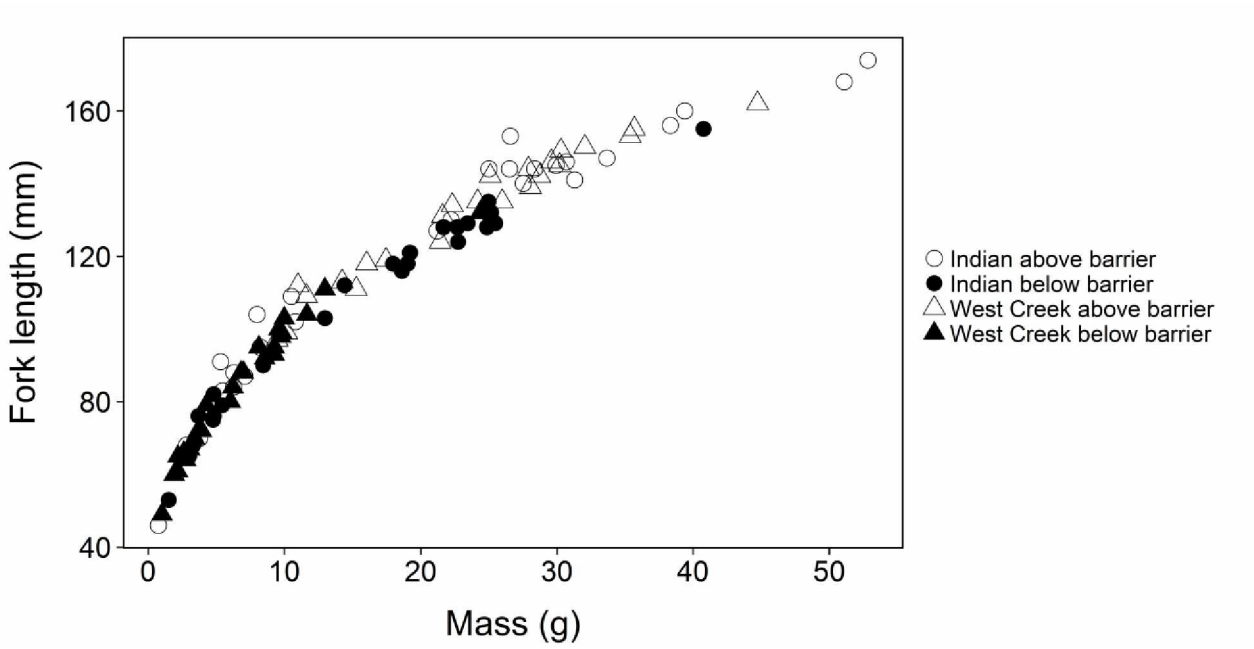

Supplementary Figure 3.1 - Relationship between mass and fork length for all Dolly Varden collected across all sampling sites.

3.11 Works Cited

AMAP, 2011. Arctic pollution 2011. Arctic Monitoring and Assessment Programme (AMAP), Oslo. vi + 38pp ISBN-13 978-82-7971-066-0

Armstrong, J.B., and Bond, M.H. 2013. Phenotype flexibility in wild fish: Dolly Varden regulate assimilative capacity to capitalize on annual pulsed subsidies. J. Anim. Ecol. 82(5): 966–975.

Armstrong, R.H. 1965. Some migratory habits of the anadromous Dolly Varden, *Salvelinus malma* (Walbaum) in southeastern Alaska. Alaska Department of Fish and Game, Informational Leaflet 51:1-27.

———. 1970. Age, food, and migration of Dolly Varden smolts in southeastern Alaska. Journal of Fisheries Research Board of Canada 27: 91-104.

———. 1974. Migration of anadromous Dolly Varden (*Salvelinus malma*) in southeastern Alaska. Journal of Fisheries Research Board of Canada 31(4): 435–444.

———. 1991. Dolly Varden char, in: Judith Stolz and Judith Schnell editors. Trout: the wildlife series. Stackpole Books Harrisburg, Pennsylvania. pp. 266-272.

Baker, M.R., Schindler, D.E., Holtgrieve, G.W., and St Louis, V.L. 2009. Bioaccumulation and transport of contaminants: migrating sockeye salmon as vectors of mercury. Enviro. Sci. Technol. 43(23): 8840–8846.

Bilby, R.E., Fransen, B.R, and Bisson, P.A. 1996. Incorporation of nitrogen and carbon from spawning coho salmon into the trophic system of small streams: evidence from stable isotopes. Can. J. Fish. Aquat. Sci. 53(1): 164–173.

Bizzotto, E.C., Villa, S., Vaj, C., and Vighi, M. 2009. Comparison of glacial and non-glacial-fed streams to evaluate the loading of persistent organic pollutants through seasonal snow/ice melt. Chemosphere 74(7): 924–930.

Blais, J.M., MacDonal, R.W., Mackay, D., Webster, E., Harvey, and C., Smol, J.P. 2007. Biologically mediated transport of contaminants to aquatic systems. Enviro. Sci. Technol. 41(4): 1075–1084.

Blais, J.M., Blais, Schindler, D.W., Muir, D.C.G., Sharp, M., Donald, D., Lafrenière, M., Braekevelt, E., and Strachan, W.M.J. 2001. Melting glaciers: a major source of persistent organochlorines to subalpine Bow Lake in Banff National Park, Canada. Ambio 30(7): 410–415.

Boening, D.W. 2000. Ecological effect, transport, and fate of mercury: a general review. Chemosphere 40 (12):1335-1351.

Bogdal, C., Schmid, P., Zennegg, M., Anselmetti, F.S., Scheringer, M., and Hungerbühler, K. 2009. Blast from the past: melting glaciers as a relevant source for persistent organic pollutants. Enviro. Sci. Technol. 43(21): 8173–8177.

Burnham, K. P., and Anderson, D. R. 2002. Model selection and multimodel inference: a practical information-theoretic approach. New York, NY: Springer.

Cyr, A., Sergeant, C.J., Lopez, J.A., and O'Hara, T.M. 2014. Developing a freshwater contaminants monitoring protocol for the Southeast Alaska Network: Summary of 2013 fish and habitat sampling in Klondike Gold Rush and Sitka National Historical Parks. Natural Resource Data Series NPS/SEAN/NRDS—2014/679. National Park Service, Fort Collins, Colorado

DeNiro, M.J., and Epstein, S., 1977. Mechanism of carbon isotope fractionation associated with lipid synthesis. Science. 197, 261-363.

DeVries, D.R., and Frie, R.V. 1996. Determination of age and growth. Pages 483-512 in B.R. Murphy and D.W. Willis, editors. Fisheries techniques, 2nd edition. American Fisheries Society, Bethesda, Maryland.

Downs, S.G., Macleod, C.L., and Nester, J.N. 1998. Mercury in precipitation and its relation to bioaccumulation in fish: a literature review. Water, Air, and Soil Poll. 108: 149-187.

Drevnick, P.E., Cooke, C.A., Barraza, D., Blais, J.M., Coale, K.H., Cumming, B.F., Curtis, C.J., Das, B., Donahue, W.F., Eagles-Smith, C.A., Engstrom, D.R., Fitzgerald, W.F., Furl, C.V., Gray, J.E., Hall, R.I., Jackson, T.A., Laird, K.R., Lockhart, W.L., Macdonald, R.W., Mast, M.A., Callie, M., Muir, D.C.G., Outridge, P.M., Reinemann, S.A., Rothenberg, S.E., Ruiz-Fernandez, A.C, St. Louis, V.L., Sanders, R.D., Sanei, H., Skierszkan, E.K., Metre, P.C., Veverica, T.J., Wiklund, J.A., and Wolfe, B.B. 2016. Spatiotemporal patterns of mercury accumulation in lake sediments of western North America. Sci. Total Environ. 568: 1157-1170.

Eagles-Smith, C.A., Ackerman, J.T., Willacker, J.J., Tate, M.T., Lutz, M.A., Fleck, J.A., Stewart, A.R., Wiener, J.G., Evers, D.C., Lepak, J.M., Davis, J.A., and Pritz, C.F. 2016. Spatial and temporal patterns of mercury concentrations in freshwater fish across the western United States and Canada. Sci. Total Environ. 568: 1171-1184. DOI: 10.1016/j.scitotenv.2016.03.229.

Edwards, R.T, D'Amore, D.V., Norberg, E., and Biles, F. 2013. Riparian ecology, climate change and management in North Pacific coastal rainforests. Pages 43–72 in Orians GH, Schoen JW, eds. North Pacific Temperate Rainforests: Ecology and Conservation. Audubon Alaska, Nature Conservancy of Alaska, University of Washington Press.

Ellings, C. S. 2003. The influence of spawning Pacific salmon (*Oncorhynchus spp.*) on the stable isotope composition, feeding behavior, and caloric intake of coastal cutthroat trout (*O. clarki clarki*). Master's thesis, University of Washington, Seattle.

Engstrom, D.R., and Swain, E.B. 1997. Recent Declines in Atmospheric Mercury Deposition in the Upper Midwest. Environ. Sci. Technol. 31(4): 960–67.

Evans, M.S., Muir, D., Lockhart, W.L., Stern, G., Ryan, M., Roach, P. 2005. Persistent organic pollutants and metals in the freshwater biota of the Canadian Subarctic and Arctic: an overview. Sci. Total Environ. 351-352: 94–147. DOI: 10.1016/j.scitotenv.2005.01.052

Faïn, X., Ferrari, C.P., Dommergue, A., Albert, M., Battle, M., Arnaud, L., Barnola, J.-M., Cairns, W., Barbante, C., and Boutron, C. 2008. Mercury in the snow and firn at summit station, Central Greenland, and implications for the study of past atmospheric mercury levels. Atmos. Chem. Phys. 8(13): 3441–3457. DOI: 10.5194/acp-8-3441-2008.

Faïn, X., Ferrari, C. P., Dommergue, A., Albert, M. R., Battle, M., Severinghaus, J., Arnaud, L., Barnola, J-M., Cairns, W., Barbante, C., and Boutron, C. 2009. Polar firn air reveals large-scale impact of anthropogenic mercury emissions during the 1970s. P. Natl. Acad. Sci. USA. 106(38): 16114–1619. DOI: 10.1073/pnas.0905117106.

Fellman, J.B., Hood, E., Raymond, P.A., Hudson, J., Bozeman, M., and Arimitsu, M. 2015. Evidence for the assimilation of ancient glacier organic carbon in a proglacial stream food web. Limnol. Oceanogr. 60: 1118–1128. DOI: 10.1002/lno.10088

Fleming, I.A., and Gross, M.R. 1990. Latitudinal clines: a trade-off between egg number and size in Pacific Salmon. Ecology 71(1): 1–11.

Fox, J. and Weisberg, S. 2011. An R companion to applied regression, second edition. SAGE Publications.

Fry, B., 2006. Stable isotope ecology. Springer Science & Business Media.

Gallant, A.L, Binnian, E.F., Omernik, J.M., and Shasby, M.B. 1995. Ecoregions of Alaska - U.S. Geological Survey Professional Paper 1567.

Galloway, J.N., Thornton, J.D., Norton, S.A., Volchok, H.L., and McLean, R.a.N. 1982. Trace metals in atmospheric deposition: a review and assessment. Atmos. Environ. 16 (7): 1677–1700. DOI: 10.1016/0004-6981(82)90262-1

Gende S.M., Edwards, R.T., Willson, M.F., and Wipfli, M.S. 2002. Pacific salmon in aquatic and terrestrial ecosystems. Bioscience. 52: 917-928. DOI: 10.1641/0006-3568(2002)052[0917:PSIAAT]2.0.CO;2

Harley, J., Lieske, C., Bhojwani, S., Castellini, J.M., Lopez, J.A., and O'Hara, T.M. 2015. Mercury and methylmercury distribution in tissues of sculpins from the Bering Sea. Polar Bio. 38: 1535–1543. DOI: 10.1007/s00300-015-1716-x

Heiser, D.W., 1966. Age and growth of anadromous Dolly Varden Char, *Salvelinus malma* (Walbaum) in Eva Creek, Baranof Island, southeastern Alaska. Alaska Department of Fish and Game. Research Report No. 5. Juneau, Alaska.

Henderson, M.A., and Northcote, T.G. 1985. Prey detection and foraging in sympatric cutthroat trout (*Salmo clarki clarki*) and Dolly Varden (*Salvelinus malma*). Can. J. Fish. Aquat. Sci. 42: 785–790.

Herzka, S.Z, and Holt, G.J. 2000. Changes in isotopic composition of red drum (*Sciaenops ocellatus*) larvae in response to dietary shifts: potential implications to settlement studies. Can. J. Fish. Aquat. Sci. 57(1): 137–147. DOI: 10.1139/cjfas-57-1-137.

Hoffman, J.C., and Sutton, T.T. 2010. Lipid correction for carbon stable isotope analysis of deep-sea fishes. Deep-Sea Res. PT I: 57(8): 956–964. DOI: 10.1016/j.dsr.2010.05.003.

Jaecks, T., and Quinn, T.P. 2014. Ontogenetic shift to dependence on salmon-derived nutrients in Dolly Varden char from the Iliamna River, Alaska. Environ. Biol. Fish. 97(12): 1323–1333. DOI: 10.1007/s10641-014-0221-3.

Jaeglé, L., 2010. Atmospheric long-range transport and deposition of mercury to Alaska: a report to the Alaska Department of Environmental Conservation. 82 pp. http://www.atmos.washington.edu/~jaegle/group/Publications_files/Alaska_Mercury_report_revised.pdf

Jarman, W.M., Hobson, K.A., Sydeman, W.J., Bacon, C.E., and Mclaren, E.B. 1996. Influence of trophic position and feeding location on contaminant levels in the Gulf of the Farallones food web revealed by stable isotope analysis. Environ. Sci. Technolo. 30(2): 654-660. DOI: 10.1021/es950392n

Jewett, S.C., Zhang, X., Naidu, A.S., Kelley, J.J., Dasher, D., and Duffy, L.K. 2003. Comparison of mercury and methylmercury in Northern Pike and Arctic Grayling from western Alaska Rivers. Chemosphere 50(3): 383–392.

Johnson, J.B., Omland, K.S., 2004. Model selection in ecology and evolution. Trends Ecol. Evol. 19 (2): 101–108. DOI: 10.1016/j.tree.2003.10.013

Kenney, L.A., von Hippel, F.A., Willacker, J.J., and O'Hara, T.M. 2012. Mercury concentrations of a resident freshwater forage fish at Adak Island, Aleutian Archipelago, Alaska. Environ. Toxicol. Chem. 31: 2647–2652. DOI: 10.1002/etc.1990.

Knott, K.K, Boyd, D., Ylitalo, G.M., and O'Hara, T.M. 2011. Concentrations of mercury and polychlorinated biphenyls in blood of southern Beaufort Sea polar bears (*Ursus maritimus*) during spring; variations with lipids and stable isotope ($\delta^{15}N$, $\delta^{13}C$) values. Can. J. Zoolog. 89: 999–1012. DOI: 10.1139/Z11-071.

Krümmel, E.M., Gregory-Eaves, I., Macdonald, R.W., Kimpe, L.E., Demers, M.J., Smol, J.P., Finney, B., and Blais, J.M. 2005. Concentrations and fluxes of salmon-derived polychlorinated biphenyls (PCBs) in lake sediments. Environ. Sci. Technol. 39(18): 7020–7026.

Krümmel, E.M., Scheer, M., Gregory-Eaves, I., Macdonald, R.W., Kimpe, L.E., Smol, J.P., Finney, B., and Blais, J.M. 2009. Historical analysis of salmon-derived polychlorinated biphenyls (PCBs) in lake sediments. Sci. Total Environ. 407(6): 1977–1989. DOI: 10.1016/j.scitotenv.2008.11.028.

Macdonald, R., Mackay, D., and Hickie, B. 2002. Contaminant amplification in the environment. Environ. Sci. Technol. 36(23): 456A – 462A. DOI: 10.1021/es022470u.

McGrew, A.K., Ballweber, L.R., Moses, S.K., Stricker, C.A, Beckmen, K.B., Salman, M.D., and O'Hara, T.M., 2014. Mercury in gray wolves (*Canis lupus*) in Alaska: increased exposure through consumption of marine prey. Sci. Total Environ. 468-469: 609–613. DOI: 10.1016/j.scitotenv.2013.08.045

McHuron, E.A., Harvey, J.T., Castellini, J.M., Stricker, C.A., and O'Hara, T.M. 2014. Selenium and mercury concentrations in harbor seals (*Phoca vitulina*) from central California: health implications in an urbanized estuary. Mar. Pollut. Bull. 83, 48–57. DOI: 10.1016/j.marpolbul.2014.04.031

McIntyre, J.K., and Beauchamp, D.A. 2007. Age and trophic position dominate bioaccumulation of mercury and organochlorines in the food web of Lake Washington. Sci. Total Environ. 372(2-3): 571–584. DOI: 10.1016/j.scitotenv.2006.10.035.

Miner, J.G, and Stein, R.A. 1996. Detection of predators and habitat choice by small bluegills: effects of turbidity and alternative prey detection of predators and habitat choice by small bluegills. T. Am. Fish. Soc. 125(1): 97–103. DOI: 10.1577/1548-8659(1996)125<0097:DOPAHC>2.3.CO;2.

Nagorski, S.A., Engstrom, D.R., Hudson, J.P., Krabbenhoft, D.P, DeWild, J.F., Hood, E., and Aiken, G. 2011. Scale and distribution of global pollutants in Southeast Alaska Network park watersheds. Natural Resource Technical Report. NPS/SEAN/NRTR-2011/496. National Park Service, Fort Collins, Colorado.

Nagorski, S.A., Engstrom, D.R., Hudson, J.P., Krabbenhoft, D.P., Hood, E., DeWild, J.F., and Aiken, G.R. 2014. Spatial distribution of mercury in southeastern Alaskan streams influenced by glaciers, wetlands, and salmon. Environ. Pollut. 184: 62–72. DOI: 10.1016/j.envpol.2013.07.040.

O'Neel, S., Hood, E., Bidlack, A.L., Fleming, S.W., Arimitsu, M.L., Arendt, A., Burgess, E., Sergeant, C.J., Beaudreau, A.H., Timm, K., Hayward, G.D., Reynolds, J.H., and Pyare, S. 2015. Icefield-to-ocean linkages across the north Pacific coastal temperate rainforest ecosystem. Bioscience. DOI:10.1093/biosci/biv027

Power, M., Klein, G.M., Guiguer, K.R.R.A., and Kwan, M.K.H. 2002. Mercury accumulation in the fish community of a sub-Arctic lake in relation to trophic position and carbon sources. J. Appl. Ecol. 39, 819–830. DOI:10.1046/j.1365-2664.2002.00758.x.

Quinn, T.P. 2005. The behavior and ecology of Pacific salmon and trout. University of Washington Press, Seattle.

Quinn, T.P., Dickerson, B.R., Vøllestad, L.A. 2005. Marine survival and distribution patterns of two Puget Sound hatchery populations of coho (*Onchorhynchus kisutch*) and chinook (*Oncorhynchus tshawytscha*) salmon. Fisheries Res. 79, 209-220. DOI: 10.1016/j.fishres.2005.06.008

R Core Team, 2015. R: A language and environment for statistical computing. R Foundation for Statistical Computing, Vienna, Austria. https://www.R-project.org/.

Riget, F., Asmund, G., and Aastrup, P. 2000. Mercury in Arctic char (*Salvelinus alpinus*) populations from Greenland. Sci. Total Environ. 245(1-3): 161–172. DOI: 10.1016/S0048-9697(99)00441-6.

Rinella, D.J., Wipfli, M.S., Walker, C.M., Stricker, C.A., and Heintz, R.A. 2013. Seasonal persistence of marine-derived nutrients in south-central Alaskan salmon streams. Ecosphere 4(10): 122. DOI: 10.1890/es13-00112.1

Rorå, A.M.B., Kvåle, A., Mørkøre, T., Rørvik, K-A., Steien, S.H., and Thomassen, M.S. 1998. Process yield, colour and sensory quality of smoked Atlantic salmon (*Salmo salar*) in relation to raw material characteristics. Food Res. Int. 31(8): 601–609. DOI: 0.1016/S0963-9969(99)00034-4

Sergeant, C.J., Armstrong, J.B, and Ward, E.J. 2015. Predator-prey migration phenologies remain synchronised in a warming catchment. Freshwater Biol. 60(4): 724–732. DOI: 10.1111/fwb.12524

Sergeant, C.J. and Nagorski, S.A. 2015. The implications of monitoring frequency for describing riverine water quality regimes. River Res. Appl. 31: 602–610. DOI: 10.1002/rra.2767

Shanley, C.S., and Albert, D.M. 2014. Climate change sensitivity index for Pacific salmon habitat in Southeast Alaska. PLOS ONE 9(8): 1-13. DOI: 10.1371/journal.pone.0104799.

Smits, A.P., Schindler, D.E., Armstrong, J.B., Brett, M.T., Carter, J.L., and Santos, B.S. 2016. Thermal constraints on stream consumer responses to a marine resource subsidy. Can. J. Fish. Aquat. Sci. DOI: 10.1139/cjfas-2015-0420.

Stark, K.J., Lee, C., Sopcak, J.M., Kilkus, K., Nadeau, A., and Amberg, S. 2012. Sitka National Historical Park Natural Resource Condition Assessment. Natural Resources Report NPS/SITK/NRR-2012/525. National Park Service, Fort Collins, Colorado.

Stopha, M. 2015. An evaluation of the Sheldon Jackson salmon hatchery for consistency with statewide policies and prescribed management practices. Alaska Department of Fish and Game, Division of Commercial Fisheries, Regional Information Report No. 5J15-07, Anchorage.

Tran, L., Reist, J.D., and Power, M. 2016. Northern Dolly Varden charr total mercury concentrations: variation by life-history type. Hydrobiologia. DOI:10.1007/s10750-016-2666-1.

Tran, L., Reist, J.D., and Power, M. 2015. Total mercury concentrations in anadromous Northern Dolly Varden from the northwestern Canadian Arctic: a historical baseline study. Sci. Tot. Environ. 509-510:154-164.

Underwood, T.J, Millard, M.J., and Thorpe, L.A. 1996. Relative abundance, length frequency, age, and maturity of Dolly Varden in nearshore waters of the Arctic National Wildlife Refuge, Alaska. T. Am. Fish. Soc. 125: 719–728. DOI: 10.1577/1548-8659(1996)125<0719

USEPA. 2001. Water quality criterion for the protection of human health: methyl mercury. https://www.epa.gov/wqc/human-health-criteria-methylmercury. Accessed: August 15, 2016.

USFDA. 2016. Guidance for industry: action levels for poisonous or deleterious substances in human food and animal feed. http://www.fda.gov/Food/GuidanceRegulation/GuidanceDocumentsRegulatoryInformation/ChemicalContaminantsMetalsNaturalToxinsPesticides/ucm077969.htm#merc. Accessed: August 15, 2016.

van der Velden, S., Reist, J.D., Babaluk, J.A., and Power, M. 2012. Biological and life-history factors affecting total mercury concentrations in Arctic charr from Heintzelman Lake, Ellesmere Island, Nunavut. Sci. Total Environ. 433: 309–317. DOI: 10.1016/j.scitotenv.2012.06.055.

Watras, C. J, Back, R.C., Halvorsen, S., Hudson, R.J.M., Morrison, K.A., and Wente, S.P. 1998. Bioaccumulation of mercury in pelagic freshwater food webs. Sci. Total Environ. 219: 183-208.

Wiener, J.G., Haro, R.J., Rolfhus, K.R., Sandheinrich, M.B., Bailey, S.W., Northwick, R.M., and Gostomski T.J. 2013. Bioaccumulation of persistent contaminants in fish and larval dragonflies in six national park units of the western Great Lakes region, 2008-2009. Natural Resource Data Series NPS/GLKN/NRDS—2013/427. National Park Service, Fort Collins, Colorado.

Vander Zanden, M.J., Hulshof, M., Ridgway, M.S., and Rasmussen, J.B.1998. Application of stable isotope techniques to trophic studies of age-0 smallmouth bass. T. Am. Fish. Soc. 127: 729–739. DOI: 10.1577/1548-8659(1998)127<0729:AOSITT>2.0.CO;2.

Zhang, X., Naidu, A.S., Kelley, J.J., Jewett, S.C., Dasher, D., and Duffy, L.K. 2001. Baseline concentrations of total mercury and methylmercury in salmon returning via the Bering Sea (1999-2000). Mar. Pollut. Bull. 42(10): 993–997. DOI: 10.1016/S0025-326X(01)00200-4

Zhang, Y., Jacob, D.J., Horowitz, H.M., Chen, L., Amos, H.M., Krabbenhoft, D.P., Slemr, F., St Louis, V.L., and Sunderland, E.M. 2016. Observed decrease in atmospheric mercury explained by global decline in anthropogenic emissions. P. Natl. Acad. Sci. USA. 113 (3): 526-531. DOI: 10.1073/pnas.1516312113

Zheng, J., Fisher, D., Koerner, R., Zdanowicz, C., Bourgeois, C., Hall, G., Pelchat, P., Shotyk, W., Krachler, M., and Ke, F. 2008. Temporal studies of atmospheric Hg deposition with ice cores and snow in the Canadian High Arctic. Synopsis of Research Conducted under the 2008–2009 Northern Contaminants Program, pp.221-225.

Chapter 4 - **Mercury concentrations in marine species from the Aleutian Islands: spatial and biological determinants** [4]

[4]Cyr, A., López, J.A., Rea, L., Wooller, M.J., Loomis, T., Mcdermott, S., O'Hara, T. 2019. Mercury concentrations in marine species from the Aleutian Islands: spatial and biological determinants. Science of the Total Environment. 664: 761-770. DOI: 10.1016/j.scitotenv.2019.01.387

4.1 Abstract

Several species found in the Bering Sea show significant spatial variation in total mercury concentrations ([THg]) longitudinally along the Aleutian Island chain. We assess [THg] in other members of the Bering Sea food web to better understand the factors shaping regional differences. We determined [THg] and stable carbon and nitrogen isotope ratios ($\delta^{15}N$ and $\delta^{13}C$ values) in muscle tissue from 1,052 fishes and cephalopods from parts of the Bering Sea and North Pacific Ocean adjacent to the Aleutian Islands. The spatial distribution of the samples enabled regional comparisons for eight species of fish and one species of cephalopod. Four species showed higher mean length-standardized [THg] in the western Aleutian Islands management area. The [THg] in yellow Irish lord were very different relative to those observed in other species and, when included in multi-species analyses drove the overall regional trends in mean [THg]. Multi-species analyses excluding measurements for yellow Irish lord showed mean length-standardized [THg] is greater in the western Aleutian Islands than in the central Aleutian Islands management area. Linear regression of [THg] and $\delta^{15}N$ values showed a significant and positive relationship across all species, varying between regions and across species. Isotopic space of all species was significantly different between the western Aleutian Islands and central Aleutian Islands, driven largely by $\delta^{13}C$ values. The stable isotope values observed follow the same regional trend of lower trophic taxa reported in the literature, with significantly lower $\delta^{13}C$ values in the western Aleutian Islands. We conclude that there are regional differences in carbon and nitrogen stable isotope ecology, as well as species-specific feeding ecology that influence [THg] dynamics in part of the marine food web along the Aleutian Island chain. These regional differences are likely contributors to the observed regional variations of [THg] in some high-level predators found in these regions.

4.2 Funding Sources

This publication is the result in part of research sponsored by the Cooperative Institute for Alaska Research with funds from the National Oceanic and Atmospheric Administration under cooperative agreement NA13OAR4320056 with the University of Alaska. This research was also sponsored by the UAF BLaST program and a 2017 North Pacific Research Board (NPRB) Graduate Student Research Award, and is referenced as publication #675. We would like to thank the Alaska Department of Environmental Conservation for supporting a portion of the mercury analysis of this research.

Work reported in this publication was in part supported by the National Institute of General Medical Sciences of the National Institutes of Health under three linked award numbers RL5GM118990, TL4 GM 118992 and UL1GM118991. The work is solely the responsibility of the authors and does not necessarily represent the official view of the National Institutes of Health.

4.3 Introduction

Mercury (Hg), a global contaminant that originates from natural and anthropogenic sources, transported via long-range atmospheric transport is deposited in a wide range of ecosystems regardless of proximity to some point sources. Hg becomes more bioavailable after it is methylated and forms monomethyl mercury, which increases biota uptake through the aquatic food web reaching concentrations of toxicological concern in some higher trophic organisms, such as Steller sea lions (*Eumetopias jubatus*), Pacific halibut (*Hippoglossus stenolepis*), or humans (Atwell et al., 1998; Bentzen et al., 2016; Fox et al., 2014; Rea et al., 2013). Monomethyl mercury in fish can be a human and wildlife health issue (Hamade, 2014) as it is a neurotoxin that can cross the blood brain barrier and act as an endocrine disrupter (Walker et al., 2012) and cause oxidative stress (Lushchak, 2011).

Various ecological and physiological processes drive differences in total Hg concentrations ([THg]) within and between species in the same ecosystem (Jarman et al., 1996; Ward et al., 2010; Willacker et al., 2013). The specific location (e.g., niche) where organisms feed and inhabit can have a significant influence on Hg exposure and accumulation. Proximity to Hg sources, or access to different food webs with different prey assemblages, can provide potential for varying degrees of bioaccumulation and biomagnification that affect observed tissue concentrations of Hg (Cyr et al., 2017). In marine ecosystems, Hg sources (Laurier et al., 2004), ocean currents, upwellings (Gill and Fitzgerald, 1987), and water mass distributions with different geochemical properties (Lehnherr, 2014; Selin, 2009) can varyingly influence how Hg is transported in open oceans and reflected in upper trophic organisms. Additionally, biological and chemical oceanographic differences across marine ecosystems can provide varying conditions for the methylation of Hg, based on factors such as pH (Kelly et al., 2003), the presence of dissolved cations and organic matter (Boening, 2000; Douglas et al., 2012)(Boening, 2000; Douglas et al., 2012), and temperature (Johnson et al., 2016). Together, these factors can provide regionally specific conditions that can influence how Hg enters and moves through the food chain in a complicated fashion.

A notable example of a regional influence on [THg] is in biota of the Bering Sea and the North Pacific along the Aleutian Islands, from east to west. A pattern of higher [THg] has been documented in Steller sea lions and Pacific halibut from the western Aleutian Islands, Alaska, when compared to populations of those species found in other regions of the Aleutian Islands and Alaska (Bentzen et al., 2016; Rea et al., 2013). A similar geographic pattern has been observed in tissues of bald eagles (*Haliaeetus leucocephalus*) and glaucous-winged gulls (*Larus glaucescens*), where [THg] increases from east to west across the Aleutians Islands (Anthony et al., 2007; Ricca et al., 2008). Significantly, Aleutian Island aggregations of Steller sea lions belonging to the western distinct population segment and some rookeries west of Samalga Pass in the western distinct population segment continue to decline in abundance (Atkinson et al., 2008; National Research Council, 2003; Fritz et al., 2014; NMFS, 2013). This pinniped management dilemma combined with the observations of [THg] in biota of the region led to this study to determine factors that may be involved related to fish.

Measurements of stable isotope ratios of carbon and nitrogen ($\delta^{13}C$ and $\delta^{15}N$ values, respectively; and together represent isotopic space) provide valuable ecological research tools that add a layer of dietary information for comparisons of [THg] within and among food webs (Cyr et al., 2017; McGrew et al., 2014; Power et al., 2002). The $\delta^{15}N$ values can be used as a proxy to infer trophic position (Peterson and Fry, 1987), while $\delta^{13}C$ values can be used to differentiate the source of the primary production for a food web (Fry, 2006; Peterson and Fry, 1987). $\delta^{13}C$ values can therefore be used to infer regional differences by differentiating the influence from different carbon sources (Budge et al., 2008; Wang et al., 2014), such as the degree of influence from marine versus terrestrial inputs (Fry, 2006; McGrew et al., 2014), or pelagic versus benthic sources (Boyle et al., 2012; Doi et al., 2010). Fish [THg] are often, but not always, correlated with increasing $\delta^{15}N$ values, and can vary with spatial influences, as elucidated by using $\delta^{13}C$ values (Cyr et al., 2017). Together, stable isotopes of carbon and nitrogen can provide information on some of the ecological influences on [THg] within and among species and locations of fish.

Fish and invertebrates sampled from across the Aleutian Islands provide an ideal study opportunity to examine regional influences on [THg] in a food web relative to wildlife management zones and oceanographic demarcations. Here we report [THg], $\delta^{15}N$ and $\delta^{13}C$ values, and associated biological data for 1,052 specimens of marine fishes and cephalopods, representing 19 species, from a portion of the Bering Sea and North Pacific Ocean adjacent to the Aleutian Islands. The primary goal of this research was to analyze patterns and comparisons of muscle [THg] in a diverse group of fish and cephalopod species from the waters along the central and western portion of the Aleutian Islands to assist with understanding observations of [THg] in upper trophic level vertebrates (fish, avian, mammalian). In particular, we examined how geographic location (Steller sea lion management zones and Amchitka Pass, a distinct oceanographic demarcation) shapes the patterns of length (proxy for age), ecology (including $\delta^{13}C$ and $\delta^{15}N$ values), and muscle [THg] of species examined.

4.4 Methods

4.4.1 Sampling

Specimens were obtained from commercial fish trawls (target and bycatch species) in 2013, 2014, and 2015; and donated subsamples from NOAA research cruises SF201401 and MS201401 in 2014 and 2015. Sampling spanned summer and winter seasons. Sampling regions along the Aleutian Islands were based on Steller sea lion management zones (western Aleutian Islands and central Aleutian Islands), located in the North Pacific Ocean and in the southern and western portion of the Bering Sea, between 51.26° N and 53.22° N, and 171.89° W and -173.76° E (Figure 4.1, York et al., 1996). Samples were also given a second regional assignment based on the longitudinal catch location in relation to Amchitka Pass, -179.98° W (Figure 4.1), which is considered a significant ecological boundary in the Bering Sea. Fish were collected from commercial trawls, frozen whole at -20°C and shipped to the University of Alaska Fairbanks for analysis. Muscle samples provided from federal research cruises were subsampled from fish measured in the field, frozen at sea and shipped to University of Alaska Fairbanks for analysis.

4.4.2 Sample processing

For specimens collected from commercial catches, fork length (in mm) and wet mass (in g) were recorded on thawed fish. Mantle length was measured for cephalopods. Approximately five grams of muscle (skin removed) was sampled from the left side of the fish from the area posterior to the pectoral fin, and ventral to the dorsal fin, or from the mantle for cephalopods. Specimens collected from federal research cruises were sampled on board the vessel, and in the lab a five gram subsample was taken from the larger subsample. All samples were freeze dried (Labcono, FreeZone 4.5 Liter) for a minimum of 48 h to remove all moisture and homogenized using a stainless-steel ball grinder (Retsch, CryoMill). Percent water content was calculated after drying using the following formula:

$$\left(\frac{wet\ weight - dry\ weight}{wet\ weight}\right) * 100 \quad \text{(Equation 4.1)}$$

4.4.3 Total Hg analysis

[THg] were measured in freeze dried samples using a Milestone DMA-80 instrument, in accordance with U.S. EPA method #7473-EPA30B, 2007 SW 846, and reported as ng/g wet weight (ww) based on percent water values (Harley et al., 2015). The method detection limit for [THg] determination for muscle was 5 ng/g ww, calculated by the following formula:

$$\left(\frac{0.5\ (g)}{Sample\ mass\ dry\ weight\ (g)}\right) * (1 - sample\ \%\ H2O) \text{ (Equation 4.2)}$$

Quality assurance and quality control measures included analyses of method blanks, Standard Reference Materials of similar matrices, and check standards. All samples were analyzed in triplicate. Samples for which the coefficient of variation among replicates was >10% were re-analyzed until <10% was reached, with the mean value for all replicates used for statistical comparisons. The standard reference materials used were DORM-4 (National Resource Council Canada; 410.0 ± 55.0 ng/g), and Lake Superior Fish (LSF, National Institute of Standards and Technology, Standard Reference Material®

1946; 433.0 ± 9.0 ng/g ww). Mean percent recoveries (± SD) for each SRM were: 100 ng/g (liquid standard), 96.7 ± 10.9%; DORM-4, 93.5 ± 7.9%; LSF, 100.3 ± 10.1%.

4.4.4 Stable carbon and nitrogen isotope analysis

Stable carbon and nitrogen isotope ratios of all samples were measured at the Alaska Stable Isotope Facility at the University of Alaska Fairbanks following the methods described in Cyr et al. (2017). Between 0.2 and 0.5 mg of freeze-dried homogenized muscle samples were analyzed using continuous-flow isotope ratio mass spectrometry (CF-IRMS, Thermo DeltaVPlus interfaced with a Costech ESC 4010 elemental analyzer via a ConfloIV system). Stable isotope ratios were expressed in δ notation as parts per thousand (‰) relative to international standards (Vienna PeeDee Belemnite – VPDB for carbon and AIR for nitrogen):

$$\delta X‰ = \left[\left(\frac{R_{Sample}}{R_{Standard}}\right) - 1\right] * 1000 \text{ (Equation 4.3)}$$

where *X* is the element of interest, *R* is the ratio of the heavy to light isotope measured for that element, *Sample* is the sample of interest, and *Standard* is the standard used, VPDB for carbon or AIR for nitrogen. Reference checks using peptone (No. P-7750 meat-based protein, Sigma Chemical Company, Lot #76f-0300) were run every 10th sample, and blanks every 20th sample, with instrument precision typically <0.2 ‰ for both carbon and nitrogen.

4.4.5 Lipid extraction and correction

Lipids are depleted in ^{13}C relative to ^{12}C compared with protein and carbohydrates, and can affect stable carbon isotope data by lowering the $\delta^{13}C$ values with increasing lipid content of a sample (DeNiro and Epstein, 1977; Sweeting et al., 2006). High C:N values present difficulties with mathematical lipid-correction formulas, and can cause significant variability between the relationship of $\Delta\delta^{13}C$ in relation to the $C:N_{Bulk}$ (Hoffman and Sutton, 2010; Post et al., 2007). A large proportion (92%) of the samples in this study had atomic C:N ratios above levels considered representative for protein, ~3.7 (Post et al., 2007;

Sweeting et al., 2006), and differed between species, individuals and regions (Supplemental Figure 4.1). To account for this influence, we lipid-extracted a subset of two hundred and forty-five samples from eight of the species following a method modified from Folch et al. (1957). Briefly, 1.0 - 2.0 g of freeze-dried sample muscle was rinsed three times in a mixture of 2:1 chloroform: methanol for 15 minutes, air dried overnight, then freeze-dried for 24 hours. These lipid-extracted samples were analyzed for $\delta^{13}C$ and $\delta^{15}N$ values as described above and recalculated C:N ratios.

We determined that the influence of lipids in samples with $C:N_{Bulk} > 10$ was considerable and introduced more variability and uncertainty than mathematical lipid-correction could reasonably account for (Supplemental Figures 1, 2 and 3), and subsequently removed ten samples with $C:N_{Bulk} > 10$ from $\delta^{13}C$ analyses. The mean C:N ratio for all lipid-extracted samples was 3.7 ± 0.1 ‰ (Supplemental Table 4.1), and thus enabled the use of the $\delta^{13}C_{Lipid\text{-}extracted}$ values to generate a mathematical correction formula. We followed the methods detailed in Post et al. (2007) by using their formula for % lipid:

$$\%\ lipid = -20.54 + 7.24 * C{:}N_{Bulk} \quad \text{(Equation 4.4)}$$

followed by the equation to determine $\Delta\delta^{13}C$ with our data:

$$\Delta\delta^{13}C = 0.45 + (0.094 * \%\ lipid) \quad \text{(Equation 4.5)}$$

and then combined the equations to generate the final correction formula (Supplemental Table 4.1, Supplemental Figure 4.3, $R^2 = 0.80$, $p << 0.001$) to mathematically correct the $\delta^{13}C_{Bulk}$ values for the remainder of the dataset:

$$\delta^{13}C_{Lipid\text{-}corrected} = \delta^{13}C_{Bulk} - 1.48 + 0.65 * C{:}N_{Bulk} \quad \text{(Equation 4.6)}$$

4.4.6 Length standardization of [THg].

To account for regional or allometric effects on [THg] and allow for inter- and intra-species and regional comparisons, we performed a length-standardization of [THg] following the methods detailed in Eagles-Smith et al. (2016). Briefly, we standardized the log-transformed [THg] using the median length

for each species by generating a linear mixed effects model with length and species as fixed covariates, and region as a random effect. We added the residuals from each fish back into the model to generate predictive [THg] values for each fish, which were then back transformed to obtain the final length-standardized [THg] for each fish.

4.4.7 Statistical analysis

All analyses were performed using R statistical computing software (R Core Team 2015). All data were checked for normality by visual inspection of normal quantile-quantile plots, and residual plots (Ciancio et al., 2008), and using either the Shapiro-Wilk's test or the Kruskal-Wallis test. [THg] were log transformed for regression analysis to comply with normality assumptions. To ensure statistical power for comparisons, we restricted our regional and inter-species comparisons to the nine species that had >10 individuals per region. Species in these comparisons were divided into two major groups: 1) darkfin sculpin (*Malacoccottus zonurus*), Pacific cod (*Gadus macrocephalus*), yellow Irish lord (*Hemilepidotus jordani*), and arrowtooth flounder (*Atheresthes stomias*) were considered piscivorous based on the percentage of diet composed of fish (Yang and Nelson, 1999; Yang, 2003); and 2) walleye pollock (*Gadus chalcogrammus*), Atka mackerel (*Pleurogrammus monopterygius*), northern rockfish (*Sebastes polyspinis*), Pacific Ocean perch (*Sebastes alutus*), and one invertebrate, the magistrate armhook squid (*Berryteuthis magister*) were considered primarily zooplanktivorous based on the percentage of diet composed of invertebrates (Yang and Nelson, 1999; Yang, 2003)

Summary statistics for [THg] are represented as geometric mean ± standard deviation (SD), all other summary statistics are represented as arithmetic mean ± SD. We conducted analysis of variance to determine the overall influence of species, region, and the interaction of species and region. Following this, we tested regional differences for individual species' mass, length, unadjusted [THg], and length-standardized [THg] using t-tests with a Holm correction to control for familywise errors. Results were considered significant at $\alpha \leq 0.05$. Rank order position for each species and region was determined using analysis of variance followed by the Tukey's Honestly Significant Difference *post hoc* test. Determining

the influence of $\delta^{15}N$ values, $\delta^{13}C$ values, the interaction of $\delta^{15}N$ or $\delta^{13}C$ values and region on [THg] was determined using generalized linear models (GLM) for each species. Differences in the isotopic space between seasons and regions for each species were tested using the Hotelling's T^2 test, comparing the mean $\delta^{15}N$ and $\delta^{13}C$ values in multivariate space (Ciancio et al., 2008; Colombini et al., 2011).

4.5 Results

4.5.1 Data summary

A total of 1,052 samples from the western Aleutian Islands and the central Aleutian Islands, representing 19 species of marine fishes and cephalopods were analyzed for [THg], and δ15N and δ13C values. Across all species, mass and length varied considerably, ranging from 15 to 16,800 g (1,303.1 g ± 1,963.4). and from 8 to 111 cm (41.3 cm ± 16.9), respectively. Unadjusted [THg] for all fish and cephalopods ranged from 7.53 to 1,578.26 ng/g ww (149.47 ± 173.74). δ15N (‰) values ranged from 5.9 to 15.0 ‰ (11.1 ± 1.5 ‰), bulk δ13C values ranged from -26.5 to -17.6 ‰ (-20.9 ± 1.5 ‰), and lipid-corrected δ13C values ranged from -22.7 to -16.5 ‰ (-19.5 ± 1.2 ‰). Statistical comparisons between central Aleutian Islands and western Aleutian Islands for the nine species with >10 individuals per region are shown in Table 4.1. Summary statistics for all other species sampled and analyzed are provided in Supplemental Table 4.2.

4.5.2 Stable isotopes

The seasonal isotopic space for each species and region was significantly different within the western Aleutian Islands in armhook squid, Atka mackerel, northern rockfish, Pacific cod, and walleye pollock, and within the central Aleutian Islands in all species except armhook squid and darkfin sculpin (Supplemental Table 4.3). These differences were small (<~1 ‰) and within analytical error and aquatic trophic level variation (Vander Zanden and Rasmussen, 2001), so we considered them not biologically significant. As a result, we pooled the stable isotope measurements within each species and region for our study.

All species occupied significantly different isotopic spaces between the central Aleutian Islands and western Aleutian Islands (Table 4.2, Figure 4.2). This is likely driven by the differences in mean lipid-corrected $\delta^{13}C$ values between regions (Δcentral Aleutian Islands-western Aleutian Islands), which was different for all species (Table 4.1), whereas only four species had statistically different (Table 4.1, $\alpha \leq 0.05$) mean $\delta^{15}N$ values between the western Aleutian Islands and central Aleutian Islands.

4.5.3 Regional comparisons

An analysis of variance model indicated that species and the interaction of species and region significantly contributed to the variability in length standardized [THg], while region alone was not significant ($\alpha \leq 0.05$). Unadjusted [THg] were statistically higher in the western Aleutian Islands for arrowtooth flounder, Pacific cod, Pacific Ocean perch, and walleye pollock (four of nine species), whereas unadjusted [THg] were statistically higher in the central Aleutian Islands for yellow Irish lord and Atka mackerel ($\alpha \leq 0.05$; Table 4.1). There was no difference in length-standardized [THg] between western Aleutian Islands and central Aleutian Islands across all fish combined ($\alpha \leq 0.05$). Since this statistic is likely driven by the magnitude of [THg] in yellow Irish lord from the central Aleutian Islands (Figure 3), a further comparison for all species combined except yellow Irish showed the mean length-standardized [THg] was significantly higher in the western Aleutian Islands ($\alpha \leq 0.001$). Intraspecies comparisons of mean length-standardized [THg] were higher in the western Aleutian Islands for arrowtooth flounder, Pacific cod, Pacific Ocean perch, and walleye pollock (four of nine species, Table 4.1, Figure 4.3). Only Atka mackerel and yellow Irish lord had higher mean length-standardized [THg] in the central Aleutian Islands (Table 4.1, Figure 4.3).

Regional comparisons based on secondary regional assignments using Amchitka Pass as the divide between western Aleutian Islands and central Aleutian Islands revealed that both mean unadjusted [THg] and length-standardized [THg] of all species combined were significantly greater in the western Aleutian Islands ($\alpha \leq 0.001$). Intraspecies comparisons demonstrated that all species except Atka

mackerel had greater mean length-standardized [THg] in the western Aleutian Islands, and statistically, the mean length-standardized [THg] of arrowtooth flounder, northern rockfish, Pacific cod, Pacific Ocean perch, walleye pollock, and yellow Irish lord were significantly greater in the western Aleutian Islands ($\alpha \leq 0.05$). Isotopic space was different between the western Aleutian Islands and central Aleutian Islands for all species ($\alpha \leq 0.01$), with consistently lower $\delta^{13}C$ values in the western Aleutian Islands.

The overall descending rank order among species for mean length-standardized [THg] was yellow Irish lord > darkfin sculpin ≥ Pacific cod > arrowtooth flounder ≥ northern rockfish ≥ Pacific Ocean perch ≥ walleye pollock ≥ Atka mackerel ≥ armhook squid (> indicates statistical difference, $\alpha < 0.05$, and ≥ indicates a greater mean value but no statistical difference). Regionally, in the western Aleutian Islands, the descending rank order for length-standardized [THg] was darkfin sculpin ≥ Pacific cod ≥ arrowtooth flounder ≥ yellow Irish lord ≥ Pacific Ocean perch ≥ walleye pollock ≥ northern rockfish ≥ Atka mackerel ≥ armhook squid (Figure 4.3). In the central Aleutian Islands, the descending rank order for length-standardized [THg] was yellow Irish lord > darkfin sculpin ≥ Pacific cod > northern rockfish ≥ arrowtooth flounder ≥ Pacific Ocean perch ≥ Atka mackerel ≥ walleye pollock ≥ armhook squid (Figure 4.3).

4.5.4 [THg] in relation to trophic position

Unadjusted [THg] increased with increasing $\delta^{15}N$ values ($R^2 = 0.31$, $p < 0.001$) across all species examined. Assessing this relationship within each species and region indicated six of the species had a significant, positive slope in the western Aleutian Islands; while four of the species had a significant, positive slope in the central Aleutian Islands (Table 4.3). Using GLM the unadjusted [THg] in Pacific cod, Pacific Ocean perch, darkfin sculpin, northern rockfish, and yellow Irish lord were significantly influenced by $\delta^{15}N$ values; and by $\delta^{13}C$ values in arrowtooth flounder, Pacific cod, Pacific Ocean perch, walleye pollock, darkfin sculpin, and yellow Irish lord (Table 4.4). Unadjusted [THg] was significantly influenced by the interaction of $\delta^{15}N$ values and region in walleye pollock, while the interaction of $\delta^{13}C$

values and region significantly influenced [THg] in arrowtooth flounder, Pacific cod, walleye pollock, northern rockfish, and yellow Irish lord (Table 4.4).

4.6 Discussion

4.6.1 Overview

We sought to gain a better understanding of the influence of region and feeding ecology on observed [THg] in fish and cephalopod species by investigating a portion of the food web of the Bering Sea and North Pacific Ocean along the Aleutian Islands. We found a pattern of higher muscle [THg] in many of the fish from the western Aleutian Islands compared to the central Aleutian Islands. We also found a consistent pattern of differences in the isotopic space ($\delta^{15}N$ and $\delta^{13}C$ values) between the western Aleutian Island and central Aleutian Island regions for all species (Table 4.2, Figure 4.2). Finally, we have demonstrated that fish muscle [THg] is highly variable and influenced by known drivers of Hg tissue concentrations.

4.6.2 Isotopes and feeding ecology

The seasonal ranges of stable isotope values measured in our fish suggest negligible biological differences and allowed us to pool the isotope data by year. The decision to do this was further supported by related feeding ecology work from the Aleutian Islands that demonstrated that the seasonal variation in stable isotopes in Steller sea lion vibrissa was 2 - 5 ‰, and 3 - 7 ‰ respectively for $\delta^{13}C$ values and $\delta^{15}N$ (Rea et al., 2015), far greater than the isotope variations measured in our fish. Doll et al. (2018) also noted the magnitude of the seasonal variation of Steller sea lion vibrissa, together with the minimal seasonal variation of their prey isotope values, and subsequently pooled their prey isotope values together seasonally.

The regional patterns of isotopic space were mostly driven by the differences in $\delta^{13}C$ values rather than $\delta^{15}N$ values. In both bulk $\delta^{13}C$ data and lipid-corrected $\delta^{13}C$ data, mean $\delta^{13}C$ values in the western Aleutian Islands were lower than those from the central Aleutian Islands for each species (Table

4.1, Figure 4.2). These measured differences in $\delta^{13}C$ values are consistent with the literature, where Schell et al. (1998) determined that the $\delta^{13}C$ values of both euphausiids and chaetognaths were lower in the western portion of the Aleutians. We suspect this is indicative of a difference in baseline stable isotope values, notably $\delta^{13}C$ values, between the western Aleutian Islands and the central Aleutian Islands. If baseline differences occur at the level of primary production, assuming other isotope factors were roughly equal in the food web, that difference would be transferred up through the food web, resulting in differences in upper trophic level prey.

Across all fishes combined, muscle [THg] increased positively and significantly with increasing $\delta^{15}N$ values, indicating biomagnification through the food web, an expected finding well supported in the literature (Atwell et al., 1998; Coelho et al., 2013; Power et al., 2002). The parameters of this correlation however, varied strongly by species and regions. Most notably, $\delta^{15}N$ values were generally lower in the western Aleutian Islands than in the central Aleutian Islands, but muscle [THg] were generally higher in the western Aleutian Islands than in the central Aleutian Islands, a pattern opposite of expected assumptions based on known biomagnification dynamics of Hg. This pattern is also consistent with previous findings, in which Pacific halibut from the western Aleutian Islands had the lowest $\delta^{15}N$ values, yet the highest muscle [THg] (Bentzen et al., 2016). The $\delta^{15}N$ values of Pacific cod, walleye pollock, arrowtooth flounder, and yellow Irish lord were all lower than those reported by Gorbatenko et al. (2008) from Cape Olutorski and Cape Navarin in the western Bering Sea. These patterns suggest regional differences in [THg] along the Aleutian Islands likely originate at the base of the food chain and are amplified through feeding ecology, but not driven strictly by feeding ecology.

The consistent trends in differences of the biology and chemistry of the biota from central or eastern and western areas of the Aleutian Islands reinforce the idea that oceanographic and ecological conditions are likely driving differences in [THg] in biota between the western Aleutian Islands and central Aleutian Islands, with these differences amplified through the food web. Feeding ecology is likely a major driver of the observed differences in [THg] of higher trophic level prey because modeling

research has demonstrated that regional deposition of [THg] across the Bering Sea and Aleutian Islands does not differ regionally (Strode et al., 2008), and Hg contributions from various sources to the Bering Sea are similar (Sunderland et al., 2009). We highlight feeding ecology because fish have limited capacity for redistributing, demethylating or eliminating THg or $MeHg^{+}$, which allows for efficient accumulation and retention of THg or $MeHg^{+}$ in muscle tissue (Amlund et al., 2007; Trudel and Rasmussen, 1997). These factors, in conjunction with the efficient assimilation of Hg in the fish gut allow biomagnification of Hg through the aquatic food web (Atwell et al., 1998; Coelho et al., 2013). Thus, higher trophic level fish tend to have higher [THg] than lower trophic fish and prey items. Our study supports this generalization as three of the species with the largest differences between western Aleutian Islands and central Aleutian Islands, arrowtooth flounder, Pacific cod, and yellow Irish lord are known to be higher trophic predators that feed primarily on fish or crustaceans (Yang, 2003). Darkfin sculpin had some of the highest mean muscle [THg], and their diet includes at least some shrimp. These four species also had the highest $\delta^{15}N$ values (Table 4.1, Figure 4.2), and occupy trophic levels ranging from 3.8 to 4.5 (Aydin et al., 2007; Gorbatenko et al., 2008; Marsh et al., 2012). All other species in this study feed almost exclusively on some type of zooplankton (Yang, 2003), and occupy trophic levels ranging from 3.0 to 3.8, a full trophic level lower on the food web, providing less potential for biomagnification.

4.6.3 Geographic trends

Our data demonstrate a general trend of higher muscle [THg] in western Aleutian Island fish compared to central Aleutian Island fish. Four of the nine species had statistically greater mean length-standardized [THg] in the western Aleutian Islands than in the central Aleutian Islands. This geographical trend in [THg] is consistent with the literature regarding other marine-based taxa, such as Steller sea lion (Rea et al., 2013), Pacific halibut (Bentzen et al., 2016), glaucous-winged gulls (Ricca et al., 2008), and bald eagles (Anthony et al., 2007). The strong influence of yellow Irish lord on the overall regional patterns of [THg] are unique and discussed in subsequent paragraphs.

Amchitka Pass on the western end of the central Aleutian Islands (Figure 4.1) is considered a discrete ecological divide in the Bering Sea, with chemical and biological oceanographic processes differing from the west to the east of the pass (Logerwell et al., 2005). The consistent differences in [THg] we found by using Amchitka Pass as the boundary for western Aleutian Islands and central Aleutian Islands are likely related to the consistent differences in isotopic spaces, where specific chemical oceanographic differences east and west of Amchitka Pass have caused differences in isotope baseline values, and then feeding ecology influences the accumulation of THg in each food web.

4.6.4 Yellow Irish lord

Although yellow Irish lord were similar in size between the western Aleutian Islands and central Aleutian Islands regions, the mean length-standardized [THg] in the central Aleutian Islands was over two times higher than the western Aleutian Islands, a regional trend that is opposite to the one detected for the other species (Table 4.1, Figure 4.3). This may be related to trophic level, as yellow Irish lord in the central Aleutian Islands had higher $\delta^{15}N$ values than those from the western Aleutian Islands. Yellow Irish lord feed on fish and benthic crustaceans (Yang, 2003), which are higher trophic level prey than the zooplankton prey that many of the other fish species in this study consume. Yellow Irish lord could also simply be older fish. Long-lived fishes will eventually reach the asymptote of their length-at-age relationship, when they will continue to age and continue to accumulate Hg, but not exhibit a related increase in length (Eagles-Smith et al., 2014). The mean length-standardized [THg] of yellow Irish lord in the western Aleutian Islands was comparable to the mean length-standardized [THg] of several other species in this study, while the length-standardized [THg] of those from the central Aleutian Islands were much greater than any other species measured in this study. Based on the longer mean fork length for yellow Irish lord in the central Aleutian Islands, we suspect that these fish may be at or approaching the asymptote of their growth curve, approximately 46 cm for males and females combined (TenBrink and Buckley, 2013), indicating they are older individuals, but this age is not reflected in their length, and has allowed a greater amount of time for the accumulation of Hg in their muscle tissue (Eagles-Smith et al.,

2014; Lange et al., 1994). Additionally, the maximum age of yellow Irish lord in the western Aleutian Islands has been reported to be less than more easterly portions of the Bering Sea (TenBrink and Aydin, 2009), further indicating the yellow Irish lord caught in the central Aleutian Islands may have been older individuals. Using only the length of a fish to understand Hg feeding ecology and accumulation dynamics would miss this level of important detail, consequently causing inappropriate comparisons of fish that are years apart in age. Age data greatly improves the ability to understand situations like this, and we recommend age estimations be conducted for fish that exhibit extreme relationships of [THg] and other metrics such as species, fish length, $\delta^{15}N$ values, or location.

4.6.5 Food web dietary exposure

The muscle [THg] of many of the fish from the central Aleutian Islands are in general agreement with other published studies of Pacific cod (Burger et al., 2014, 2007; Burger and Gochfeld, 2007), yellow Irish lord (Burger et al., 2014, 2007), and Atka mackerel (State of Alaska, 2017; Burger et al., 2007). The muscle [THg] for several species of fish from the western Aleutian Islands however, were higher than those reported in the literature, where the mean [THg] measured in Pacific cod were nearly 150 ng/g ww greater than those measured by Burger et al. (2014), or the State of Alaska Hg biomonitoring study from 2001 to 2016 (State of Alaska, 2017). The [THg] of arrowtooth flounder from the central Aleutian Islands were comparable to those identified in Oregon by Childs and Gaffke (1973), while those from the central Aleutian Islands were higher than those measured in arrowtooth flounder from the Bering Sea by Gerber et al. (2012), and those from western Aleutian Islands were higher than values reported in any literature we identified. Our [THg] for walleye pollock and yellow Irish lord were also higher than those reported by the State of Alaska (State of Alaska, 2015), and were similar to reports of halibut across Alaska (Bentzen et al., 2016). Although these comparisons demonstrate the high degree of variability of fish [THg], given the consistency of the patterns, they also reinforce the overarching regional pattern of increased [THg] in the western Aleutian Islands.

These results point to influential regional food web differences resulting in mean muscle [THg] differences along the Aleutian chain for most species we examined. Where mean [THg] are different between the western Aleutian Islands and the central Aleutian Islands, the differences are substantial, such as 92 ng/g ww difference for Pacific cod (57 % increase), or 140 ng/g ww difference for arrowtooth flounder (180 % increase). It is also important to note that regardless of region, yellow Irish lord contain elevated [THg] compared to the other species measured. These differences may translate to different Hg exposure potential between the western Aleutian Islands and central Aleutian Islands regions for Steller sea lion and other top predators occupying those areas. These differences prove to be more directly associated with Amchitka Pass, as a biogeographical divide, when compared to Steller sea lion resource management zones.

4.7 Conclusion

We compiled an extensive set of [THg] and stable isotope data for 19 species found in the Bering Sea and North Pacific along the Aleutian Islands. These data enabled us to generate and validate a mathematical lipid-correction formula for Bering Sea and North Pacific fishes with $C:N_{Bulk} < 10$. We show a general trend of elevated [THg] in fish from the western Aleutian Islands, compared to the central Aleutian Islands, when using the management regions defined for Steller sea lion. When considering a regional delineation based on ecosystem characteristics, we note that Amchitka Pass offers a clearer and more consistent explanation for the observed trends in $\delta^{13}C$ and $\delta^{15}N$ values and [THg] than those based on marine mammal species management zones. We document a consistent trend of lower $\delta^{13}C$ values in the western Aleutian Islands, providing a starting point to assess differences in primary production and feeding ecology, and subsequently the increase of [THg] through multiple trophic levels. These findings, in conjunction with previous research indicates potential regional differences in feeding ecology, resulting in both inter- and intraspecies biomagnification differences that drive higher [THg] in the western Aleutian Islands. Further research on this topic should include more comprehensive food web analysis of [THg] and stable isotopes (C and N), from primary production to top predators of the same location.

Additionally, these measurements and analyses will be useful to others interested in Hg and other contaminants in this region and for determining consumption advice for humans. As such, these data have been shared with the State of Alaska Department of Environmental Conservation for this purpose.

4.8 Acknowledgements

The authors would like to thank the crew of F/V Seafisher and F/V Ocean Peace and the crew of the National Oceanic and Atmospheric Administration (NOAA) research cruise SF201401 and MS201401 for donating fish. J.M. Castellini assisted with mercury analysis, maintenance, calibration and troubleshooting of the DMA-80. J. Harley assisted with data and statistical interpretation throughout the project. M. Campbell, E. Decker, H. Gerrish, Z. Goeden, A. Grimes, G. Johnson and K. Opp assisted with sample processing, Hg analysis, and stable isotope preparation. M. Courtney assisted with mapping. We would like to thank R. Gerlach and C. Furin with the Alaska Department of Environmental Conservation for their overall support and assistance with this project.

4.9 Figures

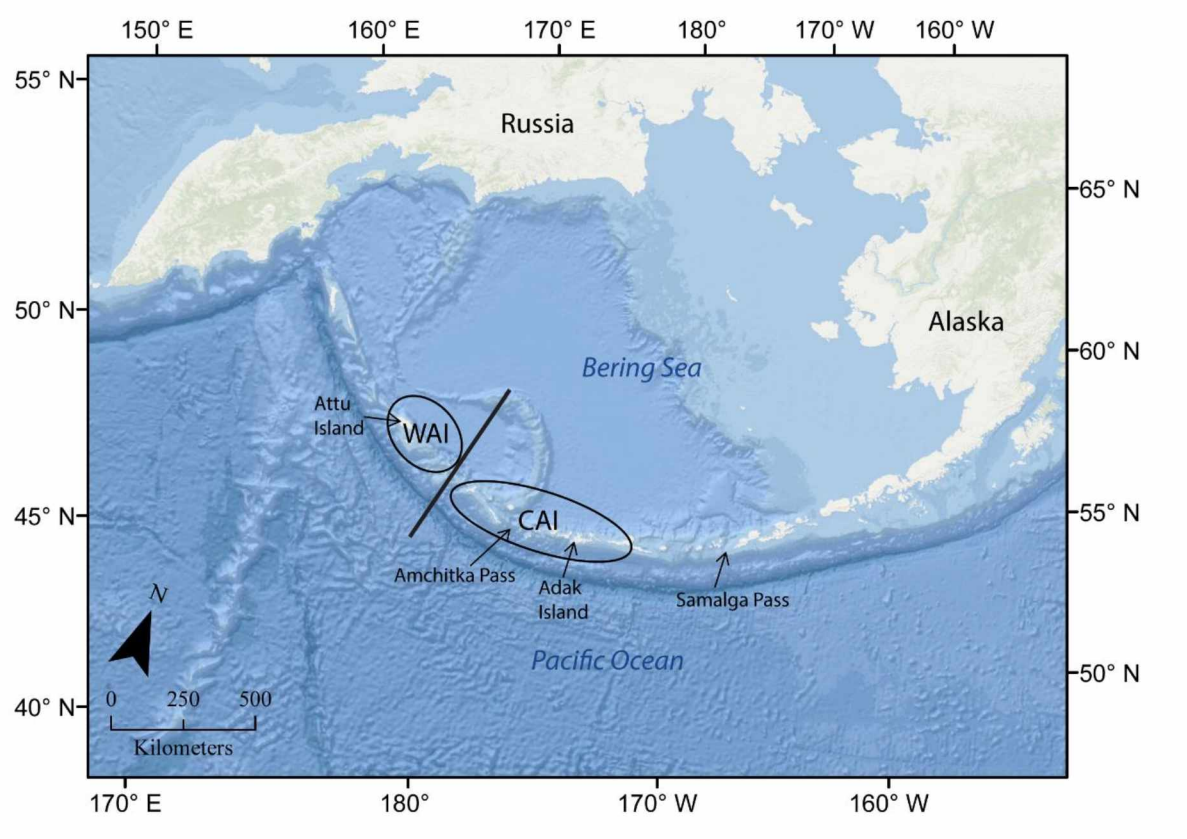

Figure 4.1 - Map depicting the approximate extent of sample collection, within the context of Steller sea lion management regions. WAI is Western Aleutian Islands, and CAI is Central Aleutian Islands.

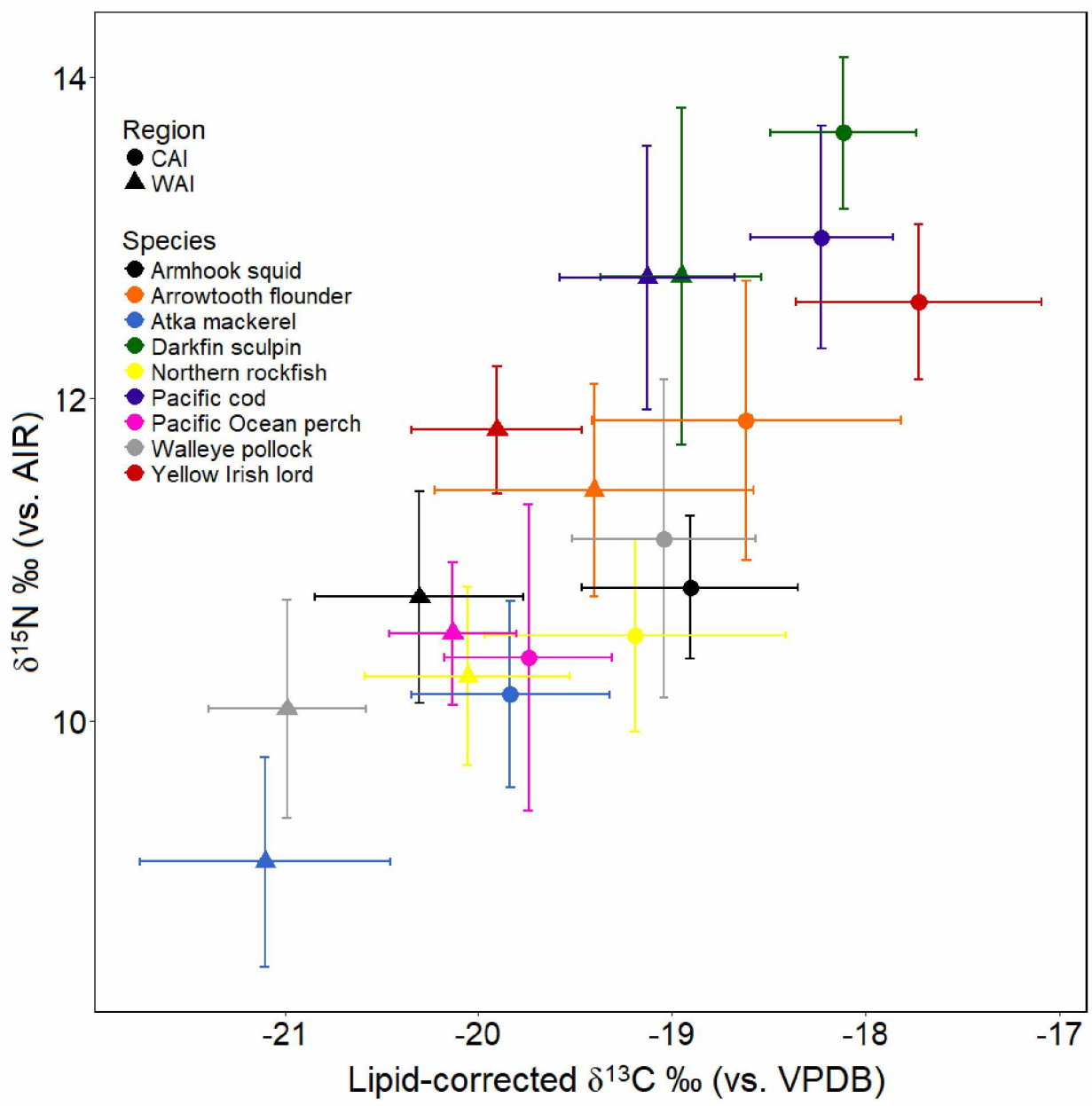

Figure 4.2 - Mean $\delta^{15}N$ and lipid-corrected $\delta^{13}C$ values (± 1 standard deviation) of muscle samples for each fish and invertebrate species, categorized by western Aleutian Islands (WAI) and central Aleutian Islands (CAI). VPDB is the isotopic standard Vienna Pee-Dee Belemnite, AIR is the isotopic standard atmospheric air.

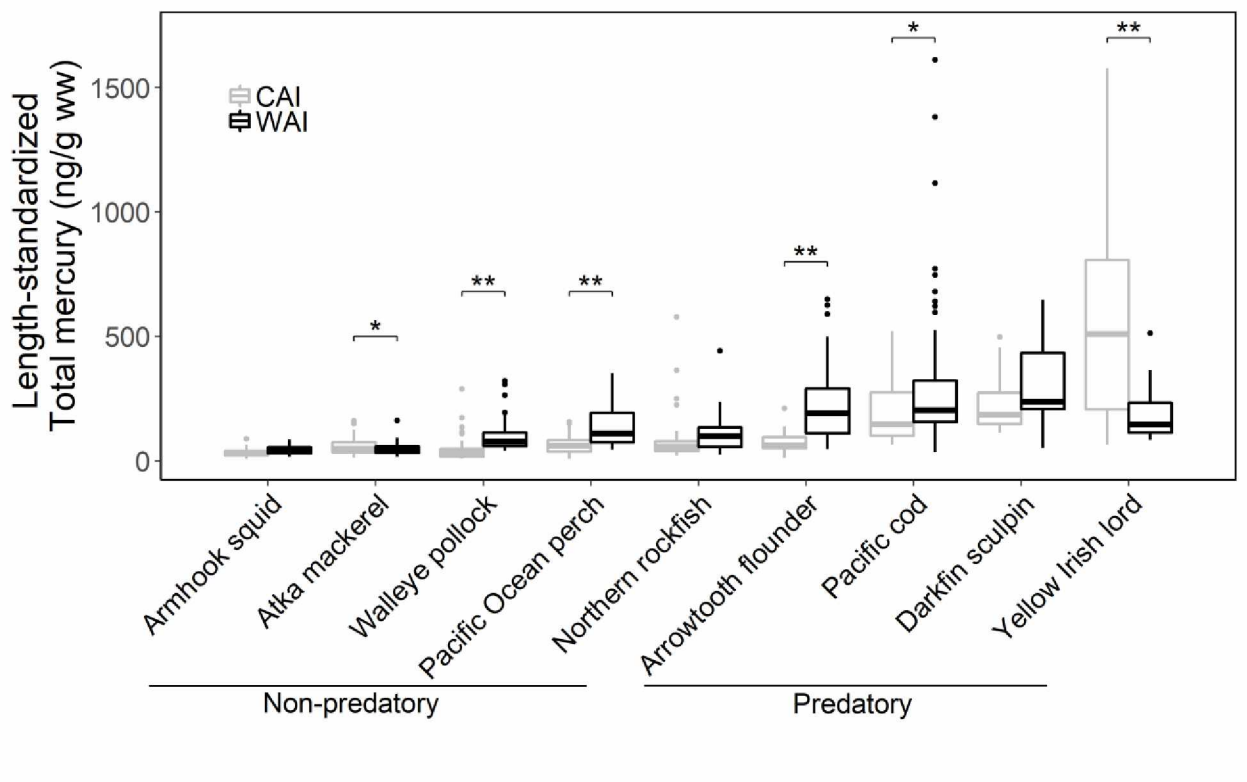

Figure 4.3 - Box and whisker plot representing the length-standardized muscle [THg] for each fish and invertebrate species, characterized by region. Data presented on a log scale on the y-axis. Bold horizontal lines inside each box represent median values, bottom and top edges of boxes represent 25th and 75th percentiles, respectively, and the ends of the vertical solid lines represent ± 1.5 * interquartile range. Length-standardized [THg] beyond this range are displayed as individual points. * denotes significance level between regions for the species indicated, $\alpha \leq 0.01$; **, denotes significance $\alpha \leq 0.001$. WAI is Western Aleutian Islands, and CAI is Central Aleutian Islands.

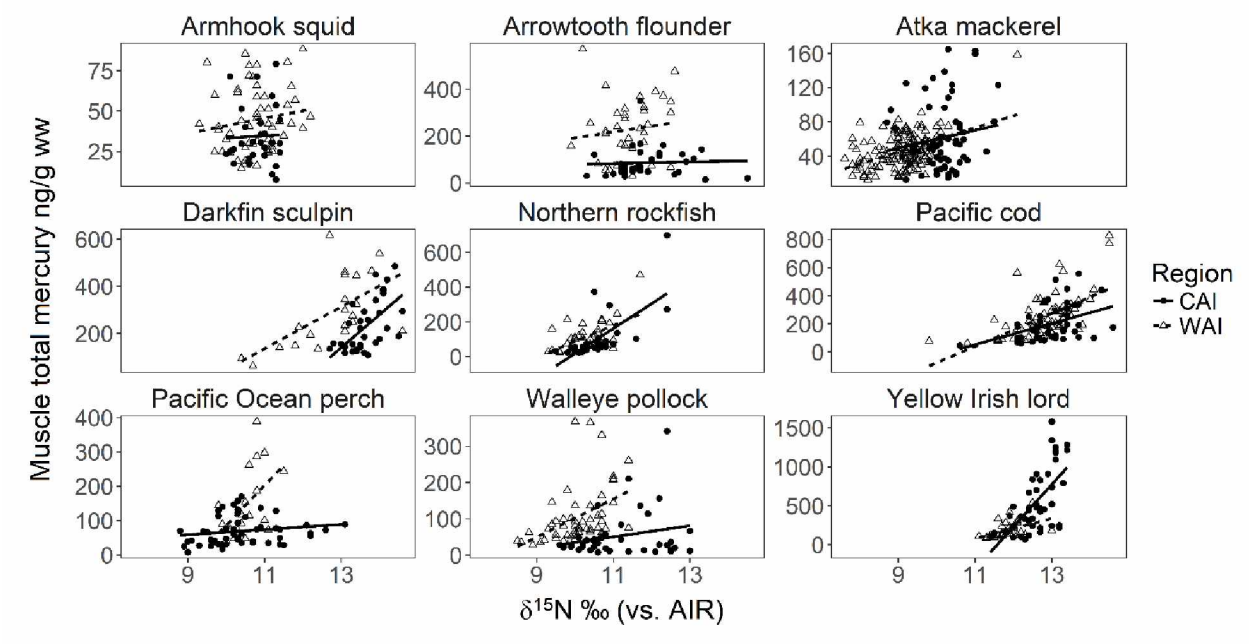

Figure 4.4 - [THg] and $\delta^{15}N$ values for muscle samples, individual species' regression slopes. WAI is Western Aleutian Islands, and CAI is Central Aleutian Islands. AIR is the isotopic standard atmospheric air.

4.10 Tables

Table 4.1 - Total mercury concentrations ([THg]) and stable nitrogen and carbon isotope values for western Aleutian Islands (WAI) and central Aleutian Islands (CAI) fishes and cephalopods. Sample sizes (N) for each region, fork length (cm), mass (g), [THg] as measured (ng/g ww), length-standardized [THg] in ng/g ww, $\delta^{15}N$ values, bulk $\delta^{13}C$ values, and lipid-corrected $\delta^{13}C$ values for each species in the dataset. Data are means ± SD, geometric mean for [THg].

Species	Region	N	Fork Length (cm)	Mass (g)	Unadjusted [THg] ng/g ww	Length-standardized [THg] ng/g ww	$\delta^{15}N$ (‰)	$\delta^{13}C$ (‰)	Lipid-corrected $\delta^{13}C$ (‰)
Armhook squid	CAI	30	22.3 ± 3.2	414.7 ± 141.6	29.1 ± 18.4	28.9 ± 18.9	10.8 ± 0.5	***-20.4 ± 0.5***	***-18.9 ± 0.6***
Berryteuthis magister	WAI	67	25.1 ± 6.2	471.6 ± 144.4	42.1 ± 22.1	39.4 ± 18.4	10.8 ± 0.7	-21.7 ± 0.5	-20.3 ± 0.5
Arrowtooth flounder	CAI	41	48.1 ± 10.2	1,226.8 ± 824.6	69.8 ± 64.0	62.4 ± 39.3	11.9 ± 0.9	***-20.4 ± 1.7***	***-18.6 ± 0.8***
Atheresthes stomias	WAI	39	***59.6 ± 17.2***	***2,705.1 ± 1,971.0***	***188.8 ± 127.9***	***184.4 ± 161.8***	11.4 ± 0.7	-22.3 ± 2.0	-19.4 ± 0.8
Atka mackerel	CAI	73	***40.2 ± 7.1***	***913.7 ± 456.8***	***50.5 ± 38.0***	***51.1 ± 37.4***	***10.2 ± 0.6***	***-22.0 ± 1.2***	***-19.8 ± 0.5***
Pleurogrammus monopterygius	WAI	148	36.8 ± 3.1	520.9 ± 239.4	42.8 ± 20.8	42.7 ± 19.4	9.1 ± 0.6	-22.8 ± 1.0	-21.1 ± 0.6
Darkfin sculpin	CAI	34	***20.2 ± 3.3***	***158.8 ± 74.3***	207.6 ± 109.7	208.0 ± 99.5	***13.7 ± 0.5***	***-19.2 ± 0.4***	***-18.1 ± 0.4***
Malacoccottus zonurus	WAI	21	16.9 ± 2.9	71.4 ± 46.3	250.2 ± 153.6	251.1 ± 158.3	12.8 ± 1.0	-20.0 ± 0.4	-19.0 ± 0.4
Northern rockfish	CAI	41	32.4 ± 3.9	485.4 ± 193.1	63.7 ± 121.0	64.3 ± 104.0	10.5 ± 0.6	***-20.3 ± 0.7***	***-19.2 ± 0.8***
Sebastes polyspinis	WAI	36	31.3 ± 3.4	496.4 ± 236.4	87.1 ± 86.8	87.6 ± 80.6	10.3 ± 0.6	-21.2 ± 0.7	-20.1 ± 0.5
Pacific cod	CAI	44	59.2 ± 11.0	2,915.9 ± 2,050.4	170.2 ± 127.6	162.5 ± 114.7	13.0 ± 0.7	***-19.3 ± 0.4***	***-18.2 ± 0.4***
Gadus macrocephalus	WAI	88	***68.9 ± 25.5***	***4,475.0 ± 4,372.7***	***225.3 ± 163.3***	***236.6 ± 279.5***	12.8 ± 0.8	-20.2 ± 0.6	-19.1 ± 0.5
Pacific Ocean perch	CAI	53	36.5 ± 2.8	700.0 ± 174.3	58.1 ± 39.9	57.5 ± 36.6	10.4 ± 1.0	***-21.4 ± 0.9***	***-19.7 ± 0.4***
Sebastes alutus	WAI	20	***39.5 ± 3.2***	***935.0 ± 306.6***	***116.1 ± 100.2***	***118.8 ± 87.3***	10.5 ± 0.4	-21.8 ± 0.8	-20.1 ± 0.3
Walleye pollock	CAI	41	54.5 ± 4.6	***1,412.2 ± 321.9***	33.7 ± 64.3	34.1 ± 87.3	***11.1 ± 1.0***	***-20.0 ± 0.5***	***-19.0 ± 0.5***
Gadus chalcogrammus	WAI	52	52.3 ± 7.5	1,051.9 ± 435.0	***85.7 ± 80.9***	***88.2 ± 62.6***	10.1 ± 0.7	-22.0 ± 0.4	-21.0 ± 0.4
Yellow Irish lord	CAI	45	***39.8 ± 3.6***	780.0 ± 225.2	***410.3 ± 408.7***	***412.2 ± 390.7***	***12.6 ± 0.5***	***-18.9 ± 0.6***	***-17.7 ± 0.6***
Hemilepidotus jordani	WAI	29	36.4 ± 5.2	627.6 ± 332.6	160.6 ± 108.9	162.9 ± 103.3	11.8 ± 0.4	-21.0 ± 0.4	-19.9 ± 0.4

Bold text indicates significant difference between WAI and CAI for the means of the given metric within a species, the larger value in bold, significance level $\alpha \leq 0.05$
WAI and CAI are Steller sea lion management sub-regions

Table 4.2 - Differences in the lipid-corrected $\delta^{13}C$ regional values (ΔCAI-WAI), and the regional difference (P values) for isotopic space comparisons for each species. Significance determined by Hotelling's T^2 test comparing mean $\delta^{15}N$ and $\delta^{13}C$ values in multivariate space.

Species	ΔCAI-WAI Lipid-corrected $\delta^{13}C$ (‰)	Isotopic space $\delta^{15}N$ ‰ and Lipid-corrected $\delta^{13}C$ (‰)
Armhook squid	1.4*	0.001
Arrowtooth flounder	0.8*	0.001
Atka mackerel	1.3*	0.001
Darkfin sculpin	0.8*	0.001
Northern rockfish	0.9*	0.001
Pacific cod	0.9*	0.001
Pacific Ocean perch	0.4*	0.01
Walleye pollock	1.9*	0.001
Yellow Irish lord	2.2*	0.001

WAI is western Aleutian Islands, CAI is central Aleutian Islands Steller sea lion management regions
* indicates a significant difference between WAI and CAI in mean lipid-corrected $\delta^{13}C$ values, $\alpha<0.05$.

Table 4.3 - Variance explained (R^2) and significance (P value) for linear regression of unadjusted total mercury concentrations ([THg]) and $\delta^{15}N$ values for western (WAI) and central (CAI) Aleutian Islands.

Species	WAI	CAI
Armhook squid	0.03 (0.2)	0.00 (0.86)
Atka mackerel	***0.17 (0.001)***	0.02 (0.28)
Arrowtooth flounder	0.01 (0.52)	0.00 (0.84)
Pacific cod	***0.51 (0.0001)***	***0.24 (0.001)***
Pacific Ocean perch	***0.27 (0.02)***	0.08 (0.06)
Walleye pollock	0.3 (0.3)	0.00 (0.6)
Darkfin sculpin	***0.55 (0.001)***	***0.36 (0.001)***
Northern rockfish	***0.35 (0.001)***	***0.62 (0.0001)***
Yellow Irish lord	***0.28 (0.01)***	***0.40 (0.0001)***

Data displayed as: R^2 (P value)
Bold text indicates significant relationship for [THg] and $\delta^{15}N$ values for each region, significance level $\alpha \leq 0.05$
WAI and CAI Steller sea lion management sub-regions

Table 4.4 - Significance (P value) from general linear models of the influence of $\delta^{15}N$ values, lipid-corrected $\delta^{13}C$ values, the interaction of $\delta^{15}N$ values and region, and the interaction of lipid-corrected $\delta^{13}C$ values and region on unadjusted total mercury concentrations ([THg]) for each fish species.

Species	$\delta^{15}N$ (‰)	Lipid-corrected $\delta^{13}C$ (‰)	Region* $\delta^{15}N$ (‰)	Region * lipid-corrected $\delta^{13}C$ (‰)
Armhook squid	n.s.	n.s.	n.s.	n.s.
Atka mackerel	n.s.	n.s.	n.s.	n.s.
Arrowtooth flounder	n.s.	0.01	n.s.	0.01
Pacific cod	0.001	0.001	n.s.	0.001
Pacific Ocean perch	0.05	0.01	n.s.	n.s.
Walleye pollock	n.s.	0.01	0.05	0.001
Darkfin sculpin	0.001	0.001	n.s.	n.s.
Northern rockfish	0.001	n.s.	n.s.	0.01
Yellow Irish lord	0.001	0.001	n.s.	0.01

n.s. indicates not significant.

4.11 Appendices

Supplemental Table 4.1 - Sample size, $\delta^{13}C_{Bulk}$ values, $\delta^{13}C_{Lipid\text{-}extracted}$ values, $C{:}N_{Bulk}$ values, $C{:}N_{Lipid\text{-}extracted}$ values, the difference in $\delta^{13}C$ values between bulk and lipid-extracted ($\Delta^{13}C$), $\delta^{13}C_{Lipid\text{-}corrected}$ values, and the difference in $\delta^{13}C$ values between lipid-extracted and lipid-corrected ($\Delta^{13}C$). Lipid-corrected values are the $\delta^{13}C$ values generated from the lipid-correction formula: $\delta^{13}C_{Lipid\text{-}corrected} = \delta^{13}C_{Bulk} - 1.48 + (0.68 * C{:}N_{Bulk})$. Data restricted to samples with $C{:}N_{Bulk} < 10$.

Species	N	$\delta^{13}C$ (‰)	Lipid-extracted $\delta^{13}C$ (‰)	Bulk C:N	Lipid-extracted C:N	Bulk – $\Delta\delta^{13}C$	Lipid-corrected $\delta^{13}C$ (‰)	Lipid-extracted $\Delta\delta^{13}C$
Armhook squid	30	-21.1 ± 0.8	-19.3 ± 0.8	3.9 ± 0.1	3.6 ± 0.0	1.8	-19.9 ± 0.8	0.6 ± 0.2
Arrowtooth flounder	24	-22.3 ± 1.6	-19.3 ± 0.5	6.5 ± 1.7	3.7 ± 0.1	3.0	-19.4 ± 0.6	0.3 ± 0.3
Atka mackerel	53	-23.0 ± 1.0	-20.5 ± 0.7	5.7 ± 1.3	3.8 ± 0.1	2.4	-20.5 ± 1.0	0.4 ± 0.3
Kamchatka flounder	8	-21.6 ± 0.4	-19.5 ± 0.3	5.5 ± 0.8	3.8 ± 0.2	2.1	-19.2 ± 0.3	0.2 ± 0.1
Northern rockfish	31	-20.9 ± 0.6	-19.9 ± 0.2	4.0 ± 0.3	3.7 ± 0.0	1.0	-19.6 ± 0.4	0.3 ± 0.2
Pacific cod	30	-19.6 ± 0.8	-18.7 ± 0.6	3.8 ± 0.3	3.6 ± 0.0	1.0	-18.5 ± 0.7	0.2 ± 0.1
Pacific Ocean perch	30	-22.1 ± 0.8	-20.1 ± 0.4	5.1 ± 0.9	3.7 ± 0.1	2.0	-20.0 ± 0.3	0.3 ± 0.2
Walleye pollock	29	-20.9 ± 1.0	-20.0 ± 1.0	3.8 ± 0.1	3.6 ± 0.0	0.8	-19.8 ± 1.0	0.3 ± 0.1

Supplemental Table 4.2 - Summary statistics of sample size (N), fork length (cm), mass (g), total mercury concentration ([THg]) in ng/g ww, $\delta^{15}N$ values, bulk $\delta^{13}C$ values, and lipid-corrected $\delta^{13}C$ values for all remaining western (WAI) and central (CAI) Aleutian Island fish and cephalopod species not included in statistical comparisons. Data are means ± SD, geometric mean for [THg].

Species	Region	N	Fork Length (cm)	Mass (g)	Unadjusted [THg] ng/g ww	$\delta^{15}N$ (‰)	$\delta^{13}C$ (‰)	Lipid-$\delta^{13}C$ (‰)
Big mouth sculpin	WAI	1	71.0	10404.0	770.6	12.0	-21.3	-19.9
Black spotted rockfish	WAI	1	30.0	374.0	200.9	12.0	-20.3	-19.1
Dusky rockfish	CAI	3	16.3 ± 1.5	na	181.8 ± 88.3	11.7 ± 0.5	-19.9 ± 0.5	-18.7 ± 0.4
Dusky rockfish	WAI	4	38.8 ± 2.2	874.0 ± 30.3	79.7 ± 109.2	10.1 ± 0.2	-21.7 ± 0.5	-20.5 ± 0.5
Pacific halibut	WAI	1	100.0	na	246.3	13.1	-20.2	-19.1.0
Kamchatka flounder	CAI	42	42.0 ± 12.4	1068.1 ± 1645.1	180.2 ± 141.5	12.2 ± 0.8	-19.8 ± 1.0	-18.5 ± 0.6
Kamchatka flounder	WAI	6	44.0 ± 13.6	1254.7 ± 1307.9	140.8 ± 73.6	12.1 ± 0.3	-21.5 ± 1.6	-19.8 ± 0.7
Longfin Irish lord	WAI	1	19.0	60.0	366.7	12.7	-19.7	-18.6
Pacific octopus	CAI	8	16.5 ± 4.4	3604.0 ± 4398.0	88.5 ± 22.1	11.2 ± 0.7	-19.8 ± 0.3	-18.7 ± 0.3
Pacific octopus	WAI	13	19.7 ± 16.3	2306.4 ± 1134.4	99.0 ± 35.5	10.8 ± 0.9	-19.9 ± 0.6	-18.7 ± 0.6
Rock sole	CAI	60	39.5 ± 2.2	681.1 ± 122.2	244.2 ± 116.3	10.5 ± 0.6	-19.4 ± 0.6	-18.3 ± 0.6
Snailfish	CAI	9	35.9 ± 6.6	916.7 ± 556.2	317.6 ± 219.3	13.1 ± 0.8	-19.3 ± 0.6	-18.1 ± 0.6
Unknown sculpin	WAI	1	22.0	na	215.3	10.7	-20.9	-19.8

na refers to no mass data available.
Samples with n = 1 do not have an associated standard deviation.

Supplemental Table 4.3 - Seasonal differences for lipid-corrected carbon ($\Delta\delta^{13}C$) and bulk nitrogen ($\Delta\delta^{15}N$) values for summer-winter for western (WAI) and central (CAI) Aleutian Islands. Significance determined by Hotelling's T^2 test comparing mean $\delta^{15}N$ and $\delta^{13}C$ values in multivariate space.

	WAI			CAI		
Species	**$\Delta\delta^{13}C$**	**$\Delta\delta^{15}N$**	**Hotelling**	**$\Delta\delta^{13}C$**	**$\Delta\delta^{15}N$**	**Hotelling**
Armhook squid	0.35	0.01	0.05	0.13	0.10	n.s.
Arrowtooth flounder	0.53	0.09	n.s.	1.19	0.95	0.001
Atka mackerel	0.35	0.03	0.01	0.22	0.39	0.01
Darkfin sculpin	0.49	0.95	ns	na	na	na
Northern rockfish	0.73	0.89	0.001	1.35	0.58	0.001
Pacific cod	0.39	0.74	0.001	0.42	0.01	0.001
Pacific Ocean perch	na	na	na	0.50	0.53	0.001
Walleye pollock	0.20	0.54	0.01	0.23	1.22	0.001
Yellow Irish lord	na	na	na	1.17	0.30	0.001

na indicates inadequate sample coverage to calculate a difference in mean values or conduct the Hotelling T^2 test.
n.s. indicates not significant

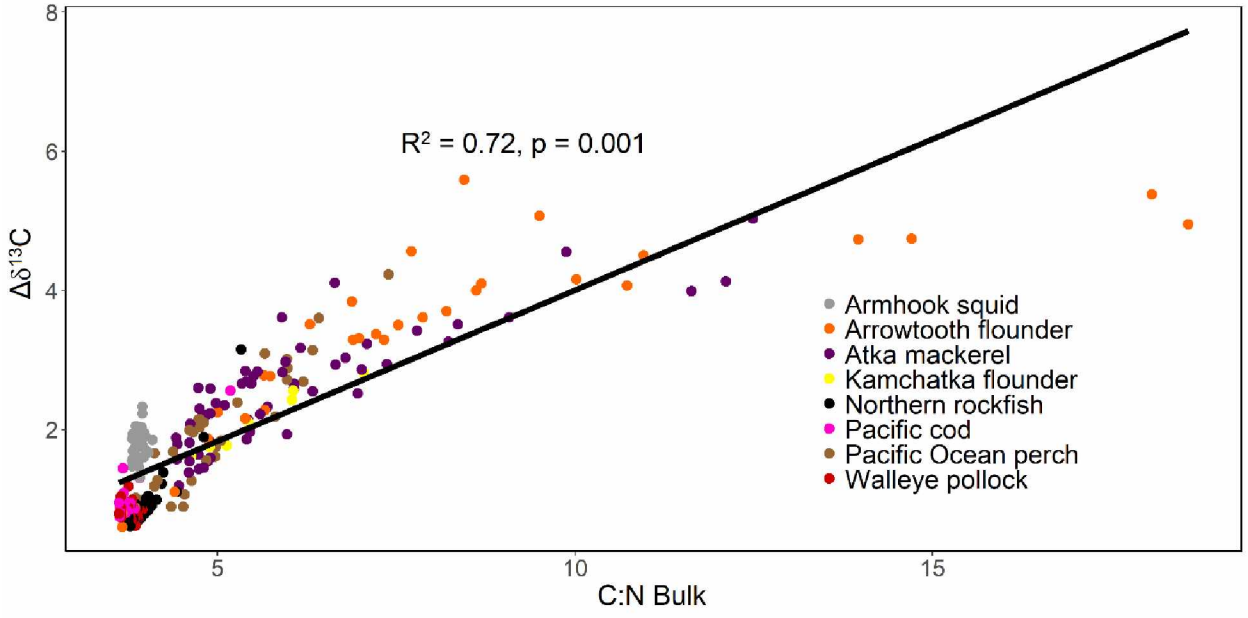

Supplementary Figure 4.1 - The difference between bulk and lipid-extracted $\delta^{13}C$ values ($\Delta^{13}C$) and $C:N_{Bulk}$ for all 245 samples.

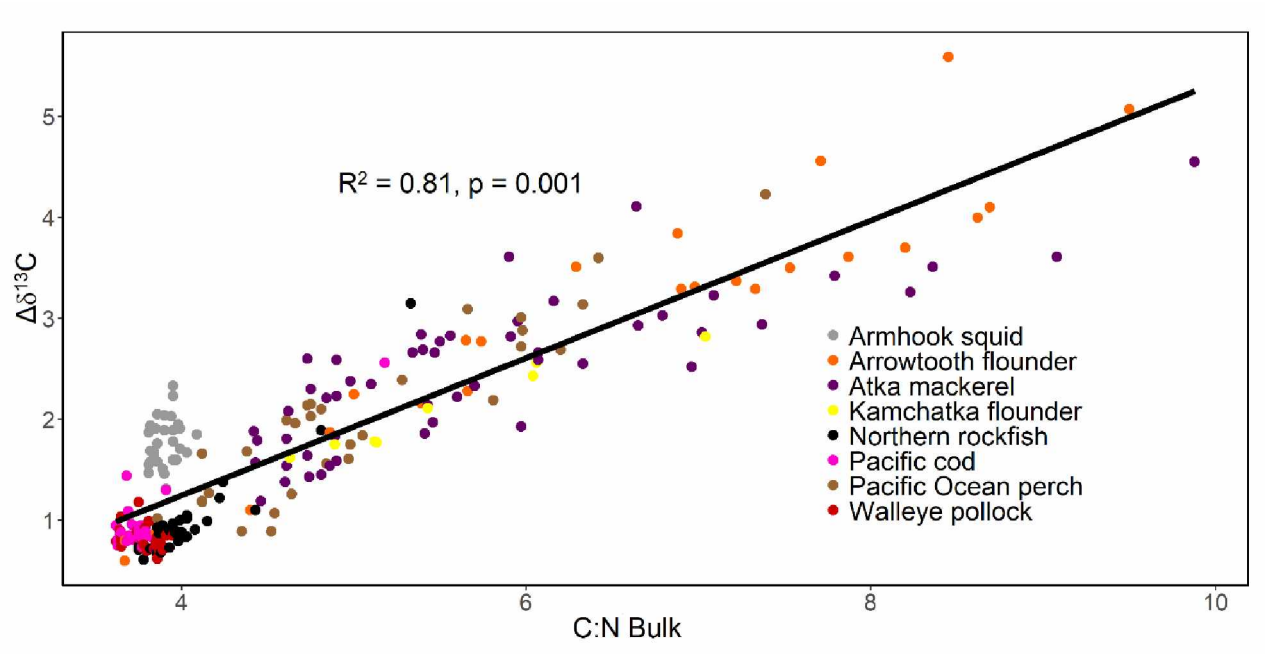

Supplementary Figure 4.2 - The difference between bulk and lipid-extracted $\delta^{13}C$ values ($\Delta^{13}C$) and $C:N_{Bulk}$ for samples with $C:N_{Bulk} < 10$.

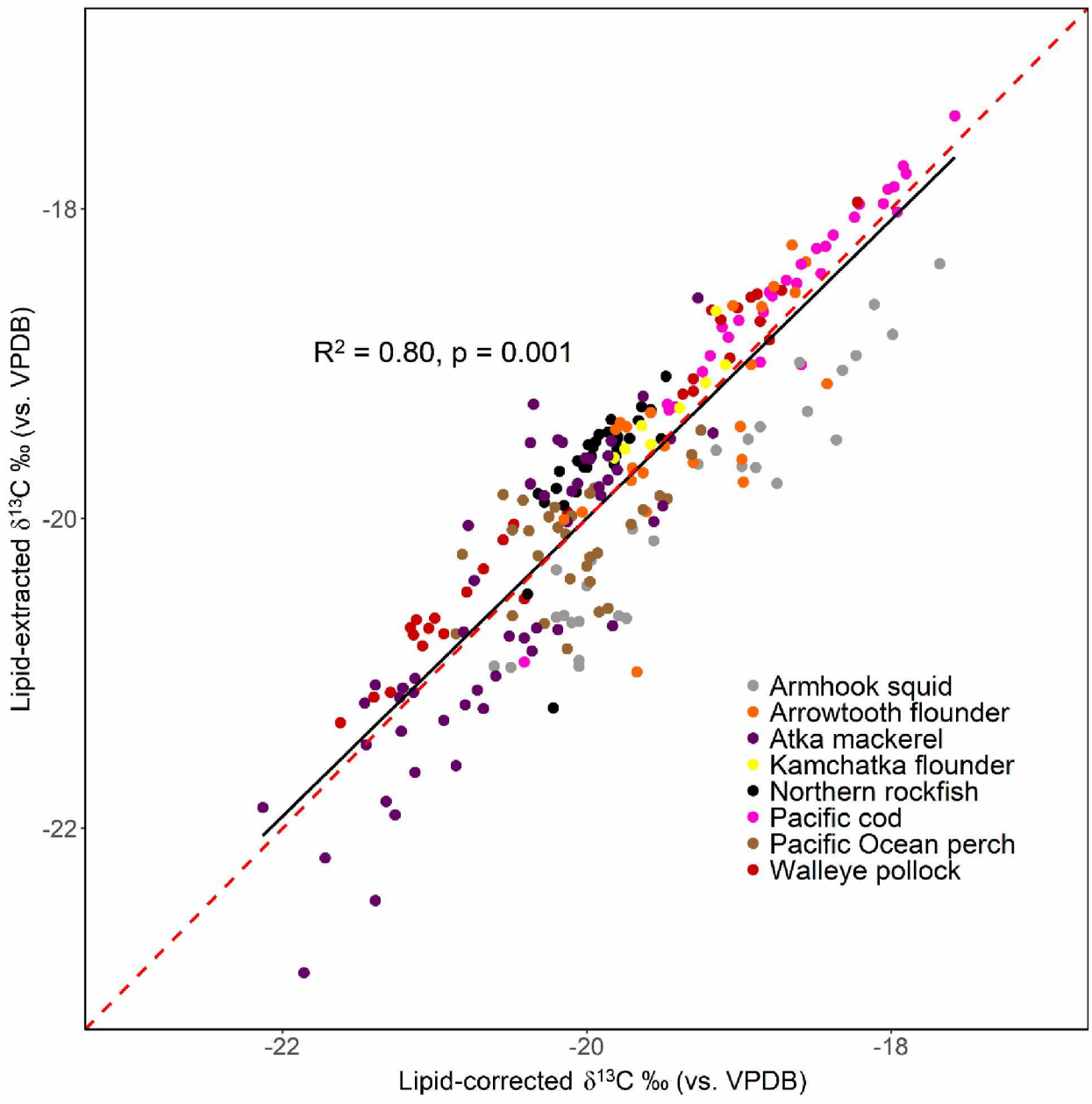

Supplementary Figure 4.3 - $\delta^{13}C_{lipid\text{-}extracted}$ values and $\delta^{13}C_{lipid\text{-}corrected}$ values, derived using the mathematical correction formula: $\delta^{13}C_{Lipid\text{-}corrected} = \delta^{13}C_{Bulk} - 1.48 + (0.65 * C{:}N_{Bulk})$. Data is restricted to $C{:}N_{Bulk} < 10$. Red dashed line is the y = x line.

4.12 Works Cited

Amlund, H., Lundebye, A.K., Berntssen, M.H.G., 2007. Accumulation and elimination of methylmercury in Atlantic cod (Gadus morhua L.) following dietary exposure. Aquat. Toxicol. 83, 323–330. doi:10.1016/j.aquatox.2007.05.008

Anthony, R.G., Miles, A.K., Ricca, M.A., Estes, J.A., 2007. Environmental contaminants in bald eagle eggs from the Aleutian archipelago. Environ. Toxicol. Chem. 26, 1843–1855. doi:10.1897/06-334R.1

Atkinson, S., DeMaster, D.P., Calkins, D.G., 2008. Anthropogenic causes of the western Steller sea lion Eumetopias jubatus population decline and their threat to recovery. Mamm. Rev. 38.

Atwell, L., Hobson, K.A., Welch, H.E., 1998. Biomagnification and bioaccumulation of mercury in an arctic marine food web: insights from stable nitrogen isotope analysis. Can. J. Fish. Aquat. Sci. 55, 1114–1121. doi:10.1139/cjfas-55-5-1114

Aydin, K., Gaichas, S., Ortiz, I., Kinzey, D., Friday, N., 2007. A comparison of the Bering Sea, Gulf of Alaska, and Aleutian Islands Large Marine Ecosystems through food web modeling. NOAA Tech. Memo. NMFS-AFSC-, 298.

Bentzen, R., Castellini, J.M., Gerlach, R., Dykstra, C., O'Hara, T., 2016. Mercury concentrations in Alaska Pacific halibut muscle relative to stable isotopes of C and N and other biological variables. Mar. Pollut. Bull. 113, 110–116. doi:10.1016/j.marpolbul.2016.08.068

Boening, D.W., 2000. Ecological effects, transport, and fate of mercury: a general review. Chemosphere 40, 1335–1351. doi:10.1016/S0045-6535(99)00283-0

Boyle, M.D., Ebert, D.A., Cailliet, G.M., 2012. Stable-isotope analysis of a deep-sea benthic-fish assemblage: evidence of an enriched benthic food web. J. Fish Biol. 80, 1485–1507. doi:10.1111/j.1095-8649.2012.03243.x

Budge, A.M., Wooller, M.J., Springer, A.M., Iverson, S.J., McRoy, C.P., Divoky, G.J., 2008. Tracing carbon flow in an arctic marine food web using fatty acid-stable isotope analysis. Oecologia 157, 117–129. doi:10.1007/s00442-008-1053-7

Burger, J., Gochfeld, M., 2007. Risk to consumers from mercury in Pacific cod (Gadus macrocephalus) from the Aleutians: fish age and size effects. Environ. Res. 105, 276–284. doi:10.1016/j.envres.2007.05.004

Burger, J., Gochfeld, M., Jeitner, C., Burke, S., Stamm, T., Snigaroff, R., Snigaroff, D., Patrick, R., Weston, J., 2007. Mercury levels and potential risk from subsistence foods from the Aleutians. Sci. Total Environ. 384, 93–105. doi:10.1016/j.scitotenv.2007.05.004

Burger, J., Gochfeld, M., Jeitner, C., Pittfield, T., Donio, M., 2014. Heavy metals in fish from the Aleutians: interspecific and locational differences. Environ. Res. 131, 119–130. doi:10.1016/j.envres.2014.02.016

Childs, E.A., Gaffke, J.N., 1973. Mercury content of Oregon groundfish. Fish. Bull. 71, 713–717.

Ciancio, J.E., Pascual, M.A., Botto, F., Frere, E., Iribarne, O., 2008. Trophic relationships of exotic anadromous salmonids in the southern Patagonian Shelf as inferred from stable isotopes. Limnol. Oceanogr. 53, 788–798. doi:10.4319/lo.2008.53.2.0788

Coelho, J.P., Mieiro, C.L., Pereira, E., Duarte, A.C., Pardal, M.A., 2013. Mercury biomagnification in a contaminated estuary food web: effects of age and trophic position using stable isotope analyses. Mar. Pollut. Bull. 69, 110–115. doi:10.1016/j.marpolbul.2013.01.021

Colombini, I., Brilli, M., Fallaci, M., Gagnarli, E., Chelazzi, L., 2011. Food webs of a sandy beach macroinvertebrate community using stable isotopes analysis. Acta Oecologica 37, 422–432. doi:10.1016/j.actao.2011.05.010

Cyr, A., Sergeant, C.J., Lopez, J.A., O'Hara, T., 2017. Assessing the influence of migration barriers and feeding ecology on total mercury concentrations in Dolly Varden (Salvelinus malma) from a glaciated and non-glaciated stream. Sci. Total Environ. 580, 710–718. doi:10.1016/j.scitotenv.2016.12.017

DeNiro, M.J., Epstein, S., 1977. Mechanism of carbon isotope fractionation associated with lipid synthesis. Science 197, 261–263. doi:10.1126/science.327543

Doi, H., Kikuchi, E., Shikano, S., Takagi, S., 2010. Differences in nitrogen and carbon stable isotopes between planktonic and benthic microalgae. Limnology 11, 185–192. doi:10.1007/s10201-009-0297-1

Doll, A.C., Taras, B.D., Stricker, C.A., Rea, L.D., O'Hara, T.M., Cyr, A.P., Mcdermott, S., Loomis, T.M., Fadley, B.S., Wunder, M.B., 2018. Temporal records of diet diversity dynamics in individual adult female Steller sea lion (Eumetopias jubatus) vibrissae. Oecologia 188, 263–275. doi:10.1007/s00442-018-4173-8

Douglas, T.A., Loseto, L.L., MacDonald, R.W., Outridge, P., Dommergue, A., Poulain, A., Amyot, M., Barkay, T., Berg, T., Chetelat, J., Constant, P., Evans, M., Ferrari, C., Gantner, N., Johnson, M.S., Kirk, J., Kroer, N., Larose, C., Lean, D., Nielsen, T.G., Poissant, L., Rognerud, S., Skov, H., Sørensen, S., Wang, F., Wilson, S., Zdanowicz, C.M., 2012. The fate of mercury in Arctic terrestrial and aquatic ecosystems, a review. Environ. Chem. 9, 321–355. doi:10.1071/EN11140

Eagles-Smith, C.A., Willacker, J.J., Flanagan Pritz, C.M., 2014. Mercury in fishes from 21 national parks in the Western United States- Inter and intra-park variation in concentrations and ecological risk: U.S. Geological Survey Open- File Report 2014-1051.

Eagles-Smith, C.A., Ackerman, J.T., Willacker, J.J., Tate, M.T., Lutz, M.A., Fleck, J.A., Stewart, A.R., Wiener, J.G., Evers, D.C., Lepak, J.M., Davis, J.A., Flanagan Pritz, C., 2016. Spatial and temporal patterns of mercury concentrations in freshwater fish across the Western United States and Canada. Sci. Total Environ. doi:10.1016/j.scitotenv.2016.03.229

Folch, J., Lees, M., Stanley, G.H.S., 1957. A simple method for the isolation and purification of total lipids from animal tissues. J Biol Chem. doi:10.1007/s10858-011-9570-9

Fox, A.L., Hughes, E.A., Trocine, R.P., Trefry, J.H., Schonberg, S. V., McTigue, N.D., Lasorsa, B.K., Konar, B., Cooper, L.W., 2014. Mercury in the northeastern Chukchi Sea: distribution patterns in seawater and sediments and biomagnification in the benthic food web. Deep. Res. Part II Top. Stud. Oceanogr. 102, 56–67. doi:10.1016/j.dsr2.2013.07.012

Fritz, L.W., Towell, R., Gelatt, T.S., Johnson, D.S., Loughlin, T.R., 2014. Recent increases in survival of western steller sea lions in Alaska and implications for recovery. Endanger. Species Res. 26, 13–24. doi:10.3354/esr00634

Fry, B., 2006. Stable Isotope Ecology. Springer Science + Business Media, LLC, New York.

Gerber, L.R., Karimi, R., Fitzgerald, T.P., 2012. Sustaining seafood for public health. Front. Ecol. Environ. 10, 487–493. doi:10.1890/120003

Gill, G.A., Fitzgerald, W.F., 1987. Mercury in surface waters of the open ocean. Global Biogeochem. Cycles 1, 199–212.

Gorbatenko, K.M., Kiyashko, S.I., Lazhentsev, A.Y., Nadtochii, V.A., Savin, A.B., 2008. Benthic-pelagic trophic interactions within the fish assemblage in the western Bering Sea shelf area according to stomach content analysis and ratios of C and N stable isotopes. Russ. J. Mar. Biol. 34, 497–506. doi:10.1134/S1063074008070092

Hamade, A.K., 2014. Fish Consumption Advice for Alaskans: A Risk Management Strategy To Optimize the Public's Health.

Harley, J., Lieske, C., Bhojwani, S., Castellini, J.M., Lopez, J.A., O'Hara, T.M., 2015. Mercury and methylmercury distribution in tissues of sculpins from the Bering Sea. Polar Biol. 38, 1535–1543. doi:10.1007/s00300-015-1716-x

Hoffman, J.C., Sutton, T.T., 2010. Lipid correction for carbon stable isotope analysis of deep-sea fishes. Deep Sea Res. Part I Oceanogr. Res. Pap. 57, 956–964. doi:10.1016/j.dsr.2010.05.003

Jarman, W.M., Hobson, K.A., Sydeman, W.J., Bacon, C.E., McLaren, E.B., 1996. Influence of trophic position and feeding location on contaminant levels in the Gulf of the Farallones food web revealed by stable isotope analysis. Environ. Sci. Technol. 30, 654–660. doi:10.1021/es950392n

Johnson, N.W., Mitchell, C.P.J., Engstrom, D.R., Bailey, L.T., Coleman Wasik, J.K., Berndt, M.E., 2016. Methylmercury production in a chronically sulfate-impacted sub-boreal wetland. Environ. Sci. Process. Impacts 18, 725–734. doi:10.1039/C6EM00138F

Kelly, C.A., Rudd, J.W.M., Holoka, M.H., 2003. Effect of pH on mercury uptake by an aquatic bacterium: implications for Hg cycling. Environ. Sci. Technol. 37, 2941–2946. doi:10.1021/es026366o

Lange, T.R., Royals, H.E., Connor, L.L., 1994. Mercury accumulation in largemouth bass (Micropterus salmoides) in a Florida lake. Arch. Environ. Contam. Toxicol. 27, 466–471.

Laurier, F.J.G., Mason, R.P., Gill, G.A., Whalin, L., 2004. Mercury distributions in the North Pacific Ocean - 20 Years of observations. Mar. Chem. 90, 3–19. doi:10.1016/j.marchem.2004.02.025

Lehnherr, I., 2014. Methylmercury biogeochemistry: a review with special reference to Arctic aquatic ecosystems. Environ. Rev. 22, 229–243. doi:10.1139/er-2013-0059

Logerwell, E.A., Aydin, K., Barbeaux, S., Brown, E., Conners, M.E., Lowe, S., Orr, J.W., Ortiz, I., Reuter, R., Spencer, P., 2005. Geographic patterns in the demersal ichthyofauna of the Aleutian Islands. Fish. Oceanogr. 14, 93–112.

Lushchak, V.I., 2011. Environmentally induced oxidative stress in aquatic animals. Aquat. Toxicol. 101, 13–30. doi:10.1016/j.aquatox.2010.10.006

Marsh, J.M., Hillgruber, N., Foy, R.J., Marsh, J.M., Hillgruber, N., Temporal, R.J.F., Marsh, J.M., Hillgruber, N., Foy, R.J., 2012. Temporal and Ontogenetic Variability in Trophic Role of Four Groundfish Species — Walleye Pollock , Pacific Cod , Arrowtooth Flounder , and Pacific Halibut — around Kodiak Island in the Gulf of Alaska. Trans. Am. Fish. Soc. 8487. doi:10.1080/00028487.2012.667042

McGrew, A.K., Ballweber, L.R., Moses, S.K., Stricker, C.A., Beckmen, K.B., Salman, M.D., O'Hara, T.M., 2014. Mercury in gray wolves (Canis lupus) in Alaska: increased exposure through consumption of marine prey. Sci. Total Environ. 468–469, 609–613. doi:10.1016/j.scitotenv.2013.08.045

National Research Council, 2003. The Decline of the Steller Sea Lion in Alaskan Waters: Untangling Food Webs and Fishing Nets. National Academy of Sciences, Washington, D.C.

NMFS, 2013. Draft status review of the eastern distinct population segment of Steller sea lion (Eumetopias jubatus), Protected Resources Division, Alaska Region, National Marine Fisheries Service, 709 W 9th St., Juneau, AK 99802.

Peterson, B.J., Fry, B., 1987. Stable isotopes in ecosystem studies. Ann. Rev. Ecol. Syst 18, 293–320. doi:10.1146/annurev.es.18.110187.001453

Post, D.M., Layman, C.A., Arrington, D.A., Takimoto, G., Quattrochi, J., Montaña, C.G., 2007. Getting to the fat of the matter: models, methods and assumptions for dealing with lipids in stable isotope analyses. Oecologia 152, 179–189. doi:10.1007/s00442-006-0630-x

Power, M., Klein, G.M., Guiguer, K.R.R.A., Kwan, M.K.H., 2002. Mercury accumulation in the fish community of a sub-Arctic lake in relation to trophic position and carbon sources. J. Appl. Ecol. 39, 819–830. doi:10.1046/j.1365-2664.2002.00758.x

Rea, L.D., Castellini, J.M., Correa, L., Fadely, B.S., O'Hara, T.M., 2013. Maternal Steller sea lion diets elevate fetal mercury concentrations in an area of population decline. Sci. Total Environ. 454–455, 277–282. doi:10.1016/j.scitotenv.2013.02.095

Rea, L.D., Christ, A.M., Hayden, A.B., Stegall, V.K., Farley, S.D., Stricker, C.A., Mellish, J.A.E., Maniscalco, J.M., Waite, J.N., Burkanov, V.N., Pitcher, K.W., 2015. Age-specific vibrissae growth rates: a tool for determining the timing of ecologically important events in Steller sea lions. Mar. Mammal Sci. 31, 1213–1233. doi:10.1111/mms.12221

Ricca, M.A., Keith Miles, A., Anthony, R.G., 2008. Sources of organochlorine contaminants and mercury in seabirds from the Aleutian archipelago of Alaska: inferences from spatial and trophic variation. Sci. Total Environ. 406, 308–323. doi:10.1016/j.scitotenv.2008.06.030

Schell, D.M., Barnett, B.A., Vinette, K.A., 1998. Carbon and nitrogen isotope ratios in zooplankton of the Bering, Chukchi and Beaufort seas. Mar. Ecol. Prog. Ser. 162, 11–23. doi:10.3354/meps162011

Selin, N.E., 2009. Global biogeochemical cycling of mercury: a review. Annu. Rev. Environ. Resour. 34, 43–63. doi:10.1146/annurev.environ.051308.084314

State of Alaska, 2017. Total Mercury in Alaska's Fish. Anchorage, Alaska.

State of Alaska, 2015. 2001-2012 Total mercury in Alaska Fish [WWW Document]. URL http://dhss.alaska.gov/dph/Epi/eph/Pages/fish/default.aspx (accessed 2.15.18).

Strode, S.A., Jaegle, L., Jaffe, D.A., Swartzendruber, P.C., Selin, N.E., Holmes, C., Yantosca, R.M., 2008. Trans-Pacific transport of mercury. J. Geophys. Res. 113, 1–12. doi:10.1029/2007JD009428

Sunderland, E.M., Krabbenhoft, D.P., Moreau, J.W., Strode, S. a., Landing, W.M., 2009. Mercury sources, distribution, and bioavailability in the North Pacific Ocean: Insights from data and models. Global Biogeochem. Cycles 23, n/a-n/a. doi:10.1029/2008GB003425

Sweeting, C.J., Polunin, N.V.C., Jennings, S., 2006. Effects of chemical lipid extraction and arithmetic lipid correction on stable isotope ratios of fish tissues. Rapid Commun. Mass Spectrom. 20, 595–601. doi:10.1002/rcm.2347

TenBrink, T.T., Aydin, K.Y., 2009. Life History Traits of Sculpins in the Eastern Bering Sea and Aleutian Islands.

TenBrink, T.T., Buckley, T.W., 2013. Life-history aspects of the Yellow Irish Lord (Hemilepidotus jordani) in the Eastern Bering Sea and Aleutian Islands. Northwest. Nat. 94, 126–136. doi:10.1898/12-33.1

Trudel, M., Rasmussen, J.B., 1997. Modeling the elimination of mercury by fish. Environ. Sci. Technol. 31, 1716–1722. doi:10.1021/es960609t

Vander Zanden, J., Rasmussen, J.B., 2001. Variation in d15N and 13C trophic fractionation: implications for aquatic food web studies. Limnol. Oceanogr. 46, 2061–2066.

Walker, C.H., Sibly, R.M., Hopkin, S.P., Peakall, D.B., 2012. Principles of Ecotoxicology, 4th ed. CRC Press, Boca Raton, FL.

Wang, S.W., Budge, S.M., Gradinger, R.R., Iken, K., Wooller, M.J., 2014. Fatty acid and stable isotope characteristics of sea ice and pelagic particulate organic matter in the Bering Sea: tools for estimating sea ice algal contribution to Arctic food web production. Oecologia 174, 699–712. doi:10.1007/s00442-013-2832-3

Ward, D.M., Nislow, K.H., Folt, C.L., 2010. Bioaccumulation syndrome: identifying factors that make some stream food webs prone to elevated mercury bioaccumulation. Ann. N. Y. Acad. Sci. 1195, 62–83. doi:10.1111/j.1749-6632.2010.05456.x

Willacker, J.J., von Hippel, F.A., Ackerly, K.L., O'Hara, T.M., 2013. Habitat-specific foraging and sex determine mercury concentrations in sympatric benthic and limnetic ecotypes of threespine stickleback. Environ. Toxicol. Chem. 32, 1623–1630. doi:10.1002/etc.2213

Yang, M.-S., Nelson, M.W., 1999. Food habits of the commercially important groundfishes in the Gulf of Alaska in 1990, 1993, and 1996, NOAA Technical Memorandum.

Yang, M.S., 2003. Food habits of important groundfishes in the Aleutian Islands in 1994 and 1997, AFSC Processed Report.

York, A.E., Merrick, R.L., Loughlin, T.R., 1996. An analysis of the Steller sea lion metapopulation in Alaska, in: McCullough, D.R. (Ed.), Metapopulations and Wildlife Conservation. Island Press, Washington, D.C., p. Pp. 259-292.

Chapter 5 - **Mercury concentrations in subsistence fish from Kotzebue Sound, Alaska: Community-based effort to understand drivers and public health**[5]

[5]Cyr, A., López, J.A., Wooller, M.J., Whiting, A., Gerlach, R., O'Hara, T. *In preparation*. Mercury concentrations in subsistence fish from Kotzebue Sound, Alaska: Community-based effort to understand drivers and public health significance. Science of the Total Environment

5.1 Abstract

The State of Alaska (SOA) assesses mercury (Hg) exposure from consumption of fish using a variety of approaches, including determination of concentrations of Hg ([Hg]) in the edible tissue (e.g., muscle) of consumed fish. The SOA programs have produced restricted consumption guidelines specifically for women of childbearing age and children in Alaska for some species of fish (e.g., some sharks), while unlimited consumption is suggested for many other fish species. These consumption guidelines have subsequently produced questions regarding the ecological drivers that influence [Hg] in fishes of dietary importance to Alaskans. This study represents a community-based effort to evaluate [Hg] in fishes from Kotzebue Sound (Alaska) and to examine potential drivers of the observed concentrations. We examined 297 individuals of marine fish, representing eight different species (Bering cisco, chum salmon, Pacific herring, humpback whitefish, sheefish, starry flounder, Pacific tomcod, and fourhorn sculpin), from Kotzebue Sound and report total Hg concentrations ([THg]) and monomethyl Hg^{+} concentrations ([$MeHg^{+}$])] in the context of factors (i.e. species, fork length, $\delta^{15}N$ and $\delta^{13}C$ values) thought to influence Hg accumulation. As expected, [THg] was positively correlated with fork length in six of the eight species analyzed, as well as with trophic level, as indicated by $\delta^{15}N$ values, in five of the eight species. [$MeHg^{+}$] was positively correlated with fork length in four of seven individual species measured for [$MeHg^{+}$] and with $\delta^{15}N$ values in the overall sample of fish species (all species), and specifically for three individual species. In six of the seven species studied, %MeHg was >80% of [THg]. This value decreased with fork length in three species, and there was no relationship with $\delta^{15}N$ values in any species. Comparison of models using AICc revealed no clear preferred model explaining [THg]. However, fork length was more commonly included among top ranked models than $\delta^{15}N$ or $\delta^{13}C$ values. The food web magnification factor for THg was 11.3, and for 12.6 for $MeHg^{+}$, indicating biomagnification is likely driving [THg] and [$MeHg^{+}$] over the entire food web; however, within species bioaccumulation is likely a stronger driver of [THg] and [$MeHg^{+}$] than feeding ecology or trophic position. All fish were considered safe for human consumption based on the State of Alaska fish consumption guidelines, with 98.7% of fish below the unrestricted consumption criteria of 200 ng of THg/g weight wet.

5.2 Introduction

Fishes are a pivotal component of the diet, culture, ancestral knowledge, and economy in rural coastal and riparian Alaska (Hamade, 2014). The community of Kotzebue, located on the northwestern tip of the Baldwin Peninsula in eastern Kotzebue Sound, an inlet in the southeastern Chukchi Sea, is a rural community that typifies fisher and subsistence lifestyles common in the Arctic. Kotzebue Sound serves as a highway and lifeline for the residents of the area and provides subsistence and commercial resources for almost 8,000 people (United States Census Bureau, 2017). Residents have a connection to fish throughout the year and this constant connection is built from diverse harvest practices, consumption preferences, and cultural traditions (Johnson et al., 2009). In these remote areas of Alaska and the circumpolar north, fish provide multiple nutritional benefits including calories, protein, long chain omega-3 polyunsaturated fatty acids, essential amino acids, vitamins A and D, selenium (Se), and iodine (Gribble et al., 2016). It is estimated that fish and marine mammals constitute 70% of the subsistence foods harvested by residents of Kotzebue and surrounding areas (Whiting, 2006). Across Alaska, subsistence consumption of fish has been estimated to account for more than 100 kg of finfish per person annually (Fall, 2018; R.J. Wolfe, 2000).

Some fish can be a significant route of exposure to Hg (AMAP, 2011; Hamade, 2014; Suchanek et al., 2008). Hg accumulates in some fish tissues mostly as the monomethyl mercury ($MeHg^+$) form. $MeHg^+$ is a global contaminant with high dietary bioavailability (Wang, 2012), crossing the blood brain barrier and placenta (Bridges and Zalups, 2005) and at certain exposure levels causes neurotoxic effects (Walker et al., 2012) and oxidative stress (Lushchak, 2011). The percent of total Hg (THg) that is $MeHg^+$ ($\%MeHg^+$) in some fish tissues has been measured to be greater than 80% (Dang and Wang, 2012; Jewett et al., 2003; Jewett and Duffy, 2007; Wagemann et al., 1997), a proportion that fuels public health concern surrounding dietary exposure to Hg (Hamade, 2014; Jewett and Duffy, 2007; Syversen and Kaur, 2012). Hg has been detected in nearly every fish tested including freshwater and marine species found around the circumpolar north (AMAP, 2011; Eagles-Smith et al., 2016). As a result, Hg is responsible for

over 80% of fish consumption advisories in the United States and Canada (Environment Canada, 2013; USEPA, 2011). The State of Alaska's Fish Monitoring Program measures trace elements (THg, $MeHg^+$, arsenic, Se, copper, lead, and cadmium) and a suite of persistent organic pollutants in important commercial, subsistence, and recreational fish and shellfish species to monitor spatial and temporal trends in fish of Alaska (Hamade, 2014). Presently the only consumption restrictions in Alaska have been placed on certain species of finfish (i.e., some halibut and sharks), specifically for women of childbearing age and children in Alaska.

$MeHg^+$ varyingly bioaccumulates in fish across species and regions, driven by numerous environmental factors and varying diet composition (Eagles-Smith et al., 2016). Relevant factors include differences in the amount of inorganic Hg present in an area, which is driven by the proximity to Hg sources, such as cinnabar ore (Carrie et al., 2012), volcanoes (Nriagu and Becker, 2003; Pyle and Mather, 2003), and some mining activities (AMAP, 2011; Goldfarb et al., 2007; Rytuba, 2003). Hg can enter ecosystems far from natural or anthropogenic sources via long range atmospheric transport (Chen et al., 2014). Conditions that affect the methylation of Hg, such as temperature (Bodaly et al., 1993; Johnson et al., 2016), the presence of dissolved ligands (Boening, 2000; Daguené et al., 2012; Douglas et al., 2012) or organic matter (Chiasson-Gould et al., 2014; Gu et al., 2012), and water pH (Kelly et al., 2003), can also influence the bioavailability of $MeHg^+$. Finally, [$MeHg^+$] in fishes is influenced by several drivers, such as fish size, age, feeding ecology, and feeding location. Access to different prey resources can also result in significant differences in Hg concentrations in the same fish species (Cyr et al., 2017). Sources of Hg, in conjunction with the varying influences of atmospheric dispersal of Hg and variation in species-specific feeding ecology, can result in differences in [THg] and [$MeHg^+$] across fish sizes, cohorts, species, and geographic regions. Understanding the differences of observed [THg] and [$MeHg^+$] in some of the fish species from Kotzebue Sound can assist in determining potential drivers of THg and $MeHg^+$ accumulation in those fish. This information is important for fish consumption advice, including potential age or size class considerations, regional differences, or species-specific concerns.

The carbon and nitrogen stable isotope composition of some tissues provide insights on the feeding ecology of an organism as a result of the fractionation of stable isotopes as these elements move through food webs. Stable carbon and nitrogen isotope data can also provide insight as to how feeding ecology and location influences [$MeHg^+$] in fishes (Cyr et al., 2017; Power et al., 2002; Willacker et al., 2013). For example, stable nitrogen isotopes ratios (expressed as $\delta^{15}N$ values) can be used to estimate trophic position (Peterson and Fry, 1987). Stable carbon isotope ratios (expressed as $\delta^{13}C$ values) can be used to differentiate sources of the primary production for a food web (Fry, 2006; Peterson and Fry, 1987), such as marine versus terrestrial (McGrew et al., 2014), or benthic versus pelagic (Boyle et al., 2012; Doi et al., 2010). Together, carbon and nitrogen stable isotope values are a useful ecological tool to understand how observed [THg] in fishes may be influenced by either feeding ecology and/or feeding location.

To assess how these ecological and biological factors drive [THg] and [$MeHg^+$], we studied the role of fork length and feeding ecology in influencing observed [THg] and [$MeHg^+$]. We measured concentrations of Hg ([THg] and [$MeHg^+$]) and determined carbon and nitrogen stable isotope values in select subsistence fish species from Kotzebue Sound. Our focus was on species of importance for human consumption or frequently caught as part of subsistence fishing activities. We report [THg], [$MeHg^+$], $\delta^{13}C$ and $\delta^{15}N$ values, and basic morphological measurements to better understand the feeding ecology in relation to Hg in fishes from Kotzebue Sound, AK that directly involves the community and assists with public health information. Finally, we interpret the [THg] and [$MeHg^+$] of Kotzebue Sound fishes in the context of published fish consumption guidelines from the SOA (Hamade, 2014).

5.3 Methods

5.3.1 Study location and fish sampling

Fish were donated by subsistence fishers (hook and line, beach seine, or gill net) during August and December of 2015, and April of 2016 and 2018. All fish were caught in Kotzebue Sound, within 15

km of the city of Kotzebue (Figure 5.1). Fish were frozen whole (intact), except when noted, either outside while on the sea ice or in a -20°C freezer and kept frozen until processed for Hg and stable isotope (carbon and nitrogen) analyses. Species sampled included Bering cisco (*Coregonus laurettae*, n = 93), chum salmon (*Oncorhynchus keta*, n = 21), Pacific herring (*Clupea pallasii*, n = 29), humpback whitefish (*Coregonus pidschian*, n = 28), sheefish (*Stenodus leucichthys*, n = 50), starry flounder (*Platichthys stellatus*, n = 24), Pacific tomcod (*Microgadus proximus*, n = 14), and fourhorn sculpin (*Myoxocephalus quadricornis*, n = 36). All species were identified using diagnostic morphological features.

5.3.2 Fish processing

Fork length (FL; in cm) and wet mass (M; in g) were determined using thawed fish. Sixteen sheefish processed by subsistence users were subsampled in the field. No length or weight measurements are available for these fish. Approximately 5 g of muscle tissue were removed from the left lateral side of the fish, ventral to the dorsal fin. Tissue samples were freeze dried (Labcono, FreeZone 6.0 Liter) for a minimum of 48 h to determine water content and homogenized using a stainless-steel ball grinder (Retsch, CryoMill). Percent moisture was determined by the following calculation:

$$\left(\frac{wet\ weight - dry\ weight}{wet\ weight}\right) * 100 \text{ (Equation 5.1)}$$

5.3.3 Total Hg concentration ([THg]) analysis

Freeze dried samples were analyzed using a Milestone DMA-80 instrument, U.S. EPA method #7473-EPA30B, 2007 SW 846, and reported as THg ng/g wet weight (ww) based on percent water values determined during the drying process. The method detection limit for [THg] determination for muscle was 2 ng/g ww, following the formula:

$$\left(\frac{0.5\ (g)}{Sample\ mass\ dry\ weight\ (g)}\right) * (1 - sample\ \%\ H2O) \text{ (Equation 5.2)}$$

Quality assurance and quality control measures were based on method blanks, Standard Reference Materials (SRMs) of similar matrices, and check standards. All samples were analyzed in triplicate, with the sample relative standard deviation among replicates (RSD; 100 * SD/$\bar{x}$) <10%. SRMs included DORM-4 (National Resource Council Canada; 410 ± 55 ng/g) and Lake Superior Fish (LSF; National Institute of Standards and Technology, Standard Reference Material® 1946; 433 ± 9 ng/g ww). Mean percent recoveries (± SD) were 100 ng/g (liquid standard), 95.9 ± 9.9%; DORM-4, 93.3 ± 4.7%; and LSF, 95.4 ± 6.7 %.

5.3.4 Monomethylmercury concentration ([$MeHg^+$]) analysis

Monomethylmercury determined in a subset of 153 samples, representing seven species (Table 1). Samples for $MeHg^+$ analysis were digested following methods detailed in Bloom (1989). Briefly, depending on [THg], 0.01–0.2 g of sample was digested in a solution of 25% potassium hydroxide (KOH) dissolved in methanol and analyzed within 2 weeks. Aliquots of digested samples and SRMs were analyzed on the Brooks Rand methylmercury cold vapor atomic fluorescence spectroscopy (CVAFS) detection system using a 7-point calibration curve. The [$MeHg^+$] was determined using the Brooks Rand Modell III detector, using the EPA method 1630 modified to incorporate the Brooks Rand MERX autosampler (USEPA, 1998; Harley et al., 2015) .

Duplicate measurements of each sample were obtained with observed RSD among sample replicates <15%. Quality assurance and quality control measures were based on method blanks, Standard Reference Materials (SRMs) and check standards. SRMs used were DORM-4 (National Resource Council Canada; 354 ± 15 ng/g ww) and LSF (394 ± 28 ng/g ww). Mean percent recoveries (± SD) were: 1 ng/g, 97.5 ± 6.8%; DORM-4, 101.2 ± 5.1%; and LSF, 102.3 ± 12.9%.

5.3.5 Carbon and nitrogen stable isotope analysis

Stable carbon and nitrogen isotope ratios in all sampled fish were measured as described in Cyr et al. (2017) at the Alaska Stable Isotope Facility (University of Alaska Fairbanks). Between 0.2 and 0.5 mg

of freeze-dried homogenized muscle was analyzed using continuous-flow isotope ratio mass spectrometry (CF-IRMS, Thermo DeltaVPlus interfaced with a Costech ESC 4010 elemental analyzer using a ConfloIV system). Stable isotope ratios are expressed in δ notation as parts per thousand (‰) relative to international standards (Vienna PeeDee Belemnite – VPDB for carbon and AIR for nitrogen):

$$\delta X‰ = \left[\left(\frac{R_{Sample}}{R_{Standard}}\right) - 1\right] * 1000 \text{ (Equation 5.3)}$$

Where *X* is the element of interest, *R* is the ratio of the heavy to light isotope measured for that element, *Sample* is the sample of interest, and *Standard* is the standard used, VPDB for carbon or AIR for nitrogen. Reference checks using peptone (No. P-7750 meat-based protein. Sigma Chemical Company, Lot #76f-0300) were run every 10th sample, and blanks every 20th sample, with instrument precision typically <0.2 ‰ for both carbon and nitrogen.

5.3.6 Lipid correction

To correct for the influence of lipids on carbon stable isotope values, we used the lipid-correction formula for Bering Sea and Arctic fishes developed in Chapter 4, which followed and amended the methods detailed in Post et al. (2007). All samples had $C{:}N_{Bulk} < 9.0$, so no samples were removed from the correction formula and subsequent analysis. The lipid correction formula is as follows:

$$\delta^{13}C_{Lipid\text{-}corrected} = \delta^{13}C_{Bulk} - 1.48 + (0.65 * C{:}N_{Bulk}) \text{ (Equation 5.4)}$$

5.3.7 Sheefish otolith age estimation

The sagittal otoliths from 37 sheefish were extracted, cleaned and stored, then processed for age estimation using the "break and burn" technique (Barber and McFarlane, 1987), by the contract lab "Mictrotech". When possible, the left sagittal otolith was cracked along the transverse plane using nail clippers, with one half held over an alcohol flame for a short time to obtain a dark brown color. The charred surface was covered with mineral oil to reveal the alternating hyaline and opaque growth rings. The otolith sections were viewed using a Leica MS5 binocular microscope at magnification ranging from

10X to 64X. The 'topography' (smoothness, luster, and opalescence) of the alternating growth rings were used for enumeration of annual growth increments and growth pattern information.

5.3.8 Statistical analysis

All analyses were performed using R statistical computing software (R Core Team, 2017). All data were checked for normality using visual inspection of histograms, normal quantile-quantile plots, residual plots, and the Shapiro-Wilk test for regression models. The THg measurement for one chum salmon (4.5% of chum salmon sample), the $\%MeHg^+$ measurements of sixteen samples from six of the species (10.3% of total fishes sampled; eight low $\%MeHg^+$ and eight high $\%MeHg^+$), and one sheefish (extreme outlier for [THg] [$MeHg^+$]) were removed from regression analyses as they were considered outliers based on the 95% confidence interval for that species and variable. Summary statistics (all samples including outliers) are represented as mean ± standard deviation (SD). Outliers are discussed as case studies in the discussion.

Bulk $\delta^{13}C$ values and lipid-corrected $\delta^{13}C$ values from each species were compared using t-tests ($\alpha \leq 0.05$). $\%MeHg^+$ of THg was calculated using two methods, first by calculating the $\%MeHg^+$ for each fish and then calculating the arithmetic mean for each species, and second by following the methods detailed in Wagemann et al. (1997), using the slope of the robust linear regression for [$MeHg^+$] and [THg]. Species comparisons and rank order for [THg], [$MeHg^+$], %MeHg, $\delta^{15}N$ values, and $\delta^{13}C$ values were determined using an ANOVA followed by a Tukey's honest significant difference (HSD) *post hoc* test. Results were considered significant at $\alpha \leq 0.05$. General linear models assessed relationships between [THg] and [$MeHg^+$] with fork length, $\delta^{15}N$ values, and lipid-corrected $\delta^{13}C$ values for each species, and fork length with $\delta^{15}N$ values. The slope of the linear regression of [THg] or [$MeHg^+$] and $\delta^{15}N$ values represents the food web magnification factor (FWMF) for all species. Corrected Akaike's information criterion (AICc), ΔAICc, and Akaike weights (w_i) were used to select the best approximating models for [THg] (Anderson and Burnham, 2002; Cyr et al., 2017). For each species, we included the same three factors as with the general linear model but also added the interaction of fork length and $\delta^{15}N$ values, to

account for the correlation of increasing trophic level as fish grow larger. We evaluated an additional model for sheefish that consisted of age, $\delta^{15}N$ values, lipid-corrected $\delta^{13}C$ values, and the interaction of age and $\delta^{15}N$ values. ΔAICc was calculated by subtracting the lowest model's AICc value from all other model AICc values. Models with ΔAICc < 2 are considered to perform comparably to the best approximating model (Anderson and Burnham, 2002). W_i values range from zero to one and represent the probability that a model is the best approximating model. As a final step, we compared the mean and 95% confidence intervals of [THg] and [$MeHg^+$] for each species to the published consumption threshold levels from the State of Alaska Department of Health Social Services (SOA DHSS) [THg] in fish (Hamade, 2014).

5.4 Results

5.4.1 Summary Results

Table 5.1 summarizes all morphological and chemical data for each species, with outliers. Mass and fork length varied considerably across all species, ranging from 6.0 to 7727 g (mean ± SD of 583.9 ± 1305.4 g), and 8.5 to 107.5 cm (35.2 ± 24.0 cm), respectively. Muscle [THg] for all fish ranged from 3.4 to 235 ng/g ww (44.9 ± 40.2 ng/g ww), and muscle [$MeHg^+$] ranged from 0.4 to 241.1 ng/g ww (38.5 ± 42.2 ng/g ww). The %$MeHg^+$ ranged from 48.4 to 119.0% (86.9 ± 14.0 %). $\delta^{15}N$ values ranged from 10.1‰ to 19.0 ‰ (13.7 ± 2.0 ‰), bulk $\delta^{13}C$ values ranged from -29.7 to -18.6 ‰ (-23.4 ± 2.2 ‰), and lipid-corrected $\delta^{13}C$ values ranged from -28.4 to -17.6 ‰ (-21.9 ± 2.3 ‰). Lipid-correction of $\delta^{13}C$ values significantly increased values in all species, with increases ranging from 1.1 to 2.7‰.

The descending rank order for mean muscle [THg]: sheefish ≥ fourhorn sculpin > humpback whitefish ≥ Pacific tomcod ≥ starry flounder ≥ Bering cisco ≥ chum salmon ≥ Pacific herring. (Figure 5.3A) ['>' indicates statistical difference ($\alpha \leq 0.05$) and '≥' indicates a larger mean value but no statistical difference]. The descending rank order for mean muscle [$MeHg^+$]: sheefish > humpback whitefish ≥ Pacific tomcod ≥ starry flounder ≥ Bering cisco ≥ chum salmon ≥ Pacific herring (Figure 5.3A, and for %$MeHg^+$ descending rank order was Bering cisco ≥ starry flounder ≥ sheefish ≥ humpback

whitefish ≥ Pacific tomcod ≥ chum salmon > Pacific herring. $\delta^{15}N$ values descending rank order: Pacific tomcod ≥ sheefish > fourhorn sculpin ≥ Pacific herring > humpback whitefish ≥ starry flounder > Bering cisco ≥ chum salmon. Bulk $\delta^{13}C$ values descending rank order: Pacific tomcod > chum salmon ≥ humpback whitefish ≥ sheefish ≥ Pacific herring ≥ fourhorn sculpin ≥ starry flounder ≥ Bering cisco, and lipid-corrected $\delta^{13}C$ values descending rank order: Pacific tomcod ≥ chum salmon ≥ Pacific herring ≥ sheefish ≥ humpback whitefish ≥ fourhorn sculpin ≥ starry flounder ≥ Bering cisco.

5.4.2 Relationship of [THg] with fork length, $\delta^{15}N$ values, and lipid-corrected $\delta^{13}C$ values

Muscle [THg] increased significantly with fork length in most species (Table 5.2, Figure 5.2) except in chum salmon (negatively correlated) and in humpback whitefish (no correlation). Across all species combined, muscle [THg] increased with increasing $\delta^{15}N$ values, with a FWMF of 11.3 ($R^2 = 0.35$, $p < 0.001$). This relationship varied strongly by species, and for species individually assessed the regression for [THg] and $\delta^{15}N$ values was significant and positive for sheefish, Bering cisco, starry flounder, Pacific herring, and fourhorn sculpin (Table 5.2). No statistically significant relationships between [THg] and $\delta^{15}N$ values were detected in chum salmon, humpback whitefish, and Pacific tomcod (Table 5.2). [THg] increased significantly with lipid-corrected $\delta^{13}C$ values in sheefish, Bering cisco, starry flounder, and humpback whitefish (data not shown).

5.4.3 [$MeHg^+$] and %$MeHg^+$ regression relationships with fork length, $\delta^{15}N$ and lipid-corrected $\delta^{13}C$ values

Muscle [$MeHg^+$] increased significantly with fork length in most species except in chum salmon (negatively correlated) and in humpback whitefish (no correlation). Across all species combined [$MeHg^+$] increased significantly with increasing $\delta^{15}N$ values, with a FWMF of 12.6 ($R^2 = 0.45$, $p < 0.001$). [$MeHg^+$] increased significantly with increasing $\delta^{15}N$ values in sheefish, starry flounder and Pacific herring. [$MeHg^+$] and lipid-corrected $\delta^{13}C$ values were significantly correlated in sheefish, Bering cisco, and starry flounder. %$MeHg^+$ decreased significantly with fork length in Bering cisco, Pacific herring, and chum salmon, however there were no significant relationships for %$MeHg^+$ with $\delta^{15}N$ values or $\delta^{13}C$

values. The range of %$MeHg^+$ varied considerably among species, however the upper bound of the 95% confidence interval for each species was above 100%.

5.4.4 Modeling [THg], fork length, $\delta^{15}N$ values, and lipid-corrected $\delta^{15}C$ values

Comparisons of general linear models based on ΔAICc values and Akaike weights revealed that no one model or variable best approximated the variation in [THg] among all species (Table 5.3). This finding was supported by the similarity of the R^2 values for the top models (ΔAICc < 2.0) from each species. Across all models considered, fork length was the most important variable, and was included alone or in conjunction with other variables in the best approximating model for seven of eight species, as well as being included in all but two of the top 25 models (Table 5.3). Lipid-corrected $\delta^{13}C$ alone was the best approximating model in humpback whitefish and was included in 13 of the top 25 models, representing every species, indicating the potential for influence from feeding location differences in those fish, such as more benthic influence. $\delta^{15}N$ was included in the best approximating model in Bering cisco, sheefish, and Pacific herring and was included in 15 of the top 25 models.

5.4.5 Sheefish age estimate relationships

Sheefish estimated ages (n=37) ranged from 8 to 29 years (17 ± 6.4 years). Sheefish age was positively correlated with muscle [THg] ($R^2 = 0.68$, $p << 0.001$), fork length ($R^2 = 0.69$, $p << 0.001$), $\delta^{15}N$ values ($R^2 = 0.58$, $p << 0.01$), $\delta^{13}C$ values ($R^2 = 0.49$, $p << 0.001$), and lipid-corrected $\delta^{13}C$ values ($R^2 = 0.53$, $p << 0.001$). General linear model results for sheefish indicated age was a significant variable influencing [THg] ($p << 0.001$). This result was further supported with ΔAICc values and Akaike weights, with the best approximating model for sheefish muscle [THg] including age (fork length removed due to high collinearity with age), and the interaction of age and $\delta^{15}N$ values.

5.4.6 [THg] comparisons with State of Alaska fish consumption criteria

The mean [THg] and [$MeHg^+$] for each species were below the 200 ng/g ww threshold for unrestricted consumption advised by the SOA DHSS (Hamade, 2014), Figure 3A. Of the 297 samples,

only four (1.0%) individual fish had muscle [THg] that were above this level, two sheefish (220.2 ng/g ww and 235.2 ng/g ww), one fourhorn sculpin (223.5 ng/g ww), and one chum salmon (202.4 ng/g ww), all within the 95% confidence interval for length of each species. The upper bound of the 95% confidence interval for each of the eight species examined was below the 200 ng/g ww level.

5.5 Discussion

5.5.1 SOA fish consumption comparisons

Every fish analyzed, but four (1.0%), was below the unrestricted consumption guideline for Hg in muscle for acceptable daily intake (SOA DHHS). In addition to the overall reassuring concentrations of Hg in these fishes, it is important to emphasize the many nutritional health benefits obtained from the consumption of marine fish including protein, long-chain omega-3 polyunsaturated fatty acids, essential amino acids, vitamins, and trace elements (Gribble et al., 2016). For example, one health benefit from additional trace elements is Selenium (Se), whereby Se can sequester and bind to Hg, rendering Hg unavailable for biological processes (Ralston and Raymond, 2010). The Se:Hg molar ratios of sheefish muscle from Kotzebue Sound are reported to be 8.35–10.3, providing an abundance of Se (Moses et al., 2009). The SOA DHHS incorporates these additional nutritional parameters of fish in conjunction with the risk of Hg exposure, which provides a comprehensive assessment of the risk and benefit tradeoffs of fish consumption (Hamade, 2014). These data are useful to others interested in Hg in this region of Alaska and for determining consumption advice for humans. In an effort to assist monitoring efforts and consumption guidelines, the [THg] and [$MeHg^{+}$] data generated as part of this research have been provided to the SOA Fish Monitoring Program.

5.5.2 Ecological drivers of mercury concentration

Trophic level, as approximated using $\delta^{15}N$ values, affected muscle [Hg] for the group of species represented. Feeding ecology drives trophic level, which influences biomagnification processes of fish

resulting in increased [Hg] in muscle in higher trophic level fishes (individuals and for species). The calculated FWMF of 11.3 indicates that THg magnified with increasing $\delta^{15}N$ values in this study.

Feeding ecology and trophic level can be influenced by several factors. One notable influence is prey assemblage of a food web, which can vary spatially and temporally, and influences the amount of Hg to which a fish is exposed due to high assimilation efficiency of $MeHg^{+}$ from the diet (Cyr et al., 2017; Johnson et al., 2015; Payne and Taylor, 2010). Another prominent influence is ontogenetic feeding changes, which can influence dietary exposure of Hg. Fish prey on different resources as they age and grow larger, either by shifting dietary resources or dietary preferences (Jaecks and Quinn, 2014), or access to different resources due to growth in gape size (Kraemer et al., 2012). These changes in feeding ecology can increase exposure to Hg by enabling feeding to occur at progressively higher trophic levels, providing more opportunity for biomagnification.

Our finding that fork length was a significant driver of muscle [THg] and [$MeHg^{+}$] in most of our individual fish species is in agreement with published literature for many other species (Burger et al., 2014; Dang and Wang, 2012; Riget et al., 2000). Length, which can be used as a proxy for age (Davis et al., 2016; Scott and Armstrong, 1972), is indicative of exposure time for bioaccumulation to occur (Dietz et al., 1990). Sheefish for example, are a relatively long-lived species, with a maximum known age of 41 (Brown et al., 2012). The sheefish examined here showed the greatest [THg] and [MeH^{+}], and had a mean estimated age of 17 y, with a maximum estimated age of 29 yrs. In contrast, chum salmon had some of the lowest [THg] and [$MeHg^{+}$], and have a maximum known age of 7 (Scott and Crossman, 1998), providing less time for the influence of bioaccumulation.

Although no single variable, or combination of variables, best approximated the true model for our fishes, we note that fork length was included in more approximating models than $\delta^{15}N$ values or lipid-corrected $\delta^{13}C$ values (Table 5.3). Resource-limited food webs, particularly in the Arctic where ice cover reduces the annual productivity (Wang et al., 2014), are shorter and contain fewer trophic levels for

biomagnification of Hg to occur (Cabana and Rasmussen, 1994). The marine food web of Kotzebue Sound has previously been described as overlapping food resources rather than distinct trophic levels (Feder et al., 2011). We hypothesize, but did not test, that the food web of Kotzebue Sound is relatively short, which allows time (age) to drive bioaccumulation in individual species more than trophic level (Gantner et al., 2010). A more comprehensive food web analysis of [THg], $\delta^{15}N$ and $\delta^{13}C$ values that encompasses plankton and invertebrate species would provide additional clarity on this process.

5.5.3 $MeHg^+$

The relatively high $\%MeHg^+$ values measured here are in agreement with published values in fish from numerous species (Amlund et al., 2007; Jewett et al., 2003; Tran et al., 2015). $MeHg^+$ has an assimilation efficiency of >85% from the fish gut (Pickhardt et al., 2006; Wang, 2012), which results in the majority of the muscle THg in many fish species being primarily $MeHg^+$ (Amlund et al., 2007; Jewett et al., 2003; Rimondi et al., 2012). Fish also have limited capacity for redistributing, demethylating or eliminating THg or $MeHg^+$, which allows for efficient accumulation and retention of THg or $MeHg^+$ in muscle tissue (Amlund et al., 2007; Trudel and Rasmussen, 1997). To account for the slightly lower $\%MeHg^+$ values of Pacific herring, we note [THg] and [$MeHg^+$] for Pacific herring were relatively low, at and slightly above the detection limit of the THg assay we used, which may have contributed to the higher data variability and low $\%MeHg^+$. Pacific herring also had the highest C:N ratio and the lowest $\%H_2O$, indicating muscle tissue likely contained a higher fraction of lipids than the other species in this study, representing a reduced capacity for $MeHg^+$ to bind with proteins (Kent, 1973). $\%MeHg^+$ has also been shown to decrease with fish age in three species of Arctic sculpins (Harley et al., 2015). We did not observe decreases in $\%MeHg^+$ with $\delta^{15}N$ values (all species) or age (sheefish); however, [THg] were much lower than the concentrations seen in Harley et al., 2015, thus the fish might not have reached a threshold of detectable demethylation (Eagles-Smith et al., 2009) as seen in older sculpin.

5.5.4 Case studies

The one chum salmon outlier had extremely high [THg] and $\delta^{15}N$ values, but was not significantly larger than the other chum, nor were the $\delta^{13}C$ values outside of the group mean. Based on these metrics, we hypothesize that this was feeding almost two full trophic levels above the rest of the sample population, allowing for more biomagnification. The one sheefish outlier had [THg] and [$MeHg^+$] that were very low, but had %$MeHg^+$ that was within range for the group mean. Despite the low [THg] and [$MeHg^+$], this fish was the 4th oldest sheefish in this study. We hypothesize that this fish was a unique fish that may have migrated in from a different location where it had been feeding on a different food web, or had selected a specific prey base low in Hg (Cyr et al., 2017). %$MeHg^+$ measurements from 16 samples were considered outliers, eight low and eight high. This can be a function of analytical precision at low concentrations, or lipid content of the sample, both of which were described in detail in the previous section.

5.5.5 Sheefish

Sheefish are one of the most important fish resources to the residents of Kotzebue; it is estimated that sheefish alone represent as much as 45% of their total fish harvested (Whiting, 2006). Sheefish were the largest fish species in this study and had greater [THg] than most other species measured (Table 5.1, Figure 5.3A), yet only two of the 50 sheefish analyzed had muscle [THg] above the SOA DHSS 200 ng/g ww criteria for unrestricted fish consumption. The [THg] measured in sheefish were comparable to those measured ten years earlier in Kotzebue Sound by Moses et al. (2009). Given the high prevalence of sheefish in the diets of many people of the Kotzebue Sound region, this is an important update.

5.6 Conclusion

We have compiled an extensive data set on the chemical feeding ecology of Hg in eight species of fish from Kotzebue Sound, Alaska; many consumed by humans. We document that across the food web of Kotzebue Sound, food web biomagnification is important for driving [THg] and [$MeHg^+$], but

within individual species fork length is a dominant driver of observed muscle [THg] and [$MeHg^+$]. We have demonstrated that except for Pacific herring, %$MeHg^+$ is consistently >80%, independent of fork length or $\delta^{15}N$ values. Finally, most fishes in this study were below the [THg] for unrestricted human consumption based on the SOA DHSS fish consumption guidelines. These data add to a detailed baseline for comparing [THg] and stable isotopes of carbon and nitrogen for a changing arctic environment. Continued monitoring of subsistence resources is vital to assuring food security for remote areas of the Arctic and for assessing other important piscivores in the region (e.g., pinnipeds, cetaceans). This allows for community involvement and understanding of Hg in their valued Sound and fishery that will enhance tribal, local and state management and outreach.

5.7 Acknowledgments

The authors would like to thank the Village of Kotzebue and the residents for all their time, assistance, and knowledge throughout the project with fish collections, transport, and logistics. J.M. Castellini assisted with mercury analysis, maintenance, calibration and troubleshooting of the DMA-80. J. Harley assisted with methylmercury analysis and troubleshooting of the Brooks Rand MERX system, as well as data and statistical interpretation throughout the project. H. Gerrish, Z. Goeden, E. Mayo, E. Audette, A. Gastaldi assisted with sample processing, mercury analysis, and stable isotope preparation. M. Courtney assisted with mapping. We would like to thank the Alaska Department of Environmental Conservation (ADEC) for supporting a portion of the Hg analysis of this research, and R. Gerlach and C. Furin for their overall support and assistance with this project. This publication is the result in part of research sponsored by the UAF BLaST program, as well as partial support from a 2017 North Pacific Research Board (NPRB) Graduate Student Research Award and is referenced as publication #675.

Work reported in this publication was supported by the National Institute of General Medical Sciences of the National Institutes of Health under three linked awards number RL5GM118990, TL4 GM 118992 and 1UL1GM118991. The work is solely the responsibility of the authors and does not necessarily represent the official view of the National Institutes of Health.

5.8 Figures

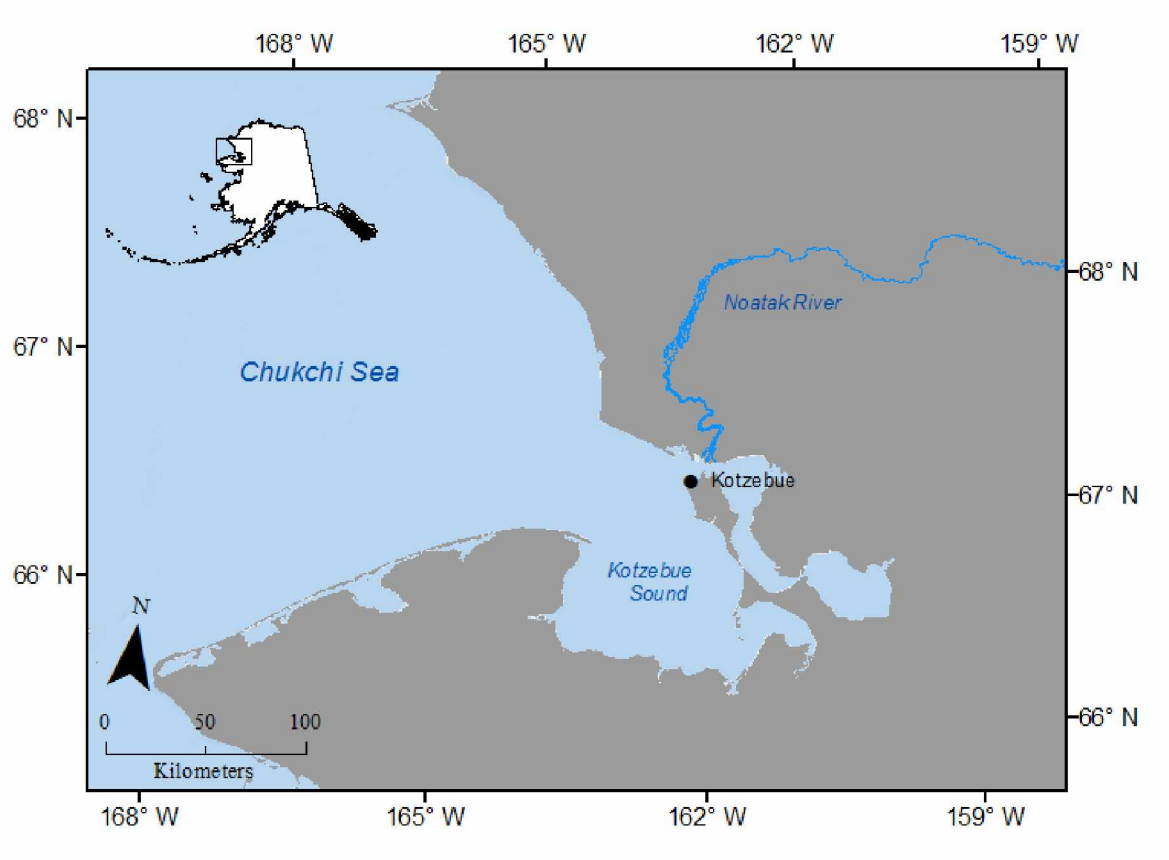

Figure 5.1 - Regional map depicting study area.

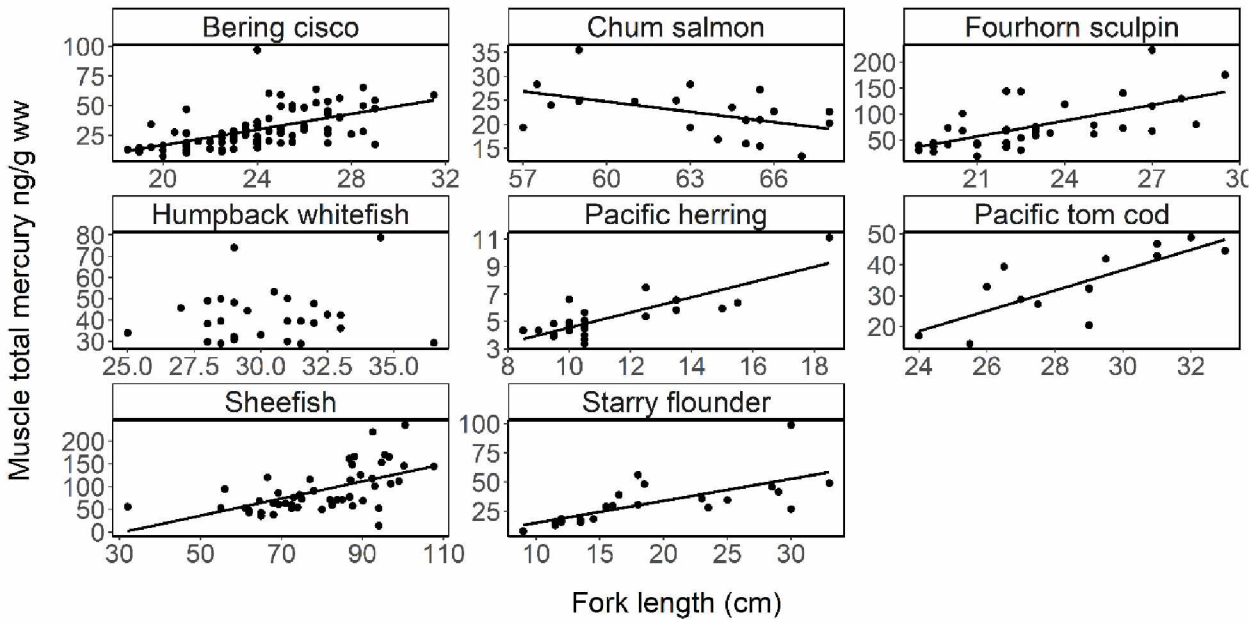

Figure 5.2 - Muscle total mercury concentrations [THg] and fork length (cm) of fishes from Kotzebue, Alaska. Absence of regression line indicates the relationship for that species was not significantly different from zero.

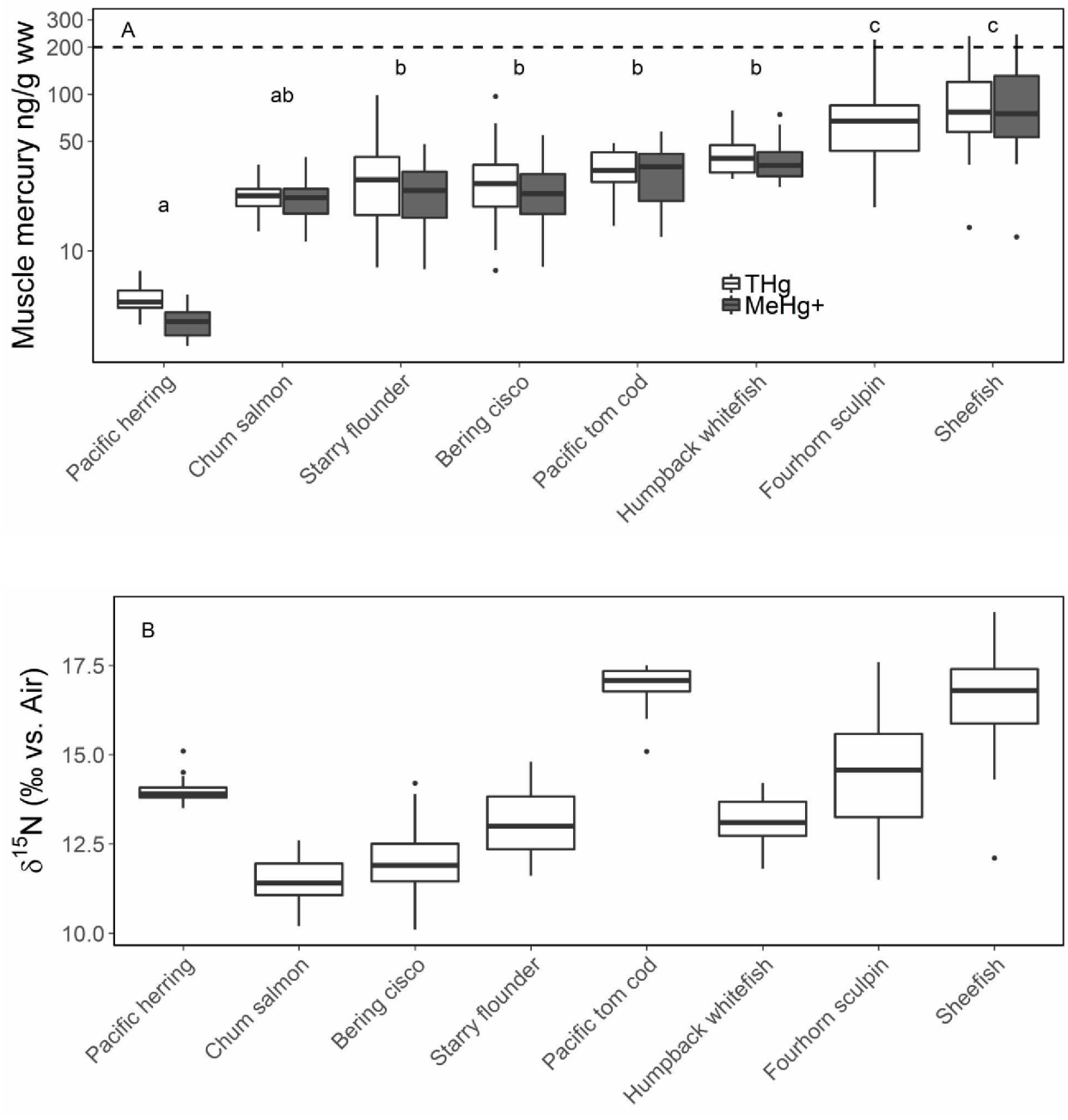

Figure 5.3A and 5.3B - Box and whisker plots of muscle total mercury concentrations [THg], methylmercury^{+} concentrations ($MeHg^{+}$], and $\delta^{15}N$ (‰) values for each fish species from Kotzebue, Alaska. Bold horizontal lines inside each box represent median values, bottom and top edges of boxes represent 25th and 75th percentiles, respectively, and the ends of the vertical solid lines represent ± 1.5 * interquartile range. Dashed line indicates the State of Alaska unrestricted consumption criteria (200 ng/g ww) for fish consumers. ww = wet weight. Letters a, b, and c indicate significant difference ($a \leq 0.05$) for mean [THg] or mean [$MeHg^{+}$] between species. $\delta^{15}N$ values compared to the isotopic standard air.

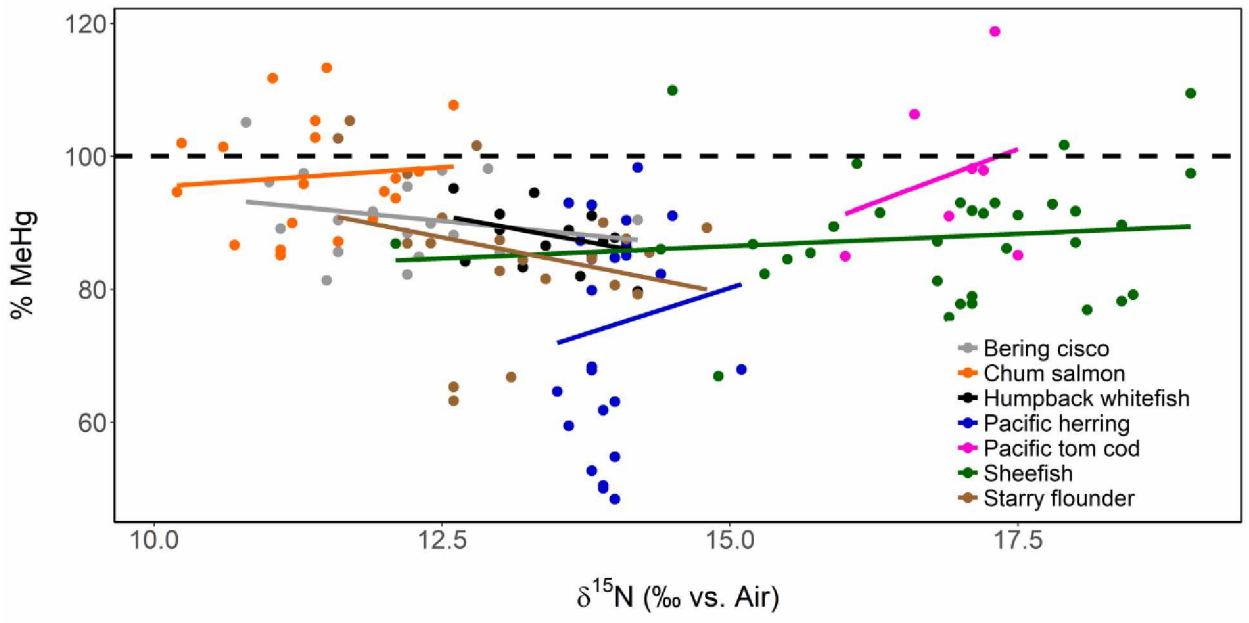

Figure 5.4 - %MeHg and $\delta^{15}N$ (‰) values for each species of fish from Kotzebue, Alaska. Dashed line indicates %MeHg = 100%. $\delta^{15}N$ values compared to the isotopic standard air.

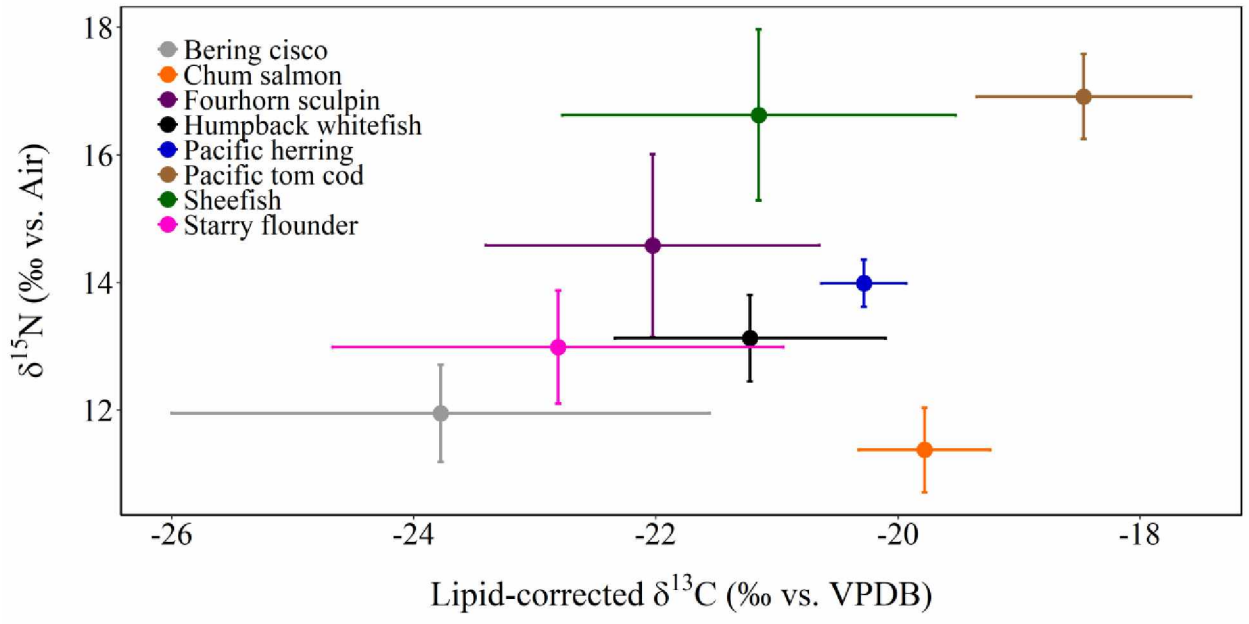

Figure 5.5 - Mean $\delta^{15}N$ (‰) and lipid-corrected $\delta^{13}C$ (‰) isotopic values ± standard deviation of muscle samples for each species of fish from Kotzebue, Alaska. $\delta^{15}N$ values compared to the isotopic standard air, and $\delta^{13}C$ values compared to the isotopic standard Vienna-PeeDee Belemnite (VPDB).

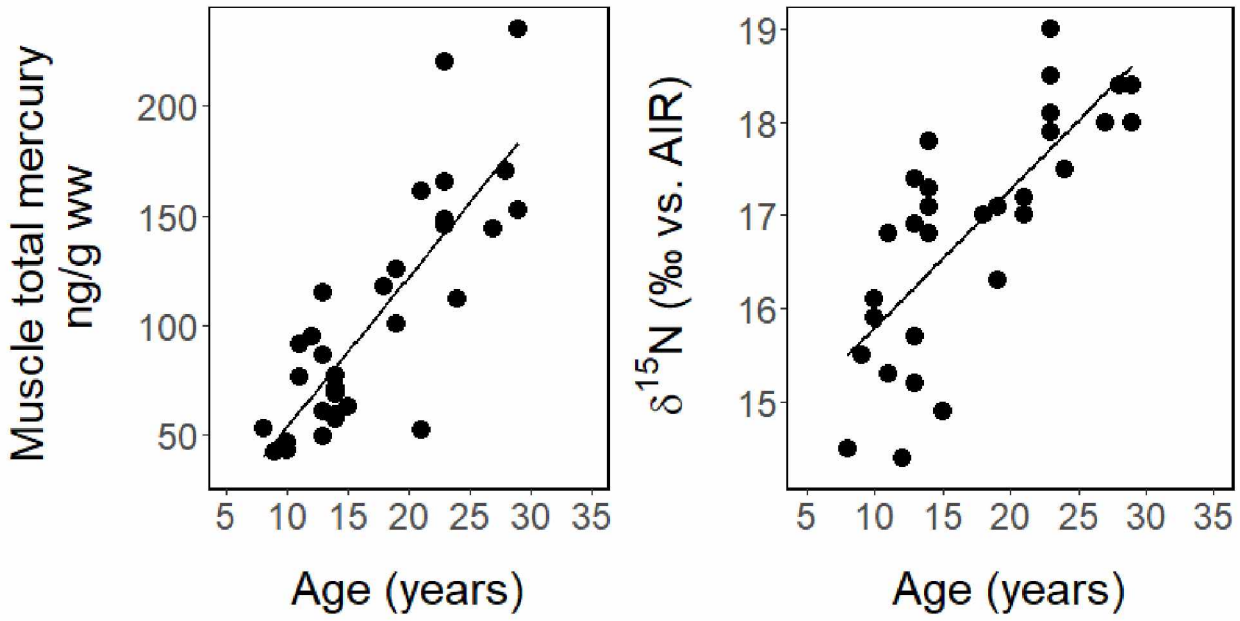

Figure 5.6 - Linear regressions for sheefish muscle total mercury concentrations [THg] with age, and muscle $\delta^{15}N$ (‰) values with age. $\delta^{15}N$ values compared to the isotopic standard air. ww = wet weight.

5.9 Tables

Table 5.1 - Sample sizes (N), fork length, mass, muscle total mercury concentrations ([THg]), muscle monomethyl mercury concentrations ([$MeHg^+$]), $\%MeHg^+$, $\delta^{15}N$ values, $\delta^{13}C$ values, and lipid-corrected $\delta^{13}C$ values for each fish species sampled near Kotzebue, Alaska. All data except %MeHg includes outliers, and is represented as mean ± SD. [THg] and [$MeHg^+$] data are represented as geometric mean ± SD ng/g wet weight in the top cell, median and (range) in the bottom cell. $\%MeHg^+$ is displayed as the mean of individual values for each species in the top cell, and the slope of the robust linear regression of [THg] and [$MeHg^+$] in the bottom cell (Wagemann et al., 1997).

Species	N	Fork Length (cm)	Mass (g)	[THg] ng/g ww	[$MeHg^+$] ng/g ww	$\%MeHg^+$	$\delta^{15}N$ (‰)	$\delta^{13}C$ (‰)	Lipid-corrected $\delta^{13}C$ (‰)
Bering cisco	93	24.1 ± 2.7	154.1 ± 57.3	26.7 ± 15.6	22.3 ± 12.8 (20)	90.8 ± 6.3	11.9 ± 0.8	-25.0 ± 2.3	-23.8 ± 2.2
Coregonus laurettae				26.9 (7.5 - 96.9)	23.3 (7.9 - 54.8)	87.8 ± 1.2			
Humpback whitefish	28	30.2 ± 2.4	324.4 ± 84.8	40.2 ± 12.4	31.0 ± 16.1 (17)	87.9 ± 4.5	13.1 ± 0.7	-22.5 ± 1.1	-21.2 ± 1.1
Coregonus pidschian				39.5 (28.9 - 78.7)	32.2 (2.3 - 74.4)	88.2 ± 1.3			
Fourhorn sculpin	36	23.0 ± 2.9	104.0 ± 54.0	65.7 ± 45.7	na	na	14.6 ± 1.4	-23.5 ± 1.3	-22.0 ± 1.4
Myoxocephalus quadricornis				67.5 (19.0 - 223.5)	na	na			
Chum salmon	22	63.9 ± 4.4	4478.1 ±	23.9 ± 38.9	22.8 ± 39.1 (22)	96.7 ± 8.6	11.7 ± 1.6	-21.4 ± 0.7	-19.8 ± 0.6
Oncorhynchus keta				22.7 (10.7 – 202.2)	22.0 (9.0 – 202.2)	96.6 ± 1.8			
Starry flounder	28	18.6 ± 7.3	114.1 ± 129.2	25.9 ± 19.5	21.2 ± 11.8 (22)	85.0 ± 11.2	13.0 ± 0.9	-23.9 ± 1.9	-22.8 ± 1.9
Platichthys stellatus				28.0 (7.9 - 98.9)	23.3 (7.7 - 48.0)	84.7 ± 1.6			
Pacific herring	29	11.1 ± 2.2	16.6 ± 16.2	5.0 ± 1.5	3.3 ± 1.1 (29)	72.8 ± 15.7	14.0 ± 0.4	-23.0 ± 0.5	-20.3 ± 0.3
Clupea pallasii				4.7 (3.4 - 11.1)	3.5 (0.4 - 5.9)	72.9 ± 3.4			
Pacific tomcod	14	28.6 ± 2.6	196.9 ± 76.7	31.5 ± 11.0	29.3 ± 16.1 (7)	96.8 ± 12.1	16.9 ± 0.7	-19.6 ± 0.9	-18.5 ± 0.9
Microgadus proximus				32.7 (14.5 - 48.8)	36.2 (12.3 - 57.9)	98.4 ± 4.6			
Sheefish	50	79.6 ± 14.7	3330.8 ±	80.6 ± 48.3	74.5 ± 50.9 (38)	87.4 ± 9.3	16.7 ± 1.3	-22.5 ± 1.6	-21.1 ± 1.6
Stenodus leucichthys				81.7 (14.2 - 235.2)	72.7 (12.3 - 241.1)	88.2 ± 1.3			

Table 5.2 - The amount of the linear regression variance explained (R^2) and the significance (P value) for linear regression of total mercury concentrations ([THg]) with fork length, with $\delta^{15}N$ values, and with the interaction of fork length and $\delta^{15}N$ values for each species. Significant regressions in bold italic text.

Species	**[THg] ~ Fork length**	**[THg] ~ $\delta^{15}N$ values**	**[THg] ~ Fork length ***
Bering cisco	***0.33 (0.001)***	***0.05 (0.03)***	***0.33 (0.001)***
Humpback whitefish	0.02 (0.5)	0.00 (0.90)	0.28 (0.25)
Fourhorn sculpin	***0.41 (0.001)***	***0.13 (0.03)***	***0.45 (0.001)***
Chum salmon	***0.38 (0.002)***	0.16 (0.07)	0.25 (0.18)
Starry flounder	***0.49 (0.001)***	***0.33 (0.003)***	***0.57 (0.001)***
Pacific herring	***0.67 (0.001)***	***0.38 (0.001)***	***0.79 (0.001)***
Pacific tomcod	***0.61 (0.001)***	0.10 (0.27)	***0.61 (0.019)***
Sheefish	***0.69 (0.001)***	***0.58 (0.001)***	***0.60 (0.001)***
All Species	***0.31 (0.001)***	***0.35 (0.001)***	***0.48 (0.001)***

Data displayed as R^2 (P values)

Table 5.3 - The top four candidate models for approximating muscle [THg] within each species of fish in Kotzebue, Alaska, including fork length (cm), $\delta^{15}N$ values, $\delta^{13}C$ values, and the interaction of fork length and $\delta^{15}N$. The best candidate model for each species is highlighted in bold text. $\delta^{13}C$ values are lipid-corrected $\delta^{13}C$ values.

Species	Model	AICc	ΔAICc	R^2	W_i
Sheefish	***Fork length + $\delta^{15}N$ + Fork length* $\delta^{15}N$***	***481.5***	***0.00***	***0.60***	***1.00***
	Fork length + $\delta^{15}N$ + $\delta^{13}C$ + Fork length * $\delta^{15}N$	483.1	1.60	0.58	0.45
	Fork length + Fork length * $\delta^{15}N$	490.3	8.83	0.52	0.01
	Fork length * $\delta^{15}N$	491.9	10.45	0.51	0.01
Bering cisco	***Fork length + $\delta^{13}C$ + Fork length * $\delta^{15}N$***	***725.46***	***0.00***	***0.45***	***1.00***
	Fork length + $\delta^{15}N$ + $\delta^{13}C$	725.80	0.34	0.45	0.84
	Fork length + $\delta^{13}C$	725.92	0.46	0.44	0.79
	$\delta^{15}N$ + $\delta^{13}C$ + Fork length * $\delta^{15}N$	726.61	1.14	0.44	0.57
Humpback whitefish	***$\delta^{13}C$***	***221.18***	***0.00***	***0.13***	***1.00***
	Fork length + $\delta^{13}C$	223.82	2.64	0.10	0.27
	$\delta^{13}C$ + Fork length* $\delta^{15}N$	223.90	2.72	0.10	0.26
	$\delta^{15}N$ + $\delta^{13}C$	223.91	2.73	0.10	0.26
Chum salmon	***Fork length***	***129.06***	***0.00***	***0.35***	***1.00***
	Fork length * $\delta^{15}N$	129.43	0.37	0.34	0.83
	Fork length + $\delta^{13}C$	130.38	1.32	0.37	0.52
	$\delta^{13}C$ + Fork length * $\delta^{15}N$	131.40	2.34	0.34	0.31
Starry flounder	***Fork length***	***201.12***	***0.00***	***0.47***	***1.00***
	Fork length * $\delta^{15}N$	201.39	0.27	0.46	0.88
	Fork length + $\delta^{13}C$	202.77	1.65	0.47	0.44
	$\delta^{13}C$	203.03	1.91	0.42	0.39
Fourhorn sculpin	***Fork length + $\delta^{13}C$***	***363.62***	***0.00***	***0.43***	***1.00***
	Fork length + Fork length * $\delta^{15}N$	364.34	0.72	0.41	0.70
	Fork length	364.45	0.83	0.39	0.66
	Fork length + $\delta^{15}N$	364.63	1.01	0.41	0.60
Pacific herring	***Fork length + $\delta^{13}C$ + Fork length * $\delta^{15}N$***	***67.65***	***0.00***	***0.80***	***1.00***
	$\delta^{15}N$ + $\delta^{13}C$ + Fork length * $\delta^{15}N$	69.21	1.56	0.79	0.46
	Fork length + $\delta^{15}N$ + $\delta^{13}C$ + Fork length * $\delta^{15}N$	69.27	1.62	0.80	0.45
	Fork length + $\delta^{15}N$ + $\delta^{13}C$	69.85	2.20	0.78	0.33
Pacific tomcod	***Fork length***	***101.17***	***0.00***	***0.58***	***1.00***
	Fork length * $\delta^{15}N$	103.57	2.40	0.50	0.30
	Fork length + $\delta^{13}C$	104.93	3.76	0.55	0.15
	Fork length + $\delta^{15}N$	105.08	3.91	0.54	0.14

5.10 Works Cited

Amlund, H., Lundebye, A.K., Berntssen, M.H.G., 2007. Accumulation and elimination of methylmercury in Atlantic cod (Gadus morhua L.) following dietary exposure. Aquat. Toxicol. 83, 323–330. doi:10.1016/j.aquatox.2007.05.008

Anderson, D.R., Burnham, K.P., 2002. Avoiding Pitfalls When Using Information-Theoretic Methods. Manag. J. Wildl. 66, 912–918.

Arctic Monitoring Assessment Program (AMAP), 2011. AMAP Assessment 2011: Mercury in the Arctic. Oslo, Norway.

Barber, W.E., McFarlane, G.A., 1987. Evaluation of three techniques to age Arctic char from Alaskan and Canadian waters. Trans. Am. Fish. Soc. 116, 874–881. doi:10.1577/1548-8659(1987)116

Bloom, N., 1989. Determination of Picogram Levels of Methylmercury by Aqueous Phase Ethylation, Followed by Cryogenic Gas Chromatography with Cold Vapour Atomic Fluorescence Detection. Can. J. Fish. Aquat. Sci. 46, 1131–1140.

Bodaly, R.A., Rudd, J.W.M., Fudge, R.J.., Kelly, C.A., 1993. Mercury concentrations in fish related to size of remote Canadian Shield lakes. Can. J. Fish. Aquat. Sci. 50, 980–987.

Boening, D.W., 2000. Ecological effects, transport, and fate of mercury: a general review. Chemosphere 40, 1335–1351. doi:10.1016/S0045-6535(99)00283-0

Boyle, M.D., Ebert, D.A., Cailliet, G.M., 2012. Stable-isotope analysis of a deep-sea benthic-fish assemblage: evidence of an enriched benthic food web. J. Fish Biol. 80, 1485–1507. doi:10.1111/j.1095-8649.2012.03243.x

Bridges, C.C., Zalups, R.K., 2005. Molecular and ionic mimicry and the transport of toxic metals. Toxicol. Appl. Pharmacol. 204, 274–308. doi:10.1016/j.taap.2004.09.007

Brown, R.J., Brown, C., Braem, N.M., Carter III, W.K., Legere, N., Slayton, L., 2012. Whitefish biology, distribution, and fisheries in the Yukon and Kuskokwim River drainages in Alaska: A synthesis of available information. U.S. Fish Wildl. Serv. Alaska Fish. Data Ser. 2012-4 2012–4, 1–330.

Burger, J., Gochfeld, M., Jeitner, C., Pittfield, T., Donio, M., 2014. Heavy metals in fish from the Aleutians: interspecific and locational differences. Environ. Res. 131, 119–130. doi:10.1016/j.envres.2014.02.016

Cabana, G., Rasmussen, J.B., 1994. Modelling food chain structure and contaminant bioaccumulation using stable nitrogen isotopes. Lett. to Nat. 372, 255–257. doi:10.1038/372255a0

Carrie, J., Stern, G. a., Sanei, H., Macdonald, R.W., Wang, F., 2012. Determination of mercury biogeochemical fluxes in the remote Mackenzie River Basin, northwest Canada, using speciation of sulfur and organic carbon. Appl. Geochemistry 27, 815–824. doi:10.1016/j.apgeochem.2012.01.018

Chen, L., Wang, H.H., Liu, J.F., Tong, Y.D., Ou, L.B., Zhang, W., Hu, D., Chen, C., Wang, X.J., 2014. Intercontinental transport and deposition patterns of atmospheric mercury from anthropogenic emissions. Atmos. Chem. Phys. 14, 10163–10176. doi:10.5194/acp-14-10163-2014

Chiasson-Gould, S.A., Blais, J.M., Poulain, A.J., 2014. Dissolved organic matter kinetically controls mercury bioavailability to bacteria. Environ. Sci. Technol. 48, 3153–3161. doi:10.1021/es4038484

Cyr, A., López, J.A., Rea, L., Wooller, M.J., Loomis, T., Mcdermott, S., O'Hara, T.M., 2019. Mercury concentrations in marine species from the Aleutian Islands: spatial and biological determinants. Sci. Total Environ. 664, 761–770. doi:10.1016/j.scitotenv.2019.01.387

Cyr, A., Sergeant, C.J., Lopez, J.A., O'Hara, T., 2017. Assessing the influence of migration barriers and feeding ecology on total mercury concentrations in Dolly Varden (Salvelinus malma) from a glaciated and non-glaciated stream. Sci. Total Environ. 580, 710–718. doi:10.1016/j.scitotenv.2016.12.017

Daguené, V., McFall, E., Yumvihoze, E., Xiang, S., Amyot, M., Poulain, A.J., 2012. Divalent base cations hamper Hg II uptake. Environ. Sci. Technol. 46, 6645–6653. doi:10.1021/es300760e

Dang, F., Wang, W.X., 2012. Why mercury concentration increases with fish size? Biokinetic explanation. Environ. Pollut. 163, 192–198. doi:10.1016/j.envpol.2011.12.026

Davis, J.A., Ross, J.R.M., Bezalel, S., Sim, L., Bonnema, A., Ichikawa, G., Heim, W.A., Schiff, K., Eagles-Smith, C.A., Ackerman, J.T., 2016. Hg concentrations in fish from coastal waters of California and Western North America. Sci. Total Environ. 568, 1146–1156. doi:10.1016/j.scitotenv.2016.03.093

Dietz, R., Nielsen, C.O., Hansen, M.M., Hansen, C.T., 1990. Organic mercury in Greenland birds and mammals. Sci. Total Environ. 95, 41–51. doi:10.1016/0048-9697(90)90051-U

Doi, H., Kikuchi, E., Shikano, S., Takagi, S., 2010. Differences in nitrogen and carbon stable isotopes between planktonic and benthic microalgae. Limnology 11, 185–192. doi:10.1007/s10201-009-0297-1

Douglas, T.A., Loseto, L.L., MacDonald, R.W., Outridge, P., Dommergue, A., Poulain, A., Amyot, M., Barkay, T., Berg, T., Chetelat, J., Constant, P., Evans, M., Ferrari, C., Gantner, N., Johnson, M.S., Kirk, J., Kroer, N., Larose, C., Lean, D., Nielsen, T.G., Poissant, L., Rognerud, S., Skov, H., Sørensen, S., Wang, F., Wilson, S., Zdanowicz, C.M., 2012. The fate of mercury in Arctic terrestrial and aquatic ecosystems, a review. Environ. Chem. 9, 321–355. doi:10.1071/EN11140

Eagles-Smith, C.A., Ackerman, J.T., De La Cruz, S.E.W., Takekawa, J.Y., 2009. Mercury bioaccumulation and risk to three waterbird foraging guilds is influenced by foraging ecology and breeding stage. Environ. Pollut. 157, 1993–2002. doi:10.1016/j.envpol.2009.03.030

Eagles-Smith, C.A., Ackerman, J.T., Willacker, J.J., Tate, M.T., Lutz, M.A., Fleck, J.A., Stewart, A.R., Wiener, J.G., Evers, D.C., Lepak, J.M., Davis, J.A., Flanagan Pritz, C., 2016. Spatial and temporal patterns of mercury concentrations in freshwater fish across the Western United States and Canada. Sci. Total Environ. doi:10.1016/j.scitotenv.2016.03.229

Environment Canada, 2013. Mercury: fish consumption advisories [WWW Document]. URL https://www.canada.ca/en/environment-climate-change/services/pollutants/mercury-environment/health-concerns/fish-consumption-advisories.html (accessed 7.10.18).

USEPA. 1998. Method 1630 Methyl Mercury in Water by Distillation , Aqueous Ethylation , Purge and Trap , and Cold Vapor Atomic Fluorescence Spectrometry.

Fall, J.A., 2018. Regional Patterns of Fish and Wildlife Harvests in Contemporary Alaska Author (s): James A . Fall Published by : Arctic Institute of North America Stable URL : https://www.jstor.org/stable/43871398 Regional Patterns of Fish and Wildlife Harvests in Cont 69, 47–64.

Feder, H.M., Iken, K., Blanchard, A.L., Jewett, S.C., Schonberg, S., 2011. Benthic food web structure in the southeastern Chukchi Sea: An assessment using δ13C and δ15N analyses. Polar Biol. 34, 521–532. doi:10.1007/s00300-010-0906-9

Fry, B., 2006. Stable Isotope Ecology. Springer Science + Business Media, LLC, New York.

Gantner, N., Power, M., Iqaluk, D., Meili, M., Borg, H., Sundbom, M., Solomon, K.R., Lawson, G., Muir, D.C., 2010. Mercury concentrations in landlocked arctic char (Salvelinus alpinus) from the Canadian arctic. Part I: Insights from trophic relationships in 18 lakes. Environ. Toxicol. Chem. 29, 621–632. doi:10.1002/etc.95

Goldfarb, B.R.J., Marsh, E.E., Hart, C.J.R., Mair, J.L., Marti, L., Johnson, C., 2007. Geology and Origin of Epigenetic Lode Gold Deposits, Tintina Gold Province, Alaska and Yukon, in: Gough, L.P., Day, W.C. (Eds.), Recent U.S. Geological Survey Studies in the Tintina Gold Province, Alaska, United States, and Yukon, Canada—Results of a 5-Year Project Edited. U.S. Geological Survey.

Gribble, M.O., Karimi, R., Feingold, B.J., Nyland, J.F., O'Hara, T.M., Gladyshev, M.I., Chen, C.Y., 2016. Mercury, selenium and fish oils in marine food webs and implications for human health. J. Mar. Biol. Assoc. United Kingdom 96, 43–59. doi:10.1017/S0025315415001356

Gu, B., Bian, Y., Miller, C.L., Dong, W., Jiang, X., Liang, L., 2012. Mercury reduction and oxidation by reduced natural organic matter in anoxic environments. Environ. Sci. Technol. 46, 292–299. doi:10.1021/es203402p

Hamade, A.K., 2014. Fish Consumption Advice for Alaskans: A Risk Management Strategy To Optimize the Public's Health.

Harley, J., Lieske, C., Bhojwani, S., Castellini, J.M., Lopez, J.A., O'Hara, T.M., 2015. Mercury and methylmercury distribution in tissues of sculpins from the Bering Sea. Polar Biol. 38, 1535–1543. doi:10.1007/s00300-015-1716-x

Jaecks, T., Quinn, T.P., 2014. Ontogenetic shift to dependence on salmon-derived nutrients in Dolly Varden char from the Iliamna River, Alaska. Environ. Biol. Fishes 97, 1323–1333. doi:10.1007/s10641-014-0221-3

Jewett, S.C., Duffy, L.K., 2007. Mercury in fishes of Alaska, with emphasis on subsistence species. Sci. Total Environ. 387, 3–27. doi:10.1016/j.scitotenv.2007.07.034

Jewett, S.C., Zhang, X., Naidu, S.A., Kelley, J.J., Dasher, D., Duffy, L.K., 2003. Comparison of mercury and methylmercury in northern pike and Arctic grayling from western Alaska rivers. Chemosphere 50, 383–392. doi:10.1016/S0045-6535(02)00421-6

Johnson, B.M., Lepak, J.M., Wolff, B.A., 2015. Effects of prey assemblage on mercury bioaccumulation in a piscivorous sport fish. Sci. Total Environ. 506–507, 330–337. doi:10.1016/j.scitotenv.2014.10.101

Johnson, J.S., Nobmann, E.D., Asay, E., Lanier, A.P., 2009. Dietary intake of Alaska Native people in two regions and implications for health: the Alaska Native Dietary and Subsistence Food Assessment Project. Int. J. Circumpolar Health 68, 109–122. doi:10.3402/ijch.v68i2.18320

Johnson, N.W., Mitchell, C.P.J., Engstrom, D.R., Bailey, L.T., Coleman Wasik, J.K., Berndt, M.E., 2016. Methylmercury production in a chronically sulfate-impacted sub-boreal wetland. Environ. Sci. Process. Impacts 18, 725–734. doi:10.1039/C6EM00138F

Kelly, C.A., Rudd, J.W.M., Holoka, M.H., 2003. Effect of pH on mercury uptake by an aquatic bacterium: implications for Hg cycling. Environ. Sci. Technol. 37, 2941–2946. doi:10.1021/es026366o

Kent, M., 1973. Hand-held instrument for fat / water determination in whole fish 47–53.

Kraemer, L.D., Evans, D., Dillon, P.J., 2012. The impacts of ontogenetic dietary shifts in yellow perch (Perca flavescens) on Zn and Hg accumulation. Ecotoxicol. Environ. Saf. 78, 246–252. doi:10.1016/j.ecoenv.2011.11.033

Lushchak, V.I., 2011. Environmentally induced oxidative stress in aquatic animals. Aquat. Toxicol. 101, 13–30. doi:10.1016/j.aquatox.2010.10.006

McGrew, A.K., Ballweber, L.R., Moses, S.K., Stricker, C.A., Beckmen, K.B., Salman, M.D., O'Hara, T.M., 2014. Mercury in gray wolves (Canis lupus) in Alaska: increased exposure through consumption of marine prey. Sci. Total Environ. 468–469, 609–613. doi:10.1016/j.scitotenv.2013.08.045

Moses, S.K., Whiting, A. V, Bratton, G.R., Taylor, R.J., O'Hara, T.M., 2009. Inorganic nutrients and contaminants in subsistence species of Alaska : linking wildlife and human health Inorganic nutrients and contaminants in subsistence species of Alaska : Linking wildlife and human health. Int. J. Circumpolar Health 68, 53–74. doi:10.3402/ijch.v68i1.18294

Nriagu, J., Becker, C., 2003. Volcanic emissions of mercury to the atmosphere: Global and regional inventories. Sci. Total Environ. 304, 3–12. doi:10.1016/S0048-9697(02)00552-1

Payne, E.J., Taylor, D.L., 2010. Effects of diet composition and trophic structure on mercury bioaccumulation in temperate flatfishes. Arch. Environ. Contam. Toxicol. 58, 431–443. doi:10.1007/s00244-009-9423-7

Peterson, B.J., Fry, B., 1987. Stable isotopes in ecosystem studies. Ann. Rev. Ecol. Syst 18, 293–320. doi:10.1146/annurev.es.18.110187.001453

Pickhardt, P.C., Stepanova, M., Fisher, N.S., 2006. Contrasting uptake routes and tissue distributions of inorganic and methylmercury in mosquitofish (Gambusia affinis) and redear sunfish (Lepomis microlophus). Environ. Toxicol. Chem. 25, 2132–2142. doi:10.1897/05-595R.1

Post, D.M., Layman, C.A., Arrington, D.A., Takimoto, G., Quattrochi, J., Montaña, C.G., 2007. Getting to the fat of the matter: models, methods and assumptions for dealing with lipids in stable isotope analyses. Oecologia 152, 179–189. doi:10.1007/s00442-006-0630-x

Power, M., Klein, G.M., Guiguer, K.R.R.A., Kwan, M.K.H., 2002. Mercury accumulation in the fish community of a sub-Arctic lake in relation to trophic position and carbon sources. J. Appl. Ecol. 39, 819–830. doi:10.1046/j.1365-2664.2002.00758.x

Pyle, D.M., Mather, T.A., 2003. The importance of volcanic emissions for the global atmospheric mercury cycle. Atmos. Environ. 37, 5115–5124. doi:10.1016/j.atmosenv.2003.07.011

Ralston, N.V.C., Raymond, L.J., 2010. Dietary selenium's protective effects against methylmercury toxicity. Toxicology 278, 112–123. doi:10.1016/j.tox.2010.06.004

Riget, F., Asmund, G., Aastrup, P., 2000. Mercury in Arctic char (Salvelinus alpinus) populations from Greenland. Sci. Total Environ. 245, 161–172. doi:10.1016/S0048-9697(99)00441-6

Rimondi, V., Gray, J.E., Costagliola, P., Vaselli, O., Lattanzi, P., 2012. Concentration, distribution, and translocation of mercury and methylmercury in mine-waste, sediment, soil, water, and fish collected near the Abbadia San Salvatore mercury mine, Monte Amiata district, Italy. Sci. Total Environ. 414, 318–327. doi:10.1016/j.scitotenv.2011.10.065

Rytuba, J.J., 2003. Mercury from mineral deposits and potential environmental impact. Environ. Geol. 43, 326–338. doi:10.1007/s00254-002-0629-5

Scott, D.P., Armstrong, F.A.J., 1972. Mercury concentration in relation to size in several species of freshwater fishes from Manitoba and Northwestern Ontario. J. Fish. Res. Board Canada 29, 1685–1690. doi:10.1139/f72-268

Scott, W.B., Crossman, E.J., 1998. Freshater fishes of Canada. Galt House Publications, Ltd.

Suchanek, T.H., Eagles-Smith, C.A., Slotton, D.G., Jamesharner, E., Colwell, A.E., Anderson, N.L., Mullen, L.H., Flanders, J.R., Adam, D.P., Mcelroy, K.J., 2008. Spatiotemporal trends in fish mercury from a mine-dominated ecosystem: Clear lake, California. Ecol. Appl. 18, 177–195. doi:10.1890/06-1900.1

Syversen, T., Kaur, P., 2012. The toxicology of mercury and its compounds. J. Trace Elem. Med. Biol. 26, 215–226. doi:10.1016/j.jtemb.2012.02.004

Team, R.C., 2017. R: A language and environment for statistical computing. R Foundation for Statistical Computing.

Tran, L., Reist, J.D., Power, M., 2015. Total mercury concentrations in anadromous Northern Dolly Varden from the northwestern Canadian Arctic: A historical baseline study. Sci. Total Environ. 509–510, 154–164. doi:10.1016/j.scitotenv.2014.04.099

Trudel, M., Rasmussen, J.B., 1997. Modeling the elimination of mercury by fish. Environ. Sci. Technol. 31, 1716–1722. doi:10.1021/es960609t

United States Census Bureau [WWW Document], 2017. URL https://www.census.gov/quickfacts/northwestarcticboroughalaska (accessed 10.19.18).

USEPA, 2011. National Listing of Fish Advisories.

Wagemann, R., Trebacz, E., Hunt, R., Boila, G., 1997. Percent methylmercury and organic mercury in tissues of marine mammals and fish using different experimental and calculation methods. Environ. Toxicol. Chem. 16, 1859–1866. doi:10.1897/1551-5028(1997)016<1859:PMAOMI>2.3.CO;2

Walker, C.H., Sibly, R.M., Hopkin, S.P., Peakall, D.B., 2012. Principles of Ecotoxicology, 4th ed. CRC Press, Boca Raton, FL.

Wang, S.W., Budge, S.M., Gradinger, R.R., Iken, K., Wooller, M.J., 2014. Fatty acid and stable isotope characteristics of sea ice and pelagic particulate organic matter in the Bering Sea: tools for estimating sea ice algal contribution to Arctic food web production. Oecologia 174, 699–712. doi:10.1007/s00442-013-2832-3

Wang, W.-X., 2012. Biodynamic understanding of mercury accumulation in marine and freshwater fish. Adv. Environ. Res. 1, 15–35. doi:10.12989/aer.2012.1.1.015

Whiting, A.A., 2006. Native Village of Kotzebue Harvest Survey program 2002–2003–2004: results of three con- secutive years cooperating with Qikiqtagrugmiut to understand their annual catch of selected fish and wildlife.

Willacker, J.J., von Hippel, F.A., Ackerly, K.L., O'Hara, T.M., 2013. Habitat-specific foraging and sex determine mercury concentrations in sympatric benthic and limnetic ecotypes of threespine stickleback. Environ. Toxicol. Chem. 32, 1623–1630. doi:10.1002/etc.2213

Wolfe, R.J., 2000. Subsistence in Alaska: a year 2000 update.

Chapter 6 - **Conclusions** [6]

[6]Cyr, A.,

6.1 Overview

Hg contamination in fishes is ubiquitous, thus investigating factors that drive [THg] and [$MeHg^+$] in fishes is important for understanding the chemical feeding ecology of Hg and its relationship to human and wildlife health. Dietary exposure of Hg, mostly as $MeHg^+$, from fish consumption is a well-known pathway for Hg exposure in humans and wildlife. In my dissertation research, I investigated some of the suspected and known drivers that influence [THg] and [$MeHg^+$] in fishes from three spatially and environmentally distinct Alaskan aquatic ecosystems. My work led to a better understanding of how fish length, age, capture location, and feeding ecology influence [Hg]. Finally, I compared the measured [Hg] of fishes from this study to State of Alaska published human consumption limits (Hamade, 2014). Chapters 3, 4, and 5 addressed a series of specific ecological questions relating to one of more of these drivers of [Hg] in fish.

6.2 Region

Region can influence fish tissue [Hg] by exposing fish to different prey resources with varying [Hg] and different water and sediments inputs of Hg with varying influences on methylation and the subsequent bioavailability of $MeHg^+$. The influence of region on the [THg] in vertebrate tissues has been noted in a variety of taxa from many locations around the world, including the Bering Sea (Anthony et al., 2007; Bentzen et al., 2016; Ricca et al., 2008). In Chapter 3 I determined that region (with respect to anadromous barriers) influenced [THg] and feeding ecology of Dolly Varden by providing them access to different prey resources, notably access to salmon eggs (roe). Chapter 4 built on previous research showing regional differences and patterns of [THg] in biota (e.g., Steller sea lions and Pacific halibut) from parts of the Bering Sea and North Pacific Ocean by expanding the number of known species exhibiting regional differences of [THg]. I determined that there are large-scale differences in the baseline values of carbon isotopes across the Bering Sea and North Pacific Ocean, and a large-scale regional difference in [THg] which then gets amplified in fishes through feeding ecology. Finally, I determined that using Amchitka Pass as an alternate spatial delineation to demarcate Aleutian Island regions

produced more consistent regional differences in [THg] across all species. This finding highlights the importance of using natural ecological and oceanographic divisions to measure and interpret observed ecological patterns. Together these regional differences demonstrate that location can play a significant role in influencing [Hg].

6.3 Feeding ecology

Trophic level is a known driver of [Hg] in some fish (Burger et al., 2014; Mason et al., 2000; McIntyre and Beauchamp, 2007; Power et al., 2002). Most of the evidence reported to date suggests that trophic level is positively correlated with [Hg], however this is not a consistent pattern. Higher $\delta^{15}N$ values do not always indicate an elevated trophic position, nor greater [Hg] in tissues. As shown in Chapter 3, Dolly Varden feeding on salmon eggs had elevated $\delta^{15}N$ values but very low [THg] in muscle. Lipid-corrected $\delta^{13}C$ values provided additional insight on the diets of these fish by indicating a marine-derived signature in part of the food web. In Chapter 4 I determined that there are consistent differences in [THg] of fishes between regions of the Aleutian Islands. I determined that within a species, the relationship of [THg] and $\delta^{15}N$ values varies depending on region and the isotopic relationships of trophic levels across a food web, including differences in baseline isotopic values of carbon. In Chapter 5 I demonstrated that among individual species, length was more influential on observed [THg] than individual feeding ecology, but biomagnification was more influential across the studied food web as a whole. These findings reinforce the notion that although $\delta^{15}N$ values may be used as indicators of trophic level, this does not consistently translate into greater [THg] and [$MeHg^{+}$]. The use of multiple metrics together can provide better context to interpret observed [Hg] by carefully separating the complex ecological relationships, and highlighting unusual individuals, populations, or species that warrant further investigation.

6.4 Fish resource Hg monitoring

Monitoring some abiotic components of the environment and select fish populations for Hg are a focus of many human and environmental health investigations. With the multitude of drivers that can

influence Hg transport, methylation, and uptake and accumulation in biota, designing effective research methods to monitor the environment for Hg is challenging. Data collected as part of this dissertation contributed to the State of Alaska (SOA) Fish Monitoring Program (State of Alaska, 2018). In addition, the data generated from the Dolly Varden study (Chapters 2 and 3) was used by the National Park Service to guide the development of a freshwater contaminants monitoring protocol. Species and site selection, and effective sampling periods were guided by the work I conducted. The wide breadth of [THg], stable isotope values, and associated biological data from the Bering Sea, North Pacific Ocean, and Kotzebue Sound (Chapters 4 and 5) were provided to the Fish Monitoring Program for future use by the SOA DHSS for ongoing fish Hg monitoring and consumption advice efforts. This project demonstrated that collaborating with various groups and agencies, such as the commercial fishing industry and subsistence fishers, can enhance relevance, sample size, spatial and species coverage, and reduce unnecessary and extraneous fish use in research, ultimately benefiting all stakeholders involved. Finally, I have shown the importance of ongoing monitoring of fish resources to keep up with changing climatic and ecological conditions and provide the most current and up-to-date information to fish consumers, researchers, and health officials.

6.5 Fish [Hg] in context of other events and research

The Minamata Bay, Japan, disaster was an example of fish Hg toxicity of drastic proportions, with a distinct point source of Hg contamination in close proximity to harvested fish resources consumed by local residents. When considering the [Hg] measured in the fishes from this project to those in fishes from the Minamata Bay disaster, we see that all of the concentrations from these fish are 50-400 times less than those from Minamata Bay. This is important to note because Minamata Bay is often cited as an example of the threat of dietary exposure to Hg from fish. In addition, none of the study areas examined in this research are near significant point sources of Hg. However, the Minamata Bay disaster underscores the importance of ongoing monitoring of fish resources to provide accurate information for consumers.

With ongoing changing climatic and ecological conditions, particularly in the Arctic, effective monitoring of fishes and environmental resources for Hg contamination should remain a priority.

A significant concern regarding reported [THg] in fishes is understanding how relevant those observed concentrations are for consumption concerns for human and wildlife health, and how they compare to other fish species, either from around Alaska or other parts of the world. The [THg] measured within my research are broadly aligned with those reported elsewhere in the literature. Nearly all of the fishes measured in this project have mean muscle [THg] comparable or lower than those reported in the literature, for example, Pacific halibut (32 ng/g ww) (Bentzen et al., 2016), Pacific cod (173 ng/g ww), yellow Irish lord (272 ng/g ww), rock sole (95.4 ng/g ww) (Burger et al., 2014), shorthorn sculpin (*Myoxocephalus scorpius*, 30 ng/g ww) (Harley et al., 2015), whitefish (163 ng/g ww), sheefish (159 ng/g ww), northern pike (*Esox lucius*, 823 ng/g ww), burbot (*Lota lota*, 96 ng/g ww) and Arctic grayling (*Thymallus arcticus*, 101 ng/g ww) (Duffy et al., 1999). Finally, in reference to dietary exposure and consumption concerns, of the 1,453 fishes measured in this study, 82.3% were below the SOA guideline for unrestricted consumption of 200 ng/g ww, and 94.8% were below the EPA screening value for recreational fishers of 400 ng/g ww. The only species with muscle [THg] at levels of potential concern were yellow Irish lord from the central Aleutian Islands, with mean muscle [THg] of 410.3 ng/g ww. This gives us confidence that regarding Hg, most fish species from Alaska that are commonly consumed are as safe or safer for consumption than many other fish species from around the world.

The majority of the fishes analyzed in this project have muscle [THg] far lower than fishes associated with severely Hg contaminated areas, such as areas in close proximity to mining activities, from other areas of North America and the world. This includes Arctic grayling (420 ng/g ww) and Dolly Varden (620 ng/g ww) near Cinnabar Creek mine, Mountain Top mine, Red Top mine, and Kolmakof mine, Alaska (Gray et al., 2000), channel catfish (*Ictalurus punctatus*, 240 ng/g ww) and largemouth bass (*Micropterus salmoides*, 1040 ng/g ww) from Clear Creek, California (Suchanek et al., 2008), or a composite mean of 840 ng/g ww from barbel (*Barbus plebejus*), chub (*Leuciscus cephalus*), roach

(*Chondrostoma genei*), and carp (*Cyprinus carpio*) from Monte Amiata Hg district, Italy (Rimondi et al., 2012).

6.6 Next steps

My dissertation research will serve as a foundation for further inquiries on the ecological dynamics of contaminants in Alaskan aquatic ecosystems. For example, do other contaminants (inorganic or organic-based contaminants) exhibit similar patterns of accumulation as those observed for Hg? If there are differences in the oceanographic conditions of the WAI and CAI, what aspects of those differences lead to elevated [THg] in individuals in the WAI as compared to those from the CAI? What is driving the [THg] in muscle in yellow Irish lords, particularly in the CAI? Is there a significant time component involved, or are there very specific feeding ecology differences driving observed [THg]? What is the full complement of chemistry and micronutrients (Cu, Se, As, Cd, Vitamins A, D, E, etc.) within each of these fish? Knowing the full complement of chemistry, what are the risk-benefit tradeoffs of consuming these fish? Some species of fish are known to accumulate Hg preferentially in different tissues, such as muscle versus liver (Harley et al., 2015; Murillo-Cisneros et al., 2018; Raldua et al., 2007). Do these differences help explain measured differences of [THg] and [$MeHg^{+}$] between species? These questions demonstrate that additional research is needed to extend our knowledge of mercury dynamics in aquatic ecosystems and in fishes in particular, the full complement of chemistry that occurs within an individual fish and ecosystem, and the implications for human and wildlife consumption of these fish.

One of the most informative pieces of information that I believe this research could benefit from is a more comprehensive food web analysis, extending from primary producers to top predators. We know that $MeHg^{+}$ accumulates efficiently from the diet in fish, but we also know that there is significant variability in [$MeHg^{+}$] within the same fish population or region. What causes this? How much variability is there in other taxa or trophic levels? In conjunction with a more comprehensive food web analysis, compound-specific stable isotope analysis, in addition to bulk stable isotope measures, could prove

particularly valuable to better differentiate the trophic relationships between predator and prey resources and help us understand why observed [THg] are often highly variable with respect to bulk $\delta^{15}N$ values. The use of compound-specific stable isotope analysis of $\delta^{15}N$ values has proven effective in trophic studies, demonstrating that the $\delta^{15}N$ values of glutamic acid, a non-essential amino acid, change in a consistent manner with trophic steps (Chikaraishi et al., 2014). This would enable a comprehensive and detailed approach to understanding the specific mechanisms that influence muscle [THg]. Finally, a series of detailed controlled feeding experiments can address specific feeding and accumulation questions.

The ecological dynamics of Hg in the aquatic environment is a vital area of research. The data, results, and comparisons presented in this dissertation address, in various small steps, several key components of chemical feeding ecology of Hg. The data generated here also informs monitoring protocols, augments existing databases of [Hg] in fish for Alaska, and provide guidance on future research steps.

6.7 Works cited

Anthony, R.G., Miles, A.K., Ricca, M.A., Estes, J.A., 2007. Environmental contaminants in bald eagle eggs from the Aleutian archipelago. Environ. Toxicol. Chem. 26, 1843–1855. doi:10.1897/06-334R.1

Bentzen, R., Castellini, J.M., Gerlach, R., Dykstra, C., O'Hara, T., 2016. Mercury concentrations in Alaska Pacific halibut muscle relative to stable isotopes of C and N and other biological variables. Mar. Pollut. Bull. 113, 110–116. doi:10.1016/j.marpolbul.2016.08.068

Burger, J., Gochfeld, M., Jeitner, C., Pittfield, T., Donio, M., 2014. Heavy metals in fish from the Aleutians: interspecific and locational differences. Environ. Res. 131, 119–130. doi:10.1016/j.envres.2014.02.016

Chikaraishi, Y., Steffan, S.A., Ogawa, N.O., Ishikawa, N.F., Sasaki, Y., Tsuchiya, M., Ohkouchi, N., 2014. High-resolution food webs based on nitrogen isotopic composition of amino acids. Ecol. Evol. 4, 2423–2449. doi:10.1002/ece3.1103

Duffy, L.K., Scofield, E., Rodgers, T., Patton, M., Bowyer, R.T., 1999. Comparative baseline levels of mercury, Hsp 70 and Hsp 60 in subsistence fish from the Yukon-Kuskokwim delta region of Alaska. Comp. Biochem. Physiol. - C Pharmacol. Toxicol. Endocrinol. 124, 181–186. doi:10.1016/S0742-8413(99)00055-9

Gray, J.E., Theodorakos, P.M., Bailey, E.A., Turner, R.R., 2000. Distribution, speciation, and transport of mercury in stream-sediment, stream-water, and fish collected near abandoned mercury mines in southwestern Alaska, USA. Sci. Total Environ. 260, 21–33. doi:10.1016/S0048-9697(00)00539-8

Hamade, A.K., 2014. Fish Consumption Advice for Alaskans: A Risk Management Strategy To Optimize the Public's Health.

Harley, J., Lieske, C., Bhojwani, S., Castellini, J.M., Lopez, J.A., O'Hara, T.M., 2015. Mercury and methylmercury distribution in tissues of sculpins from the Bering Sea. Polar Biol. 38, 1535–1543. doi:10.1007/s00300-015-1716-x

Mason, R.P., Laporte, J.-M., Andres, S., 2000. Factors controlling the bioaccumulation of mercury, methylmercury, arsenic, selenium, and cadmium by freshwater invertebrates and fish. Arch. Environ. Contam. Toxicol. 38, 283–297. doi:10.1007/s002449910038

McIntyre, J.K., Beauchamp, D.A., 2007. Age and trophic position dominate bioaccumulation of mercury and organochlorines in the food web of Lake Washington. Sci. Total Environ. 372, 571–584. doi:10.1016/j.scitotenv.2006.10.035

Misarti, N., Finney, B., Maschner, H., Wooller, M.J., 2009. Changes in northeast Pacific marine ecosystems over the last 4500 years: evidence from stable isotope analysis of bone collagen from archeological middens. The Holocene 19, 1139–1151. doi:10.1177/0959683609345075

Murillo-Cisneros, D.A., O'Hara, T.M., Castellini, J.M., Sánchez-González, A., Elorriaga-Verplancken, F.R., Marmolejo-Rodríguez, A.J., Marín-Enríquez, E., Galván-Magaña, F., 2018. Mercury concentrations in three ray species from the Pacific coast of Baja California Sur, Mexico: Variations by tissue type, sex and length. Mar. Pollut. Bull. 126, 77–85. doi:10.1016/j.marpolbul.2017.10.060

Power, M., Klein, G.M., Guiguer, K.R.R.A., Kwan, M.K.H., 2002. Mercury accumulation in the fish community of a sub-Arctic lake in relation to trophic position and carbon sources. J. Appl. Ecol. 39, 819–830. doi:10.1046/j.1365-2664.2002.00758.x

Raldua, D., Diez, S., Bayona, J.M., Barcelo, D., 2007. Mercury levels and liver pathology in feral fish living in the vicinity of a mercury cell chlor-alkali factory. Chemosphere 66, 1217–1225. doi:10.1016/j.chemosphere.2006.07.053

Ricca, M.A., Keith Miles, A., Anthony, R.G., 2008. Sources of organochlorine contaminants and mercury in seabirds from the Aleutian archipelago of Alaska: inferences from spatial and trophic variation. Sci. Total Environ. 406, 308–323. doi:10.1016/j.scitotenv.2008.06.030

Rimondi, V., Gray, J.E., Costagliola, P., Vaselli, O., Lattanzi, P., 2012. Concentration, distribution, and translocation of mercury and methylmercury in mine-waste, sediment, soil, water, and fish collected near the Abbadia San Salvatore mercury mine, Monte Amiata district, Italy. Sci. Total Environ. 414, 318–327. doi:10.1016/j.scitotenv.2011.10.065

State of Alaska, 2018. Contaminants in Alaska's fish [WWW Document]. State of Alaska. URL https://dec.alaska.gov/eh/vet/fish-monitoring-program/

Suchanek, T.H., Eagles-Smith, C.A., Slotton, D.G., Jamesharner, E., Colwell, A.E., Anderson, N.L., Mullen, L.H., Flanders, J.R., Adam, D.P., Mcelroy, K.J., 2008. Spatiotemporal trends in fish mercury from a mine-dominated ecosystem: Clear lake, California. Ecol. Appl. 18, 177–195. doi:10.1890/06-1900.1